EVALUATING THE ECONOMIC FEASIBILITY OF THERMAL SCREENS IN NEW ZEALAND USING A MATHEMATICAL MODEL

A thesis

submitted in partial fulfilment

of the requirements for the degree

of

Master of Horticultural Science

in

Horticultural Engineering

at

Massey University

Todd Litchfield Newman

1991

ABSTRACT

A mathematical model of the greenhouse environment was developed to ascertain the annual savings in heating expenditure achieved by thermal screens. Thirteen materials with thermal screening potential were investigated. Each material was modelled within glass, *Agphane*, and twin skin *Agphane* covered greenhouses, 300m^2 and 1000m^2 in floor area, heated with diesel, coal, electricity, natural gas, or L.P.G., to set points of 15°C and 20°C, in Auckland and Christchurch.

The model consisted of two phases. Phase 1 was a steady state model of the greenhouse environment based on a series of energy and mass balances. The temperatures within the greenhouse and the quantity of heat required to hold the house at a specified set point were predicted by solving these balances simultaneously. This process enabled the average U-value for each greenhouse to be estimated.

In Phase 2 of the model the annual heat load for combinations of each house size and type, cover, screen, set point, and location were estimated using average U-values from Phase 1 and meterological data indicative of Auckland and Christchurch. Using current fuel prices, annual heat loads were converted into annual heating expenditures.

Using annual heating expenditure, screen life expectancy, and screen installation cost an economic analysis was conducted using internal rate of return as a measure of thermal screen feasibility.

In terms of savings in heating expenditure, Black Polythene, *Infrane*, and Clear Polythene recorded the highest internal rate of return. It was decided that before a formal recommendation could be made further research was required to evaluate screens as summer shading or photoperiod control devices and to consider the practical problems associated with some of the screens.

It was shown that returns from thermal screening were greater in Christchurch than Auckland, greater at a 20°C set point than at a 15°C set point, greater for a 1000m² house than a 300m² house, greatest with diesel heating in Auckland, and greatest with diesel and L.P.G. heating in Christchurch.

TABLE OF CONTENTS

PAGE

LIST OF FIGURES

LIST OF TABLES

LIST OF PLATES

LIST OF FREQUENTLY USED SYMBOLS

A	advective heat transfer (Wm^{-2})
Al	aluminium
AUX	auxiliary heating or cooling (Wm^{-2}floor)
C	cloud fraction, conductive heat flux density (Wm^{-2})
$^{\circ}C$	degrees Celsius
CAI	cover area index
Cp	specific heat capacity of dry air at 20°C ($1.01Jg_{DA}^{-1}{}^{\circ}C^{-1}$)
D	diffusive heat transfer (Wm^{-2})
e	water vapour pressure (Pa)
E	energy of one photon (J), evaporative heat transfer coefficient ($Wm^{-2}{}^{\circ}K^{-1}$)
Eb	total emissive power of a blackbody (Wm^{-2})
EMF	evaporative cooling, misting, or fogging ($g_v s^{-1} m^{-2}$)
EVA	ethylene vinyl acetate
ERR	external rate of return (%)
f	frequency (s^{-1})
F	FIR
FIR	far infra-red radiation
g	gram
h	convective heat transfer coefficient ($Wm^{-2}{}^{\circ}K^{-1}$), Plank's constant (6.63×10^{-34} Js^{-1})
H	rate of heat loss (Wm^{-2}), solar radiation ($MJm^{-2}day^{-1}$), convective heat flux density (Wm^{-2})
$\mathcal{H}$	enthalpy of moist air (Jg_{DA}^{-1})
IR	infra-red (long wave) radiation
IRR	internal rate of return (%)
J	joule
k	thermal conductivity ($Wm^{-1}{}^{\circ}K^{-1}$)
K	thermal conductance ($Wm^{-2}{}^{\circ}K^{-1}$)
$^{\circ}K$	degrees Kelvin
$\mathcal{L}$	latent heat of vaporization of water at 20°C ($2454Jg_v^{-1}$)
L	latent heat loss (Wm^{-2})
LAI	leaf area index
m	metre
mm	millimetre
M	molecular mass ($gmol^{-1}$), mass transfer ($g_v s^{-1} m^{-2}$)

N	NIR, number of air changes per second (s^{-1})
NIR	near infra-red radiation
$\varnothing$	permeance ($g_v s^{-1} m^{-2} Pa^{-1}$)
P	PAR
PAR	photosynthetically active radiation
PE	polyethylene
PVC	polyvinyl chloride
q	conductive heat flux density (Wm^{-2})
r	resistance (sm^{-1})
R	Universal gas constant ($8.314 Jmol^{-1} {}^{\circ}K^{-1}$)
s	second
S	solar radiation (Wm^{-2})
T	temperature
U	overall heat loss coefficient, thermal transmittance, U-value ($Wm^{-2}floor {}^{\circ}C^{-1}$ or $Wm^{-2}floor {}^{\circ}K^{-1}$)
UV	ultra-violet
v	velocity of light in a vacuum (3×10^6 ms^{-1})
V	greenhouse volume (m^{-3})
VA	vinyl acetate
W	watt
x	direction of heat flow (m)
Z	water vapour flux density ($g_v s^{-1} m^{-2}$)

GREEK ALPHABET

α	absorptivity
ϵ	emissivity
γ	slope of enthalpy lines on the psychometric chart ($Pa {}^{\circ}K^{-1}$)
δ	slope of the saturated vapour pressure curve ($Pa {}^{\circ}K^{-1}$)
θ	equivalent temperature ($^{\circ}C$)
λ	wavelength (m)
μm	micrometre
ρ	reflectivity, density of gas (gm^{-3})
σ	Stefan-Boltzmann constant (5.67×10^{-8} $Wm^{-2} {}^{\circ}K^{-4}$)
τ	transmissivity
Φ	advective heat transfer coefficient ($Wm^{-2} {}^{\circ}K^{-1}$)

χ	water vapour density or absolute humidity ($g_v m_{DA}^{-3}$)
ω	humidity ratio ($g_v g_{DA}^{-1}$)
Ω	diffusive heat transfer coefficient ($Wm^{-2} {}^{\circ}K^{-1}$)

SUBSCRIPTS

a	inside air
c	cover
DA	dry air
f	floor
F	FIR
i	inside air
l	lower surface of thermal screen
N	NIR
o	outside air
p	plant
P	PAR
q	quiescent airspace
s	thermal screen
sky	sky
s1	soil layer 1
s2	soil layer 2
s3	soil layer 3
s4	soil layer 4
v	water vapour
vap	water vapour
u	upper surface of thermal screen
w	wet bulb

ACKNOWLEDGEMENTS

The author wishes to express sincere gratitude to his supervisors, Dr. Gavin Wall, Acting H.O.D (Agricultural Engineering) and Mr. Colin Wells. Their assistance and advice throughout this study were gratefully appreciated.

The author also wishes to acknowledge Mr. Ian Painter, Mr. Leo Bolter, and Mr. Paul Turner for the construction of experimental apparatus and technical advice, Kitrina Shapleske for her help collecting and collating data, and to other postgraduates and staff of the Agricultural Engineering Department for assistance when needed.

The competitiveness and assistance of masterate colleague Phil Heatley was appreciated. Phil's humour, sanity and conversation kept wearisome moments to the minimum and his companionship and consolation during times of frustration and personal stress will be remembered. Thanks also to my long suffering room mate, landlord, and friend Richard, and the flatties and frequent visitors of 21 Glasgow St for friendship and laughs. Special thanks goes to Leigh Mitchell for her help in typing this thesis and to Roy for his devoted Thursday night therapy on the squash court.

The financial support of the New Zealand Fruitgrowers Federation, the C. Almar Baker Trust, the Robert Gibson Methodist Trust, the Frank Sydenham Scholarship and the J.A. Anderson Scholarship are gratefully acknowledged.

Finally, I wish to acknowledge my parents for their love, support and prayers, and Basil and Nancy Christensen and family, whose hospitality, amazing meals, and friendship have made my stay in Palmerston North truly memorable. To these people I dedicate this thesis.

CHAPTER I

INTRODUCTION

1.1 BACKGROUND

A greenhouse is a structure designed to facilitate the control or modification of environmental factors affecting plant growth. By controlling the environment, variations and hazards associated with weather are eliminated. Temperature, humidity, day length, gas composition (carbon dioxide and oxygen), and light can be regulated with varying degrees of precision; damage from wind and rain is avoided; and injury from plant diseases and insects is reduced. Growing media, moisture content, nutrition, and fertility levels can also be adjusted to meet plant requirements. Consequently crops can be produced for specific market dates; grown more rapidly with greater uniformity, and yield a product with less variation in quality.

Compared to field production, greenhouse crop culture is characterised by high capital, labour and fuel costs. The cost of erecting a manually controlled plastic covered house was around 40-55 $\$/m^2$ in 1990; the cost for a glass covered house was around 80-100 $\$/m^2$ (Faber, 1990; Tailor, 1990; Williams, 1990; and Young, 1990). To offset capital cost of this magnitude, efficient and intensive year round production are important management strategies.

As heating is a major component of greenhouse management (Burit et al, 1978),

intensive production effectuates a high heating cost. It follows that price premiums arising from superior quality and timing production to coincide with the short or non-existent supplies from field sources, are intrinsic when justifying greenhouse heating cost (Breuer, 1985a).

Fuel cost in New Zealand stands out as the one economic factor which is expected to escalate at a rate higher than inflation (Breuer 1985a). The price of oil based fuels fluctuate depending on political action in oil producing countries. Recent events in the Middle East have caused the price of petrol in New Zealand to increase by about 20%. By improving both energy efficiency and independence, New Zealand's greenhouse industry will become increasingly cost competitive and more able to withstand shortfalls or discontinuity in energy supply.

Modern glass or plastic covered houses have been designed for maximum light transmission without particular regard for heat conservation. They are usually leaky structures, having thin walls with high U-value (overall heat loss). As a result they tend to be expensive to heat especially in windy conditions (Hurd and Sheard, 1981).

Measures which reduce the heating requirement of a greenhouse include:

a) **Self-evident measures:** The grower may delay planting or lower the heating set point of the greenhouse. Such measures however may cause reduced and later yields (Hurd and Sheard, 1981). Other options include converting to a more economic heating system, insulating heating pipe work, checking thermostats regularly for proper operation, using reflectors behind pipe work, regularly checking flue gas temperature and carbon dioxide to maintain combustion efficiency, and constant monitoring of temperature levels (Hurd and Sheard, 1981; and Winspear, 1978).

b) **Greenhouse shape:** Since heat loss is directly proportional to surface area, greenhouse geometry has a marked affect on heat loss. Small houses and houses

rectangular in plan have relatively large surface to plan area ratios. Large houses domical in shape minimize heat loss. Paraboloid is the next best shape followed by square (Burit et al, 1978).

c) **Shelter:** The rate of heat loss from a glasshouse is given by:

$$H = U(T_i - T_o)$$

where H = rate of heat loss (Wm^{-2})
U = the overall heat loss coefficient for the glasshouse ($Wm^{-2}\,^{\circ}C^{-1}$)
T_i = air temperature inside the glasshouse ($^{\circ}C$)
T_o = air temperature outside the glasshouse ($^{\circ}C$)

(Burit et al, 1978)

Sheard (1978) investigated the effects of wind on greenhouse heat loss and came up with the following U-value relationships:

Glasshouses	$U = 4.04 + 0.65W$
Single skin plastic	$U = 4.76 + 0.52W$
Inflated two skin plastic	$U = 4.06 + 0.25W$

where W = wind speed (ms^{-1})

It follows that the heat loss of an exposed greenhouse is reduced be installing suitable windbreaks.

d) **Alternative or renewable heat sources:** Solar storage, geothermal energy sources, and waste heat recovery are possible approaches for achieving resilience to conventional fuel pricing and availability (Breuer 1985a).

Internationally, solar heat storage has been shown to reduce annual energy consumption by 5-20% (Breuer, 1985a). Bellamy and Ward (1984) examined the

application of solar storage to New Zealand greenhouses and concluded that an attractive option was solar storage coupled with heat pumps.

Geothermal energy is a New Zealand resource which is well suited to greenhouse heating (Breuer 1985a). In general most geothermal bores produce water at 90-150°C. Although its use has been long-standing for water and space heating in the Taupo-Rotorua region, geothermal energy is now used to heat a number of commercial greenhouses in this region.

The use of recovered waste heat is an economic heating method. Many industries recover heat for internal re-use, but cannot easily accommodate an ancillary industry. Power generation stations however, provide an ideal host since land is often available in their buffer zone. More than half of the energy generated by a thermal power station is rejected as low grade heat in the condenser cooling water. Internationally most stations have large flows of cooling water available at temperatures from 22-80°C. In this country cooling water seldom exceeds ambient by 15°C. This combined with our mild climate highlights technical and economic shortcomings (Breuer, 1985a).

e) **Increasing thermal resistance:** Increasing the thermal resistance of a greenhouse reduces heat loss. The resistance must be increased in a controlled manner so that transmission of solar radiation is not impeded (White, 1980). Increased thermal resistance is achieved by reducing air leakage, layering the cladding, or installing a thermal screen.

Air leakage is a significant heat loss mechanisms in New Zealand greenhouses. Air leakage rates as high as 4 air changes per hour are not atypical (Breuer, 1985a). Up to 12% of the total heat loss may arise from air leakage (Burit et al, 1978). Mending torn plastic, erecting wind breaks, sealing glass laps with transparent adhesive sealing compounds, and restricting leakage around loose fitting doors and vents, are management strategies for reducing air leakage. Fuel saving from lap sealing alone range from 5% to 30%, depending on the original condition of the

roof (Breuer, 1985a).

The use of twin covering materials offer energy savings of up to 40% (White, 1980; Winspear, 1978). Benefits are often offset by the loss in revenue from delayed or reduced cropping caused by light loss (Winspear, 1978). With the exception of shade-loving ornamental plants the benefits of twin-skinning are often not justified (White, 1980). Tests in New Zealand (Levin) show a 15% reduction in annual fuel consumption with minimal effects on greenhouse lighting and yields when a clear polyethylene sheet is attached to the interior end and side walls of a greenhouse. Attaching clear polyethylene to the ceiling gives a 24% reduction in annual heating but a 10% light transmission reduction (Breuer, 1985b).

The thermal screen; also known as thermal curtain, night curtain, thermal blanket or internal blind, is a relatively new technology aimed at increasing the thermal resistance of a greenhouse. The screen system consists of a flexible material constructed and supported so that it completely encloses the crop and heating system at night. The thermal screen is movable to enable storage during the day. The thermal effectiveness of a screen is related to the type of greenhouse used, the screen material, outside weather conditions, the way it is mechanised, the ratio of covered crop volume to unheated above screen volume, and the air tightness of the screen (Breuer, 1985b).

As 70-80% of the total heat loss occures at night, more is gained by insulating at night (Breuer, 1985b).

1.2 STATEMENT OF THE PROBLEM

Nocturnal heat loss is a problem facing many greenhouse growers. Although thermal screens are an accepted panacea in Europe, the United States, and Japan (Breuer, 1985b), their use has met much grower scepticism in New Zealand. As a rule New Zealand growers are reluctant to change from traditional practice until

they have clear evidence of improved returns. Many continue to use relatively inefficient heating systems as they are not convinced the returns from thermal screens justify their installation. Unfortunately the environmental and economic conditions faced here prevent the application of overseas findings. At present thermal screen research in this country is sparse. As a result controversy over their economic effectiveness and the severity of their drawbacks limits widespread adoption. Under such conditions of uncertainty growers choose to minimise risk through inaction.

In short, as growers can not afford to experiment with new technologies, the heat saving potential of thermal screens in New Zealand will continue unnoticed unless research by a recognised institution for New Zealand conditions eventuates.

Conducting a real-life investigation of thermal screens in an actual greenhouse is both costly and time consuming. By modelling the greenhouse environment mathematically a large number of greenhouse, screen, and climate combinations can be simulated and evaluated without fitting screens to a actual greenhouses and running numerous trials. With this in mind a research programme was proposed aimed at developing a mathematical model to investigate the economic feasibility of thermal screens in New Zealand.

1.3 SCOPE OF THE STUDY

The economic feasibility of sixty two greenhouse and thermal screen combinations were assessed by performing an internal rate of return (IRR) analysis on thirteen materials with thermal screen potential within four different greenhouses. The greenhouses investigated were:

1. A small glasshouse ($300m^2$)
2. A large glasshouse ($1000m^2$)
3. A large single skin *Agphane* house ($1000m^2$)
4. A large double skin *Agphane* house ($1000m^2$)

Agphane is an ethylene vinyl acetate (EVA) film. In New Zealand EVA films are commonly used to cover greenhouses. In this study *Agphane* was assumed to be representative of EVA materials in general.

The screen materials investigated were:

1. ***LS 13***
2. ***LS 15***
3. ***LS 18***
4. ***LS 18F***

(narrow strips of polyester and aluminised polyester sewn together in varying ratios)

5. ***Marix*** (spun bonded polyester fabric)
6. **Clear Polythene** (125μm)
7. **Black Polythene** (125μm)
8. ***Infrane X 30*** (a 80μm single layer extrusion of infra-red absorbing Polythene, commonly known as *Infrane*)
9. ***Infrasol*** (a 150μm three layer co-extrusion of infra-red absorbing Polythene, containing antifogging agents, antistatic additives, and ultra-violet stabilizers)
10. ***Durafilm*** (a 150μm EVA containing slip additives, condensation inhibitors, and a HALS ultra-violet stabilizer)
11. ***Duratherm*** (a 150μm EVA containing a CIL antifog agent)
12. ***Hyerlyte*** (400μm, Polyvinyl chloride)
13. ***Agphane*** (150μm EVA)

Each combination was analysed for Auckland and Christchurch climates, since the majority of greenhouses are in this region, at heating set points of 15°C and 20°C. Economic analysis was based solely on the fuel savings achieved when diesel, electricity, coal, natural gas and L.P.G. were used as heating fuels. The analysis did not make allowance for the value thermal screens have as shade cloth or photoperiod control. Nor did it penalise combinations based on practical problems associated with humidity buildup beneath impermeable screens.

Screen life expectancy was taken from manufacturers' data. It was assumed that the strength and durability of the material and its support system enabled it to fulfil its role throughout this period.

CHAPTER II

LITERATURE REVIEW

The first application of moveable screens in greenhouses was with year round production of chrysanthemums (Bailey, 1978a). Chrysanthemums are one of the most commonly grown plants exhibiting a response known as photoperiodism whereby flower development depends on the relative length of day and night periods. In its natural state the chrysanthemum flowers when days are short and nights are long. When natural day length is too long for bud development, short day length is simulated by drawing a blackout screen over the plants at dawn and dusk. Early experiments by Bailey and Winspear (1975) in England assessed the effect of such blinds on heat consumption in a large glasshouse. They found fuel savings of 38% when wind speed was $2ms^{-1}$. Further experiments were run with equally encouraging results.

It was soon apparent (Winspear, 1977) that considerable savings could be achieved with photoperiod blinds (blackout covers). However, as these systems were designed to be opaque to light (ie. short wave radiation in the 0.3-0.7μm range) rather than opaque to long wave radiation (2.5-100μm) they could hardly be called 'thermal screens'. To be a thermal screen a more appropriate material would have to be operated primarily as a nocturnal, thermal radiation barrier (Winspear, 1977).

Thermal screens have been investigated and used extensively throughout the world. To date the majority of research has been conducted in Europe, Japan and the

United States. In 1972, researches at the National Institute of Agricultural Engineering (England) began an investigation of fuel saving possibilities of thermal screens. They found that a black polythene thermal screen reduced the night-time heat requirement in a commercial glasshouse by 35 %; resulting in an overall annual saving of 20 % (Dawson and Winspear, 1976). Europe's work in thermal screens has by in large been in application to the glass type greenhouse. Japanese work has been primarily related to glass and Polyvinyl chloride, and work in the United States (Rutgers, Penn State, and Cornell Universities) has been aimed at glass and polythene (Breuer, 1985a).

Subsequent research led to the development of aluminised plastic materials which reduce night-time energy consumption by up to 60 % (Bailey, 1978a).

The efficacy of a thermal screen depends largely on its ability to reduce heat transfer from a greenhouse. A literature review of thermal screens is therefore incomplete without a brief mention of the nature of heat movement within a greenhouse. The three modes of heat transfer are discussed in Appendix 1.

2.1 HEAT MOVEMENT IN GREENHOUSES

During the day solar energy is absorbed by the floor, crop, cover and any other opaque surface within the greenhouse. The layer of air immediately in contact with these surfaces is warmed by conduction and carried to the roof by convective air currents. When outside air is cooler than inside air, heat conducts through the covering material to the roofs outer surface. From here heat is carried away by outside convection currents or lost as cover radiance. Convective loss increases with wind speed. Cloud cover and atmospheric water vapour influence the cover's radiative heat loss.

When liquid water evaporates from the soil or crop, latent heat is absorbed by the water molecules escaping from the liquid surface. Air movment over the floor, or

crop, picks up this 'energy laden' vapour and carries it to the roof. If the roof temperature is below dew point, condensation will form on the underside of the roof releasing latent heat in the process. The cover material conducts this heat through to its outer surface where once again it is lost as convection and radiation. Since absolute humidity within a greenhouse is usually higher than that outside, when air is exchanged by ventilation or infiltration, water vapour and hence energy is lost.

The floor, crop and cover all give off long wave radiation. At night the roof receives radiation from the floor and the crop and radiates energy to the cold sky. As the floor and crop are similar in temperature the net radiation exchange between these two is relatively small.

Greenhouse plastic films, especially polyethylene, are transparent to long wave radiation. Warm surfaces within the house can therefore 'see' straight through the cover to the cold sky. This may cause significant radiation loss from the crop and floor to the sky. Glass on the other hand is opaque to the long wave radiation. Crop and floor radiation can therefore only 'see' the glass roof. Radiative heat loss is therefore reduced.

Figures 2.1 and 2.2 summarise the main heat transfers in a screened and non-screened greenhouse at night. Note that radiative heat loss has been reduced by installing a screen. Thermal screens also reduce the volume of house air being heated. For this reason screens are more effective in large span houses or when pulled from gutter to gutter rather than from gutter to ridge (Badger and Poole, 1979).

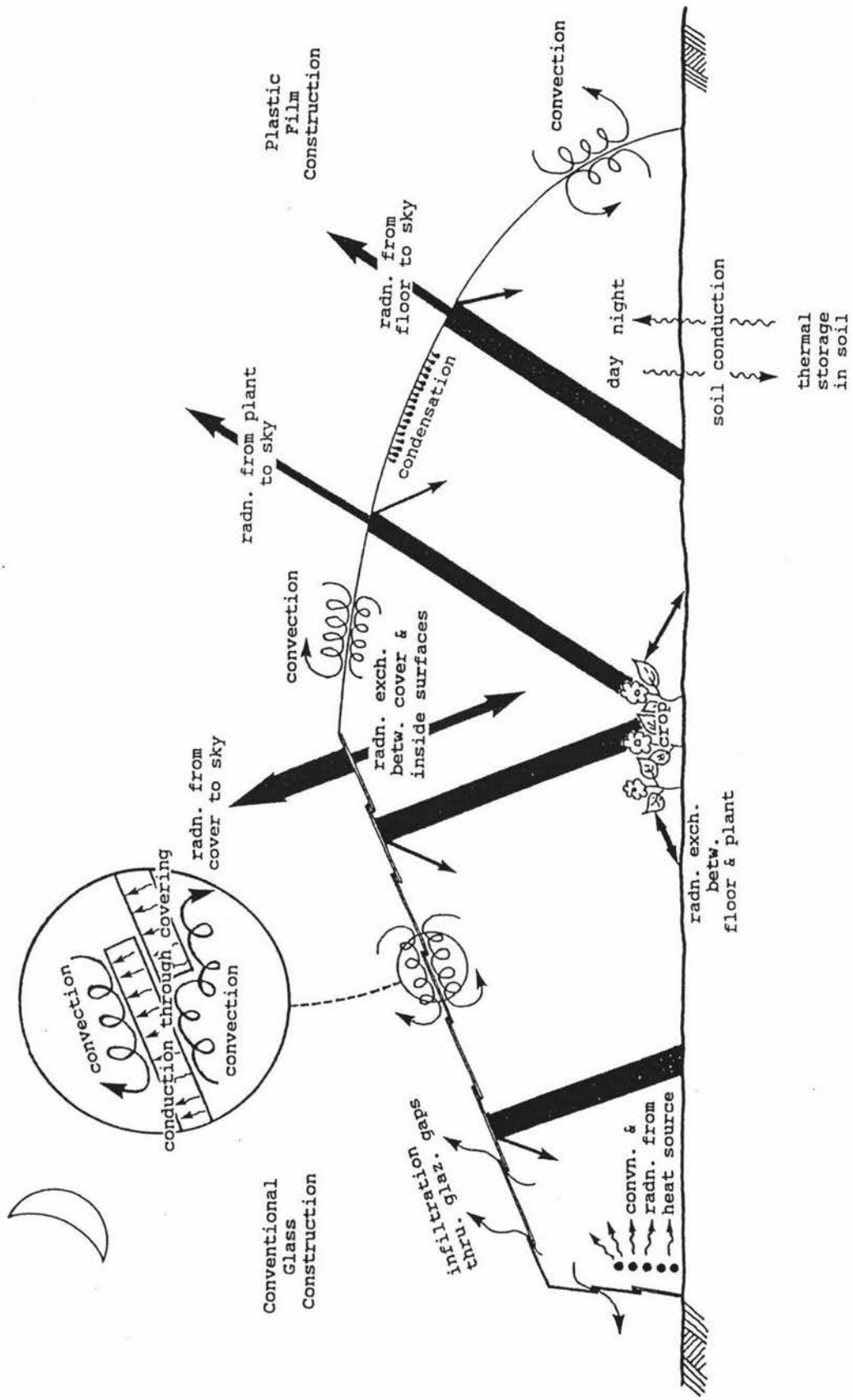

Figure 2.1 **Heat transfers of a screenless greenhouse at night.**

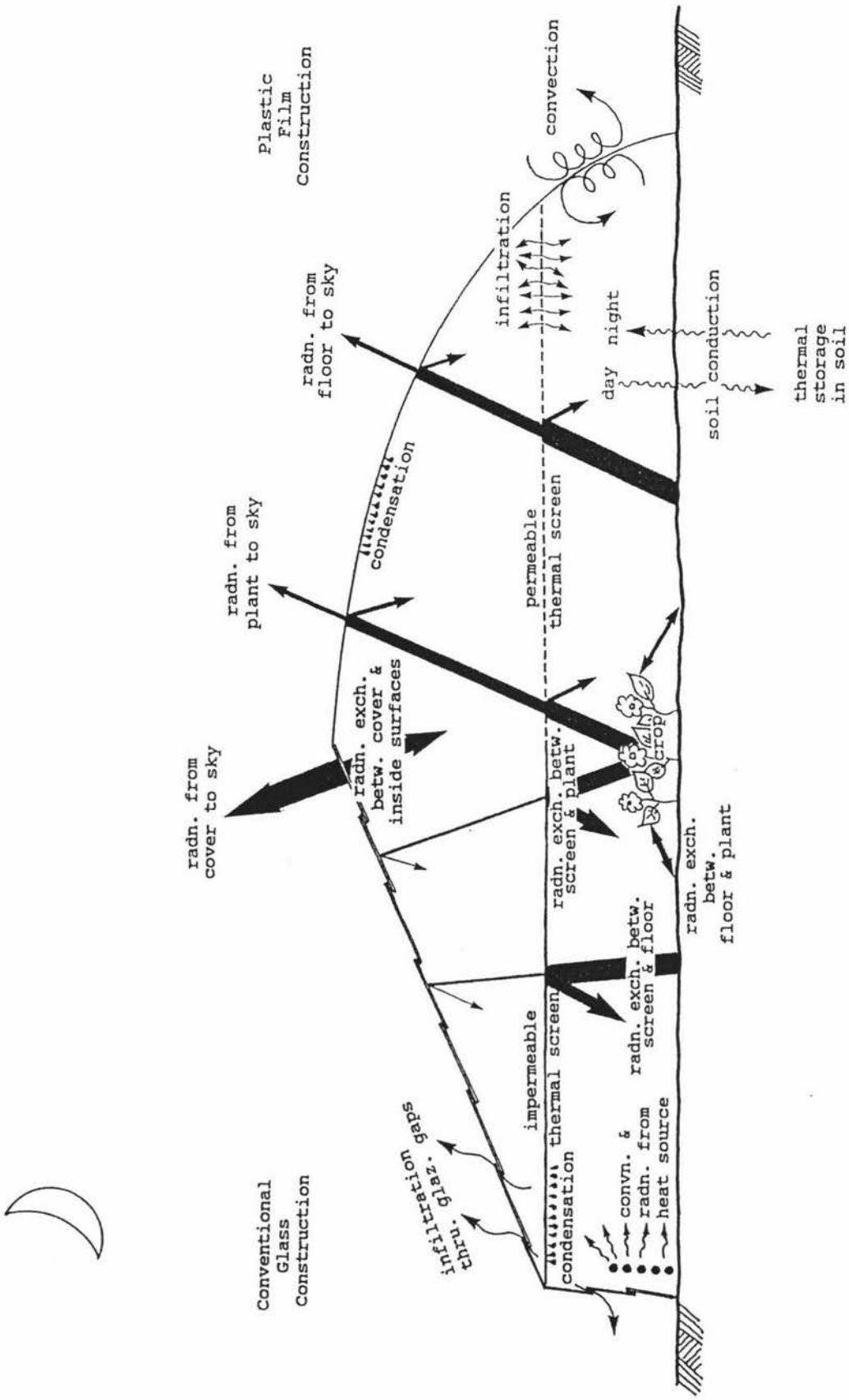

Figure 2.2 Heat transfers of a screened greenhouse at night.

2.2 SCREENING MATERIALS

The first thermal screen materials; polyethylene, polypropylene, polyester and acrylic, were superseded by materials with superior long wave reflectivity and emissivity such as silver coated and aluminised screens (Bailey, 1978a). Polyvinyl chloride and ethylene vinyl acetate type materials are also available (Breuer, 1985b).

2.2.1 POLYETHYLENE

Polyethylene (PE) is the most widely used greenhouse plastic film covering in New Zealand and goes by the accepted common name polythene. As its name indicates, the material is a homopolymer of many ethylene units. The ethylene units are joined in a chain-like manner forming a long molecule. The number of units per molecule, the degree of cross linking between chains, and the presence of ultra-violet (UV) stabilisers, determine the physical characteristics of PE (White, 1984).

PE is produced in two forms, low density for film extrusion and high density for fibre production. The mechanical properties of PE depend on its density. As density increases so too does tensile strength, stiffness and brittleness. Tear strength and flex life decrease (Bailey, 1978a).

PE is subject to photodegradation and stress cracking by the blue to UV range of wavelengths in sunlight which possess enough energy to break the polymer bonds (Breuer, 1985b). Initial breakdown can be followed by a chain reaction within the film. Deterioration of PE film is evident as loss of flexibility and stretch, increased brittleness, and discolouration (White, 1984). Photodegradation is slowed by incorporating retardant compounds (stabilisers) into the film resin during manufacture. These stabilisers absorb the injurious radiation in a thin surface layer and convert it to heat, thus protecting the bulk of the material (Breuer, 1985b).

PE does not absorb water nor is it permeable to water vapour. Films of PE can be joined readily by welding at 115-120°C (Bailey, 1978a).

2.2.2 POLYPROPYLENE

This is similar to high density PE but has higher tensile strength, greater stiffness (Bailey, 1978a), and less permeability to air (Breuer,1985b). It is more affected by heat and UV than PE. UV stabilisers are used to reduce the rate of degradation. The fibres have high tenacity and good resistance to abrasion (Bailey, 1978a).

2.2.3 POLYESTER

Polyester is the generic name given to polymers which use an ester to form the links in the polymer chain; individual polyesters are known by the manufacturers' trade name for example, *Terylene*, *LS 56*, *Reemay 2016*, and *Floratex 80.* The common polyesters are made from ethyl glycol and terephthalic acid. Polyesters have greater resistance to UV than PE, and are light weight. Although they absorb small amounts of water, their properties are not affected by wetting. The fibres are elastic and have good abrasion resistance. The films have high tensile strength but low tear strength (Bailey, 1978a).

2.2.4 ACRYLIC

Acrylic is the generic name given to fibres which contain more than 85% acrylonitrile. They have very high resistance to degradation by UV and heat, and age slowly.

The fibres are strong, elastic and have good abrasion resistance. Water absorption is higher than that of polyesters but the properties are unaffected by wetting.

Although acrylics are flammable, using burn resistant modacrylic fibres which contain between 35-85% acrytonitrite alleviate this problem.

2.2.5 ETHYLENE VINYL ACETATE

As a greenhouse film PE has been generally supplanted by a copolymer derivative manufactured by enriching a PE resin with vinyl acetate (VA). The resulting copolymer, polyethylene vinyl acetate, is commonly called ethylene vinyl acetate or EVA. The VA content in EVA films ranges between 5-40% (Dartiguepeyrou, 1986). Characteristics of EVA films depend on the proportions of VA in the copolymer as well as the properties of the PE and UV stabilises in the film (White, 1984). Increasing levels of VA lower the film's long wave transmission, increase compatibility with mineral fillers and enhance resistance to splitting (Dartiguepeyrou, 1986). EVA films become more elastic as the VA component increases. Such films have low tensile strength and are therefore hard to tension during greenhouse construction (Wells, 1989b). Increasing VA levels also reduce permeability to gases and resistance to stretching (Dartiguepeyrou, 1986).

2.2.6 POLYVINYL CHLORIDE

Polyvinyl chloride (PVC) also suffers from light induced breakdown. It is less subject to oxidative breakdown than PE but more subject to thermal breakdown. PVC greenhouse films contain plasticisers (to render pliablity), UV absorbers and heat stabilisers (White, 1984).

2.2.7 ALUMINIUM

Pure aluminium is used in the construction of some thermal screen materials. When used as a screen constituent the aluminium is usually laminated to a thin

plastic film through a vacuum deposition process (see Figure 2.3). The aluminium is sometimes coated with a lacquer to reduce oxidation and attack by water (Bailey, 1979a).

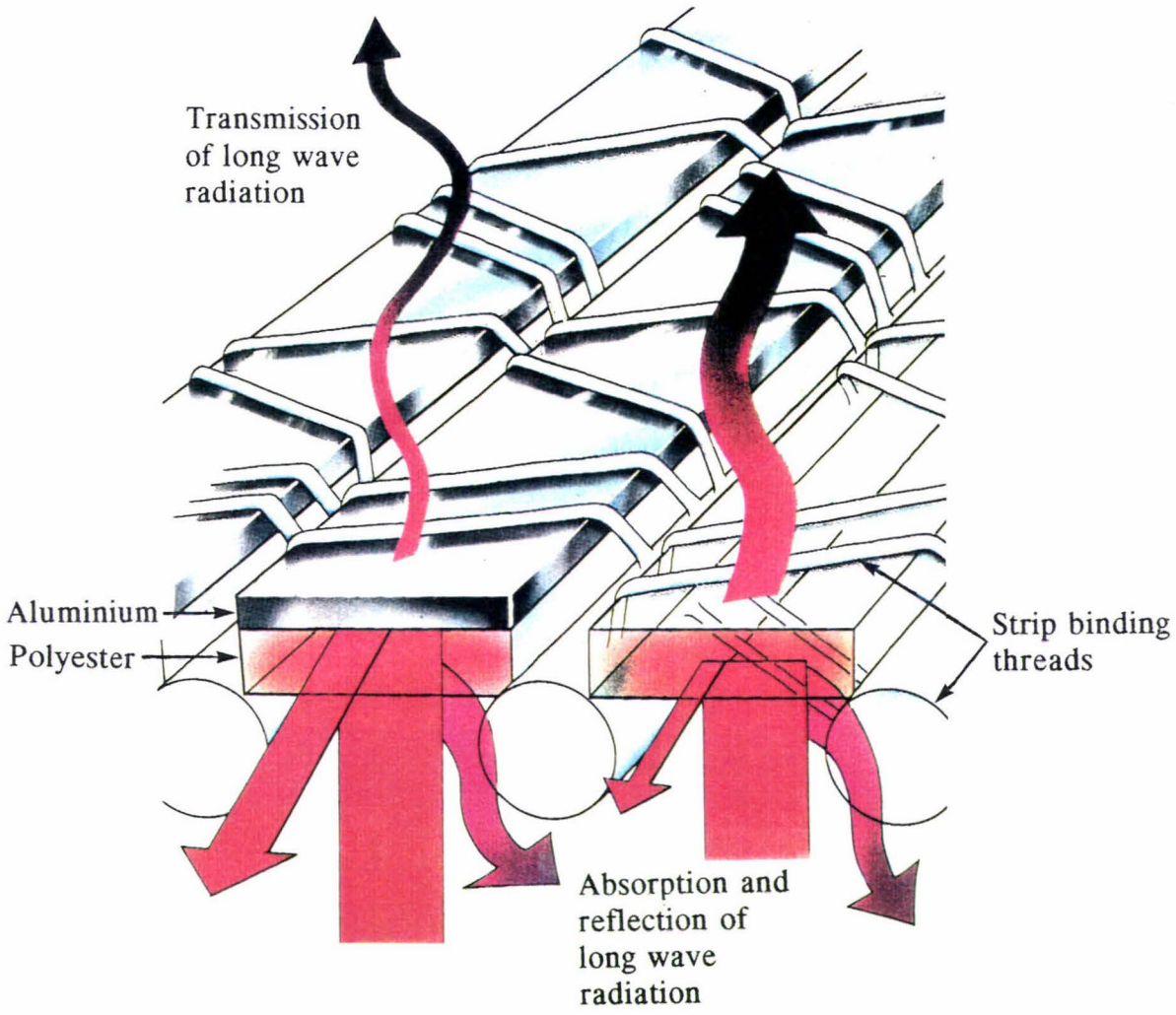

Figure 2.3 **Strip structure of an aluminised polyester Ludvig Svensson screen. (Ludvig Svensson International, 1989).**

2.3 MATERIAL CONSTRUCTION

The screen constituents outlined above can be produced as fibres and, with the exception of acrylic, films.

2.3.1 FILM

Continuous polymer films are produced by extrusion. In this process molten resin of the polymer is forced through an annular die causing an air inflated flowing bubble. Once cooled in air the long continuous tube of film is slit to form the normal flat film (White, 1984). The films usually encounted in horticulture vary between 25μm and 400μm in thickness (Bailey, 1978a). Film width in New Zealand varies between 1.2 and 6m. Overseas, extruders produce films up to 20m in width (White, 1985).

Ludvig Svensson, a Swedish greenhouse screen manufacturer, have developed a series of screens suitable for thermal screening. They are constructed from narrow strips of polyester and aluminised polyester, at varying ratios, all running in one direction (Figure 2.3 and Plate 2.1)

2.3.2 FIBRE

Fibre may be used to produce three types of fabric, woven, non woven and knitted (Wells, 1990a).

2.3.2.1 Woven Fabric

Weaving is the traditional way of producing fabrics in which two sets of fibres are inter-woven at right angles. The manner in which the two sets are interlaced affects the characteristics of the fabric. A closely woven fabric will have low permeability while a fabric with loose weave will readily permit the passage of air (Bailey, 1978a).

2.3.2.2 Non-woven Fabric

Non-woven fabrics can be produced using either continuous lengths of fibre (continuous filament) or short lengths (staple). Continuous filament fabrics are made from thin flat webs containing a random arrangement of fibres which,

because of their lack of cohesion, are bonded immediately after formation (spun bonded). The web of a staple fabric consists of carded fibres. Bonding can be achieved by an adhesive which is cured by heating. A method developed by ICI uses bi-component fibres in which the two components are arranged as a core and sheath or spun side by side. The process of making these bi-component fibres into fabrics is known as melding (melting and welding). Fabrics made from staple can be produced in a variety of thicknesses. They are more flexible than continuous filament fabrics, but are generally not as strong. As with woven fabrics these non-woven fabrics are permeable (Bailey, 1978c).

2.3.2.3 Knitted Fabric

The fibres of knitted fabric are bound to each other by a knitting process. The elasticity of knitted fabric is superior to woven fabric (Wells, 1989b).

2.4 SCREEN PROPERTIES

The properties of thermal screen materials depend partly on their constituents and partly on their physical construction (Bailey, 1978a). Screen properties may be categorised into:

- Flexibility
- Durability and life expectancy
- Long wave transmission
- Permeability

2.4.1 FLEXIBILITY

Flexibility enables the screen to be furled or folded into a small parked bundle, minimising crop shading during the day (Bailey, 1978a). Plate 2.2 shows an

aluminised Ludvig Svensson screen in a parked (withdrawn) position.

Jensen (1977) states the major problem with internal screens, especially in small greenhouses, is screen storage when open. This may result in crop shading problems and inconvenience for personnel movement.

Hurd and Sheard (1981) state crop shading is an unfortunate feature of present generation thermal screens. Light losses of 5-10% have been recorded beneath parked screens; corresponding to yield losses of similar magnitude. Light losses are minimised by parking screens beneath roof trusses (Figure 2.4).

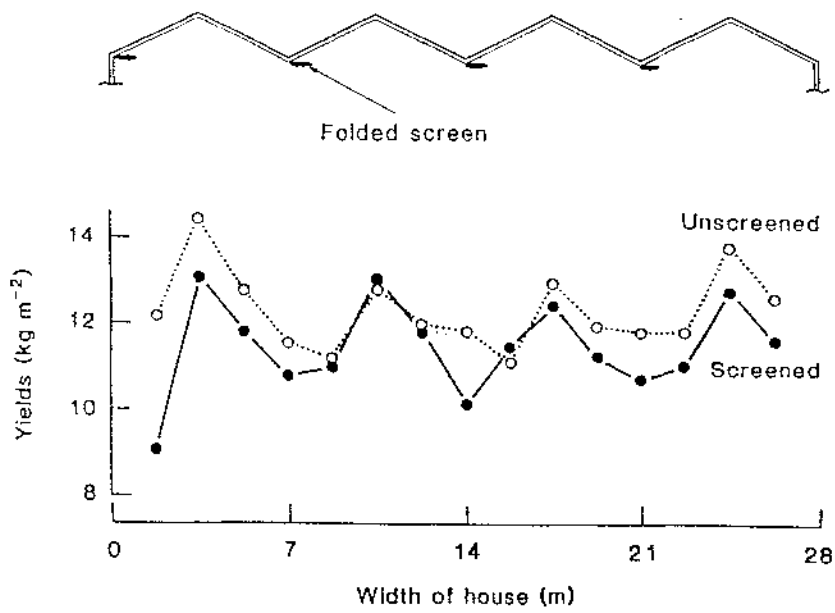

Figure 2.4 **Tomato yields across a screened and unscreened house (Hurd and Sheard, 1981).**

Hoeflak (1990) claims that light losses are less than 5% for some modern installations in New Zealand.

2.4.2 DURABILITY AND LIFE EXPECTANCY

An important consideration when selecting a screening material is life expectancy. A material with reasonable life is attractive in light of replacement cost. Unfortunately, since many of the materials are relatively new, little is known of their durability (Bailey, 1978b).

The method of suspending the screen is one factor influencing its life. Wear and tear and mechanical damage can ruin a screen long before any aging effect. To prolong screen life, friction between the material and supporting wires must be minimised. This can be done by coating wires with plastic or by fixing the screen to moveable pulleys, suspended on racks (Bailey, 1978b).

The other major factor influencing screen life is polymer degradation by UV light. Glass roofs prevent the entry of UV light. The life of UV sensitive screens is therefore enhanced when beneath glass. Plastic houses however are transparent to UV. As a result they offer less protection to UV sensitive screens (Bailey, 1978b). Open ventilation promotes deterioration as it allows direct UV to reach the screen (Meinders et al, 1984). Sometimes screen materials age faster at certain spots for instance at girders and trailing tubes, as they are heated by the sun (Meinders et al, 1984).

In England, thermal screens composed of clear polythene, not UV stabilised, have to be replaced annually (Sturrock, 1981). Four years satisfactory service have been obtained in England for dense black polythene photoperiod control screens (Bailey, 1978b).

Knowning the effects of sunlight on various polymers, Bailey (1978b) ranked the following screens in order of increasing stability: polypropylene, polyethylene, polyester and acrylic. If the material's surface is coated with aluminium, resistance to UV degradation is increased. Aluminised polyester screens developed by Ludwig Svensson, available in New Zealand, come with a world wide five year warrantee. The economic life of Ludwig Svensson screens in New Zealand is up

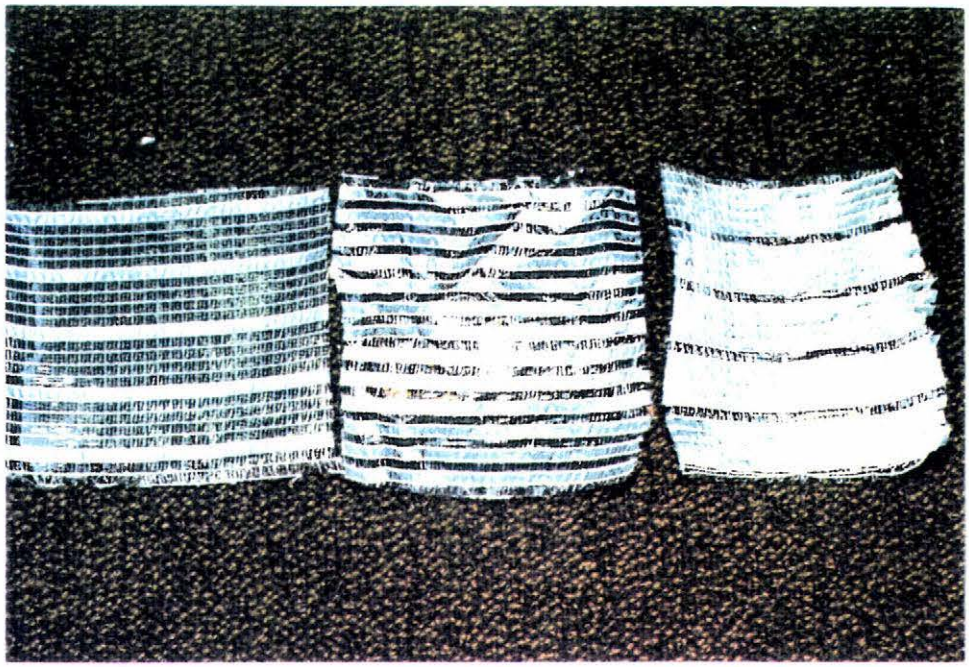

Plate 2.1 Three aluminised polyester materials. From left to right: *LS 13*, *LS 15*, and *LS 18*

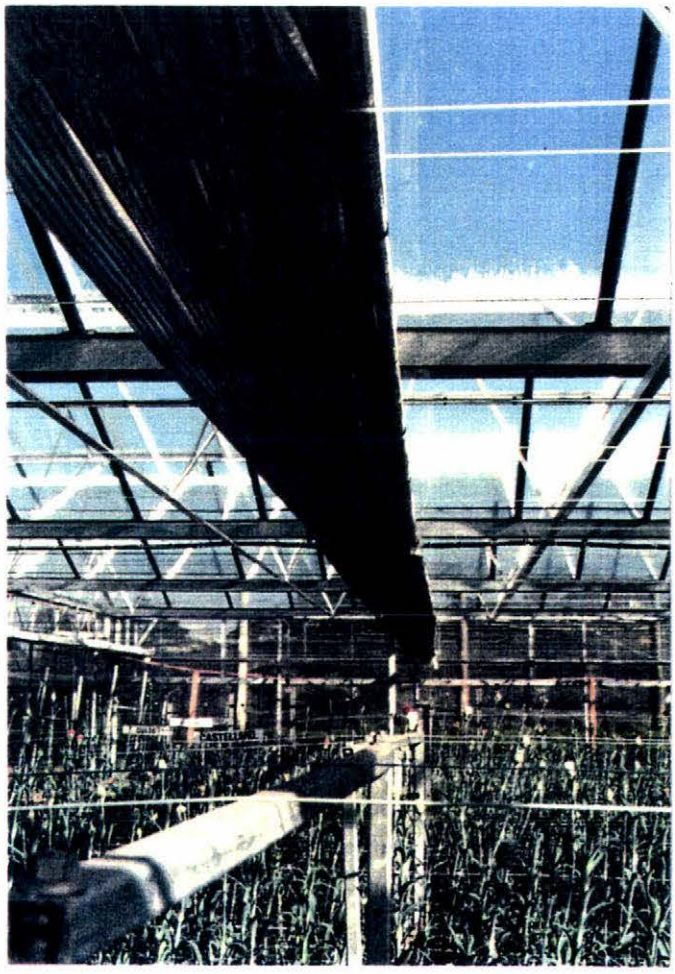

Plate 2.2 Aluminised Ludvig Svensson screen in parked position

to nine years (Hoeflak, 1990). Table 2.1 gives the economic life of some of the more common screening materials.

Table 2.1 Economic life in years of selected thermal screen materials (Meinders et al, 1984).

Form	Material	Name or Type	Economic Life
Film	PE	Transparent	1.5
	PE	Black	4
	PE + VA additive	EVA (18% VA)	1.5
Film-strip	Polyester	*LS 12*	5
		LS 15	5
Knitted	Polyester	Terylene *LS 56*	4.5
		Terylene *LS 100*	5
Spun bonded	Polyester	*Reemay 2016*	5

The properties which enable the screen to fulfil its role should not change as the material ages (Bailey, 1978b). Bailey and Cotton (1977) report that some aluminised materials develop a crazed appearance with age and portions of aluminium may flake off. Sturrock (1981) reports that the life of aluminised screens are enhanced when coated with lacquer or another sheet of polythene. The effect rubbing had on the emissivity of three materials was investigated by Bailey (1981). The materials were abraded with a rough paper tissue; passing the paper 10 times over the surface constituted 'light abrasion', and 50 strokes constituted 'heavy abrasion' (Table 2.2). The lacquer protection on the lacquered aluminised polyester screen did not appear sufficient as the emissivity increased markedly. The spun bonded polyolefin was also adversely affected.

Table 2.2 Effect of abrasion on emissivity of aluminised screen materials (Bailey, 1981a).

Material	Surface	Abrasion		
		None	Light	Heavy
Lacquered aluminised PE	Aluminium	0.07	0.11	0.26
	PE	0.27	0.29	0.29
Lacquered aluminised polyester laminated to black PE	Aluminium	0.07	0.07	0.06
Spun bonded polyolefin aluminised/black	Aluminium	0.25	0.36	0.56

The screen material should withstand the effects of the greenhouse environment, not be affected by UV radiation, high temperature, high humidity, condensation, pesticides and fungicides, and have high resistance to abrasion (Bailey, 1978b).

2.4.3 LONG WAVE TRANSMISSION

Fuller et al (1984) state thermal screens reduce energy demand by:

(i) reducing losses by convection,
(ii) reducing latent heat losses associated with mass movement of water vapour from leaves to cover,
(iii) reducing the heated air volume, and
(iv) reducing long wave radiation losses.

(i), (ii) and (iii) can be achieved with virtually any impermeable screen material but to reduce long wave losses however, screens must be opaque to long wave radiation (τ=0). Complete opacity to long wave radiation prevents surfaces beneath the screen 'seeing' surfaces beyond the screen (a condition necessary for radiant heat transfer). Practical considerations determine whether or not the screen should be

highly reflective or highly absorptive to long wave radiation. It would seem logical (Badger and Poole, 1979) to install highly reflective screens with the reflectorised surface facing down to reflect all the radiation back to the crop. However, as good reflectors are poor absorbers if the reflectorised surface faced downward only a small fraction of the radiant energy would be absorbed. The screen would therefore stay cool increasing the liklihood of condensation on the screen (Arinze et al, 1986).

Condensation on the screen is undesirable for three reasons. Firstly it can fall onto the crop and reduce flower or fruit quality and create conditions favourable disease development. Secondly, the increased weight of a wet screen may make removal in the mornings difficult (Bailey, 1981a). Thirdly, when water vapour condenses on the screen latent energy is transferred to the screen. The air surrounding the crop has therefore lost latent heat (Winspear, 1977).

If a reflectorised surface faces out and a black surface faces in, the screen absorbs energy and stays warmer. This reduces condensation and run off problems. Radiation beyond the screen is minimised as the lowest emitting surface is exposed to the outside. Table 2.3 lists radiation properties of selected plastic and aluminised screen materials.

In Table 2.3 screens with a pure aluminised surface show the highest reflectivity ($\rho = 0.95$). Reflectivity decreases slightly when the aluminium layer is protected by a thin layer of lacquer, (0.80-0.93), but markedly (0.43) when protected by a polyester film. A material containing aluminium powder between films of clear polyethylene (*Silver Polyto*) has a low reflectivity of 0.21, this is attributed to the diffuse nature of the aluminium/polyethylene interface. All materials that contain aluminium (except *Silver Polyto*) have zero long wave transmission.

Plate 2.1 shows three unlacquered, aluminised polyester screen material available on the New Zealand market. Figure 2.3 illustrates how long wave radiation is retained by Ludvig Svensson screens.

Table 2.3 Long wave properties of selected screen and cover materials.

Material	Surface	τ	ϵ	ρ	Ref.
Black PE (150μm)		0.15	0.40	0.45	1
Clear PE (100μm)		0.70-0.77	0.05-0.28	0.02-0.20	1,2&4
IR stabilised clear PE (200μm)		0.43	0.54	0.03	2
Infrane X30		0.35	0.45	0.20	1
PVC (100μm)		0.24-0.33	0.64-0.71	0.05-0.12	3&4
EVA		0.38-0.64	0.33-0.58	0.02-0.03	2&4
Polypropylene		0.50	0.45	0.05	4
Polyester (100μm)		0.76	0.13	0.11	3
Reemay 2016 (white spun bonded polyester)		0.20-0.31	0.60-0.70	0.10-0.09	5&6
Aluminium (Al) film		0	0.04	0.96	2
Lacquered aluminised PE	Lacquered Al	0	0.20	0.80	7
	Clear PE	0	0.34	0.66	
Polyester aluminised on both surfaces (unlacquered)		0	0.05	0.95	8
Polyester aluminised on one side (lacquered)	Lacquered Al	0	0.07	0.93	8
	Polyester	0	0.57	0.43	
Lacquered Al polyester laminated to clear PE	Lacquered Al	0	0.08-0.16	0.84-0.92	7&8
	Clear PE	0	0.46-0.48	0.52-0.54	
Lacquered Al polyester laminated to black PE	Lacquered Al	0	0.07	0.93	9
	Black PE	0	0.91	0.09	
Silver Polyto		0.10	0.73	0.29	8
Polycarbonate		0	0.91	0.09	4
Glass		0	0.90	0.10	2

Table references:

1. Badger and Poole, 1979
2. Tantau, 1981
3. Horiguchie et al, 1982
4. Nijskens et al, 1984
5. Bailey, 1978b
6. Breuer, 1985a
7. Bailey and Cotton, 1977
8. Bailey, 1981a
9. Bailey and Cotton, 1980

2.4.4 PERMEABILITY

One of the modes of heat loss from a greenhouse is infiltration (air leakage). Another is convection of heat from the crop zone to the cover. Large reductions in air movement are possible if impermeable thermal screens are installed and sealed without gaps around their periphery. However, reduced air movement increases relative humidity which in turn raises the likelihood of condensation.

A high humidity environment is an ideal breeding ground for the myriad of fungal diseases plaguing the greenhouse grower. Trials on a commercial scale in England have shown that humidity under a screen increases as the plants mature, reaching 100% when fully grown. This is concerning as research shows the incidence of *Cladosporium fulvum* and *Botrytis cinerea* increase markedly as relative humidity approaches 100% (Bailey, 1978c).

In a non-screened glasshouse, water vapour condenses on the inner surface of the glass; this prevents the dew point of the glasshouse air from exceeding the glass temperature by more than 1 or 2°C and consequently imposes a limit on the absolute humidity of the glasshouse air. When the greenhouse contains a thermal screen the house dew point climbs because crop air is no longer in direct contact with the cold glass. Consequently the restraints on absolute humidity relax and the

relative humidity beneath the screen increases. If the dew point of the air beneath the screen rises much above the screen temperature condensation forms on the underside of the screen. This has been noticed with polythene thermal screens over cucumber crops. The added weight of water prevented operation of the screen (Bailey 1978c).

If a screen permits the exchange of air, condensation on the glass (which is colder than the screen) exerts a controlling influence on the humidity beneath the screen; the final humidity would depend on the rate of air exchange (Bailey, 1978c).

A convenient way of allowing the mixing of air above and below a thermal screen is to use a permeable screen. Air movement through a permeable screen occurs as a result of air temperatures difference above and below the screen. Such a screen however is less effective at reducing the heat loss as convective transfers, both latent and sensible, are iscreased (Bailey, 1978c).

In the late 1970s semi-permeable screens were introduced into England. Although they saved less fuel they virtually eliminated condensation and humidity build-up beneath the drawn screen. In old leaky houses these screens also prevented the collection and ponding of rain, which can be damaging to the fabric. Permeable screens of woven fibres offer dual purpose shading and screening and the more recently introduced aluminised permeable screens combine high fuel savings with the advantages of the permeable types (Sturrock, 1981).

2.5 OPERATION

2.5.1 TOWING AND SUPPORT

Screens may be pulled gutter to gutter, gutter to ridge (not preferable), or truss to truss. In quonset-type greenhouses (tunnel houses) the screen may be pulled from end to end (Badger and Poole, 1979). Special attention to support members is

required in plastic tunnel houses as the tensioned support cables exert considerable force on the end walls. Bracing is necessary to prevent wall distortion (Hoeflak, 1990).

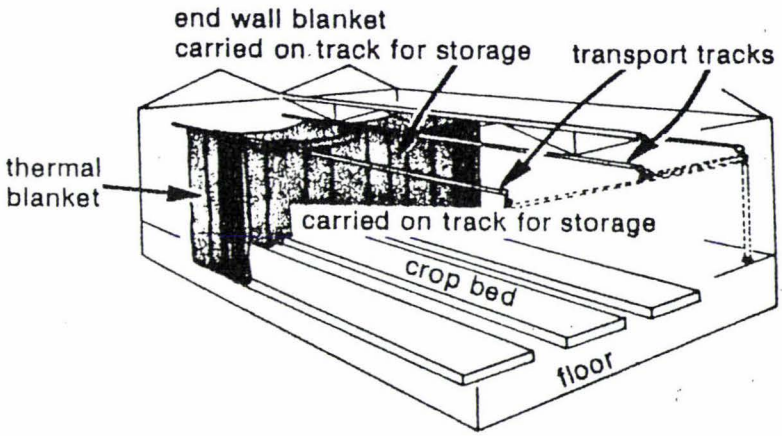

Figure 2.5 A track type thermal screen with side and end curtains (Badger and Poole, 1979).

Support for screens can be track, cable, wire or a combination of these (Breuer, 1985b). For long spans track is preferable as it distributes the load more evenly onto the greenhouse structure (Figure 2.5) The track is supported by hangers fixed to the roof structure (Badger and Poole, 1979).

According to Bailey (1978a) in the majority of houses, the screen rests on horizontal wires or cables, often called static lines, which span the house. One end of the screen is fixed to the house structure while the opposite end is attached to a wooden or metal tube approximately 40mm in diameter. It is important to have the tube lying true across the greenhouse (parallel to end walls) to prevent misalignment. A rigid member is required here to ensure that the screen travels back and forth in a straight line otherwise jamming may occur. The tube is drawn over static lines by cords attached to a rotating torque tube driven either manually or by a geared reversible electric motor (Plate 2.3). The torque tube may be of galvanised water pipe 50mm in diameter. Although not practised in New Zealand (Hoeflak, 1990), the ends of the house can be screened by extending the main

horizontal cover. The sides of the house may be screened using separate side covers, operated either by hand using a cord and pulley system, or coupled to the main operating system.

Plate 2.3 Reversible electric motor, torque tube, and cable support system.

To reduce air leakage past the screen the leading edges may be butted into foam rubber sealing strips when the screen is closed (Bailey, 1979a).

Figure 2.6 illustrates a system used in clear span freestanding greenhouses where crops are not supported from the trusswork. Individual small pulleys support the screen material on powered cables which are spaced 3-4m apart. Static lines between the drive cables also support the screen. The screen is normally stored in the south wall (in the southern hemisphere) to minimise shading. In wide houses, over 13m, the screen is drawn from each side toward the middle (Breuer, 1985b).

One of the problems associated with cable support systems, (Fuller et al, 1984), is the method of attachment to the moving cables and the fixed supporting wires.

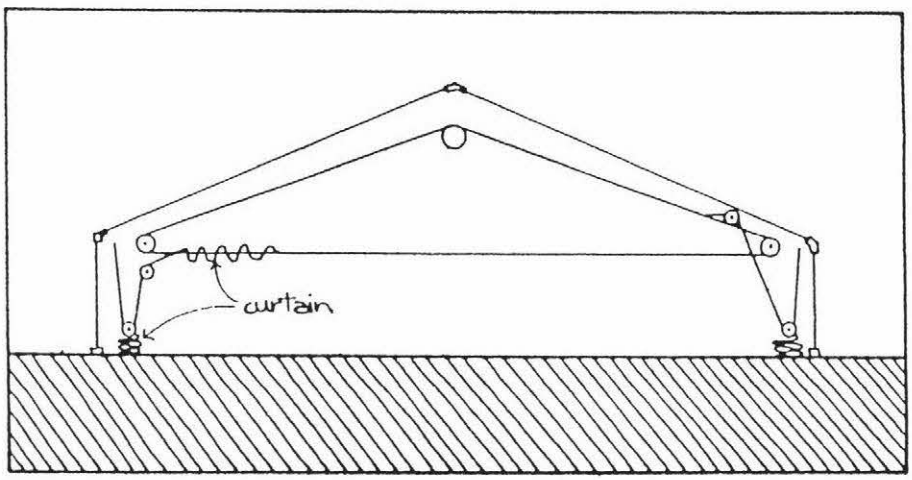

Figure 2.6 Curtain system for a clear span greenhouse (Breuer, 1985a).

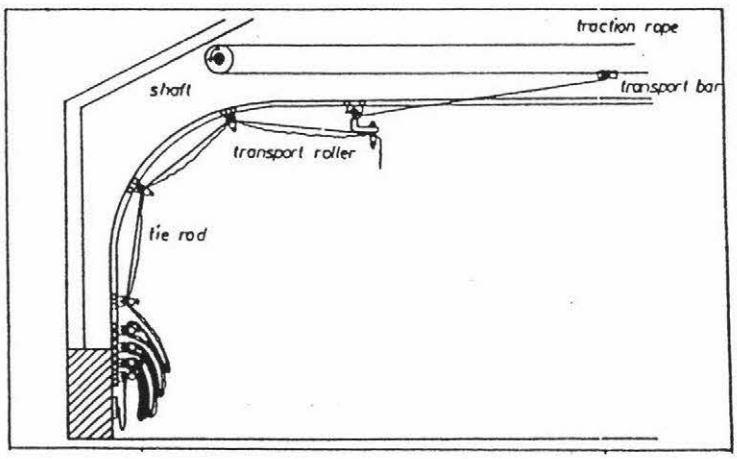

Figure 2.7 Details of the mechanical system (Meyer, 1981).

High stresses on the material at the point of attachment can lead to damage and a shortened life. Screen efficiency is affected if holes or tears appear in the material. An alternative method which reduces screen wear and lessens the force necessary to move the screen is to fix it to cable operated, moveable, low friction pulleys suspended from aluminium tracking (Figure 2.7).

2.5.2 CONTROL

Thermal screens may be opened and closed manually or automatically using an electric motor. The motor is usually coupled to a gearbox which reduces the shaft output of the motor to a workable speed of around 10 RPM. Limit switches are positioned in such a way to operate when the screen has reached the end of its travel.

The motor is initiated by signals coming from a time clock or a photo cell. With a time clock the screen would be opened at say 7:30am and drawn at say 5:30pm. With a photo cell the screen would open when light levels reached $30Wm^{-2}$ and drawn when they fell below $30Wm^{-2}$ in the evening (Marsh et al, 1984).

Seginer and Albright (1980) indicate that the savings due to a thermal screen increased approximately 6% when operated on a radiation level basis rather than by time clock. Special controls may be needed to automatically open the screen slowly in the morning to prevent cold shock. Automatic control however is not necessary. A manually operated system reduces capital cost significantly and eliminates the need for an electric motor, gearbox, time clocks and limit switches (Fuller et al, 1984).

A variety of defaults may also be built into the system (Albright, 1983). For example the curtain should not open and close repeatedly during intermittent sunshine nor should it open late in the morning or close early in the evening if light levels are erroneous.

2.6 EFFECTS IMPOSED BY THERMAL SCREENS

The fuel saving cababilities of thermal screens have been proven world wide (Table 2.4). Crop performance under screens however are highly variable. Although most ornamental foliage crops are not affected by screening, tomatoes, cucumbers and other vegetable crops, while occasionally yielding as well as unscreened crops, more often yield less. Crops harvested over a long period often show changed patterns of production. The advantage of fuel economy is sometimes outweighed by these disadvantages (Sturrock, 1981).

Table 2.4 Reported fuel savings by thermal screening.

Country	City or State	Fuel Saving (%) *	Ref.
England	Bedfordshire	35-50	1
Holland		25-80	2
Germany	Hanover	32-71	3
France		32-52	4
USA	New Jersey	22-58	5
	Pennsylvania	50	6
Australia	New South Wales	30-40	7
New Zealand	Christchurch	50	8

* The magnitude of the fuel saving depends on screen type, screen age, house type, house age, and wind speed.

Table references
1. Bailey, 1978c
2. Meinders et al, 1984
3. Tantau, 1981
4. Baille et al, 1985
5. Roberts et al, 1981
6. Rebuck et al, 1977
7. Fuller et al, 1984
8. Harford, 1990

2.6.1 LIGHT TRANSMISSION AND SHADING

Sturrock (1981) states that evaluation trials in Britain indicate shading from parked screens during the day can be held partly responsible for reduced tomato yields of 2-12%. There is evidence that some tomato cultivars do better under screens than others, for example Sonatine. In contrast to Sonatine some other cultivars have given small increases in early yields but reductions in total yield (Sturrock, 1981).

Dutch growers have experienced less setting and development of tomato fruit with screens. This has led to grower scepticism (Sturrock, 1981).

Bailey (1981a) investigated the shading effect of screens during the day with tomatoes, by measuring the transmission of photosynthetically active radiation (PAR) across the glasshouse. PAR sensors were mounted above the glasshouse ridge and within the house. The ratio of the two signals indicated the house transmittance. The variations in transmittance along identically located traverses in screened and non-screened multispan and single one span houses are shown in Figures 2.8a and 2.8b respectively.

The transmission maxima in the multispan non-screened house occurred beneath the roof trusses. On average the overall reduction in PAR transmission by the screened house was 3.0%. This was mainly due to the 80mm deep steel members placed under the gutters for support because the angle braces had to be removed to accommodate the screen. In the single span house the maximum reduction in light, of 17%, was recorded immediately beneath the parked screen. When averaged over the whole house however, the reduction was equivalent to 1.5%.

Work done by Grange and Hurd (1983) using solarimeters showed an initial reduction in light transmission of 11%, was reduced to 3% when an improved parking method was employed.

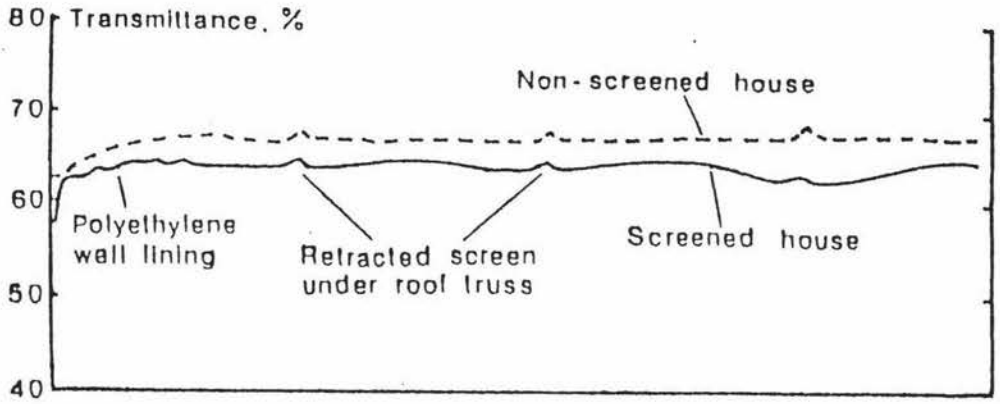

Figure 2.8a PAR transmission of a multi-span glasshouse (Bailey, 1981b).

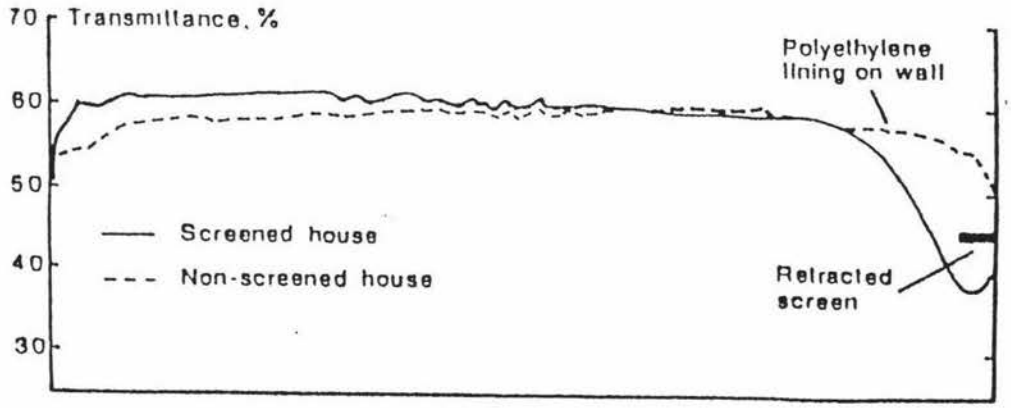

Figure 2.8b PAR transmission of a single span glasshouse (Bailey, 1981b).

2.6.2 LEAF TEMPERATURE

In a glasshouse, at night, the upper leaves of the crop lose energy by long wave radiation to the greenhouse cover or thermal screen (Bailey 1981c). As the temperature of the screen is higher than that of the cover, radiative heat loss from plants is less with a screen. This results in higher plant temperatures.

Using a radiation thermometer Bailey (1981c) measured the temperatures of the uppermost leaves of a tomato crop in a multi and single span house both fitted with aluminised screens. Results showed that leaves in the screened house were approximately 1 $^{\circ}$C higher than those in a non-screened house.

2.6.3 HUMIDITY AND CONDENSATION

The relative humidity in both screened and non-screened houses increase as plants grow. Two processes limiting relative humidity are infiltration and condensation. When the humidity is low the major mode of water removal is infiltration. As humidity increases so too does the dew point of the air. When it exceeds the temperature of the glasshouse cover (generally the coldest surface in the glasshouse), condensation occurs. Bailey and Cotton (1977) found that in non-screened houses the temperature of the glass imposed a limit on the dew point temperature of the glasshouse air. On average the dew point temperature was 1.5°C above that of the cover. Figure 2.9 demonstrates the influence of glass temperature on dew point.

When a thermal screen was drawn the average rate of air loss from the crop zone dropped from 2.1 to 1.3 air changes per hour. This reduced the water vapour reaching the cover hence increasing the absolute humidity and dew point of the air beneath the screen. The difference in dew point temperature and cover temperature was found to increase to 5.0°C. With highly emissive screens, screen temperature remains above dew point so condensation rarely occurs. With highly reflective screens, or where air leakage is low, screen temperature controls dew point in much the same way as glass temperature does for an unscreened house. Condensation will occur on the underside of the screen.

There are several methods for alleviating high humidity under screens (Bailey and Cotton, 1977). These include artificial ventilation, de-humidification by air conditioning, or periodic withdrawal of screens. The first two methods involve increased capital cost and energy consumption. The latter method causes warm air to be lost. Another means of keeping humidity in check is to use a permeable screen material. This permits the passage of water vapour from the crop zone to the roof thus lowering the humidity in the crop zone. Such a material however permits the passage of air thus increasing the convective heat loss to the cover.

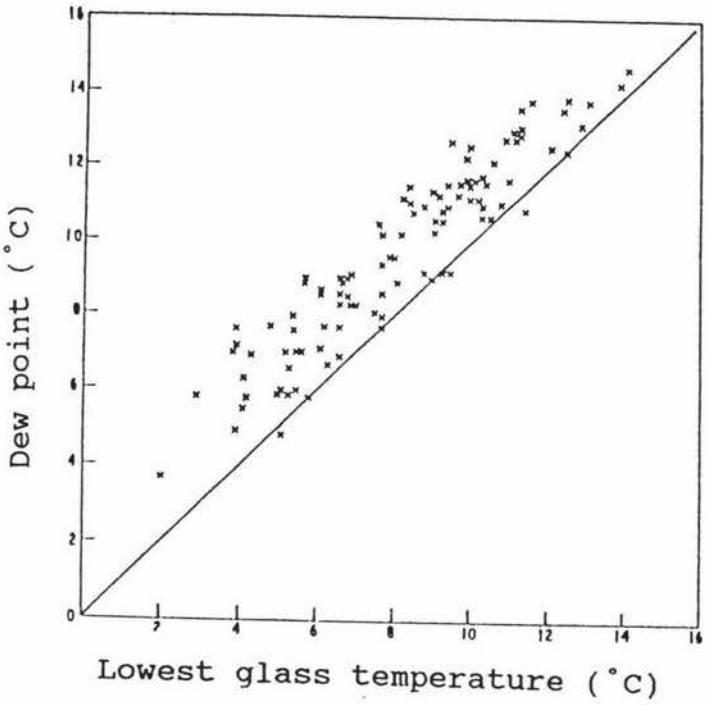

Figure 2.9 Influence of glass temperature on the dew point of glasshouse air (Bailey and Cotton, 1977).

2.6.4 WIND SPEED AND HEAT LOSS

The overall heat loss of a greenhouse (also known as U-value, thermal transmittance and overall heat transfer coefficient) was first measured by Hoare and Morris (1955). Since then it has remained the most useful single expression of greenhouse heat loss ever since. The U-value, defined as the quantity of heat lost per unit area of greenhouse surface per unit time per unit temperature difference between inside and outside air, is usually expressed in units of $Wm^{-2}\,^{\circ}C^{-1}$ (White, 1984b). Table 2.5 lists U-values for various covers under New Zealand conditions.

Bailey (1979b) illustrated the effect wind had on night-time heat loss from a non-screened glasshouse (Figure 2.10). Figure 2.10 also illustrates how thermal screening could eliminate the influence of wind.

Table 2.5 U-values for common greenhouse coverings (Breuer, 1985a).

Cover	Material	U-Value
Hort. glass		7.4
Lap sealed glass		6.2
Durolite	Tedlar-coated, fibreglass-reinforced acrylic panels	5.0
Acrylflute	Impact modified acrylic resin	4.2
Novaroof	Rigid corrugated PVC	5.8
Agphane	EVA	5.3
Twin skin Agphane	EVA	3.6
Hyperlyte	PVC	5.1
Twin skin Hyperlyte	PVC	2.6

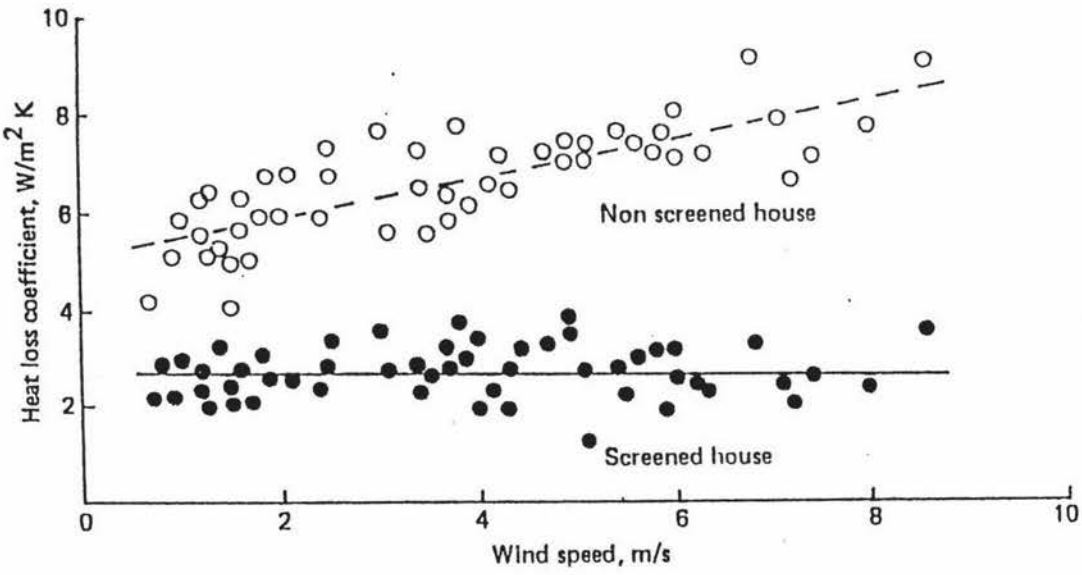

Figure 2.10 Heat loss coefficient (U-value) of glasshouses at night (Bailey, 1979b).

Using appropriate correlation equations Bailey (1979b) assembled tables for percentage reductions in thermal transmittance of different thermal screens at different wind speed. Results are summarised in Table 2.6.

Table 2.6 Percentage reduction in U-value by thermal screening.

Thermal Screen	Wind Speed (ms^{-1})				Ref.
	0	2	4	6	
Clear PE	33	41	46	50	1
Black PE	32	37	41	44	1
Silver Polyto	*28*	*40*	*47*	*53*	1
Aluminised Polyester	43	50	56	60	1
Aluminised PE	52	56	59	61	2
Aluminised polyester-clear PE laminate	50	54	57	59	2
Reemay 2016	*32*	*40*	*46*	*50*	2

Table references
1. Winspear, 1977
2. Bailey and Cotton, 1977

2.6.5 INDIRECT EFFECTS

Soil, plant and air temperatures may be lower than in non-screened houses since thermal screens reduce the need for auxiliary heating. This may lead to reduced production. Some crops may take on the appearance of having been grown at low temperatures (Sturrock, 1981).

Opening screens in the morning can result in sudden chilling of crops as the air that was held above the screen suddenly descends. The use of permeable screens or the provision of heating above the screen may negate this eff[illegible], especially in cold climates (Sturrock, 1981).

Thermal screens have been shown to reduce air stratification in greenhouses, This factor promotes plant uniformity (Badger and Poole, 1979).

2.7 ECONOMICS OF THERMAL SCREENS

To be a profitable investment of time, labour and money a thermal screen system should: a) come with a reasonable life expectancy, b) have a total cost competitive with alternative fuel saving techniques, c) be used with high return crops in cold climates, and d) have a dual use eg. shading or photoperiod control.

In New Zealand the life expectancy of a thermal screen can range from one year for non UV stabilised polythenes to around ten years for Ludvig Svensson aluminised screens.

Due to its geographic nature New Zealand has diverse climatic conditions. Climate types extend from warm humid conditions in the north to cool conditions in the south. Growers in Christchurch face mean daily winter temperatures 4-5 $^{\circ}$C below those in Auckland. Consequently the potential for heat saving is greater in Christchurch. It is therefore likely that screening outlays' are more attractive in Christchurch in comparison to Auckland.

In New Zealand total cost (screen cost + labour cost + support and control cost) for a thermal screen installation range from about \$7/m^2 to about \$15/m^2 depending on the size of the installation, type of screen, type of house, level of control, and whether or not the grower assists with installation (Hoeflak, 1990; Mac Donald, 1990; and Tayor, 1990).

The thermal screen system is more economic if it can be put to a secondary use. Screens capable of reducing the light intensity below 20 lux (Bailey, 1978) can be used for day-length control of photoperiodic crops. Tight fits of mating surfaces are necessary for effective light control. Semi-transparent thermal screens may be

used as shade screens. Reducing the amount of sunlight reaching the plants cuts the ventilation requirement; reducing fuel cost ventilating with fans (Badger and Poole, 1979).

It is both difficult and expensive to retrofit thermal screens to existing houses especially if structural support posts and roof hung trellis systems are present. Similarly heat and water pipes and lighting may have to be relocated. Lowering unit heaters may cause safety problems (Badger and Poole, 1979)

2.8 REVIEW OF GREENHOUSE MODELS

Models are simplified representations of reality. As a result they aid the study of real systems.

A model can be physical or mathematical. Physical models are usually scale replicas of real systems whereas mathematical modelling applies mathematics to real systems. A mathematical model is usually defined and described by a mathematical equation or set of equations. These equations quantitatively represent the assumptions and hypotheses made regarding the real system. When solved they produce predicted values which can be used to test different system designs, foresee problems, compare alternative systems and anticipate future events.

During the last thirty years many models of the greenhouse environment system have been developed. The number of models reported in literature reflects the increasing use of models in applied sciences. This in itself, can be traced to the availability of computing power necessary to solve complex models using numerical techniques. Over this period of time there has been a progression in the complexity of the models produced to describe the response of the greenhouse environment, from simple analytical models with one dependent variable, to highly complex models, with many dependent variables, requiring numerical solutions (Wells, 1990b).

A review of models was conducted by Kano and Sadler, (1985) for publications up to 1983. Five categories of model were identified: black-box (ie. empirical models), steady-state single component models, steady-state multiple component models, dynamic multiple component models, and models that include the carbon dioxide exchange of the crop.

2.8.1 BLACK-BOX MODELS

In this class of model the system outputs (greenhouse environment responses) are related directly to the system inputs (control actions and weather disturbances), without attempting to explain the internal operation of the system.

Black-box models have been developed to determine the heating requirements of greenhouses (Schockert and Von Zabeltitz, 1980; Strom and Amsen, 1981). The model of Schockert and Von Zabeltitz relates energy consumption to prevailing wind speed for single and double glass structures, while the model of Strom and Amsen relates energy usage to mean outside temperature.

Black-box models have also been used to study the control characteristics of greenhouses (Udink ten Cate, 1983; Hesketh et al, 1986; Davis, 1984). The model of Udink ten Cate was used to compare the response of conventional PI (proportional integral) controllers, modified PI controllers, and adaptive control algorithms for controlling air temperature in a Dutch greenhouse with natural ventilation and pipe heating.

Davis (1984) used ARMAX (autoregression moving average exogenous variable) and TF (transfer function) models to develop adaptive controllers for a greenhouse ventilation system. These were compared to conventional proportional and PI algorithms and found to be superior.

Hesketh et al (1986) developed a discrete polynomial model of a greenhouse with fan ventilation and forced convection heating. From this a polynomial controller was developed and its performance simulated. It was predicted that this new controller would have markedly better performance than a conventional on/off controller, particularly if the control outputs were allowed to vary continuously.

2.8.2 STEADY-STATE SINGLE COMPONENT MODELS

This class of model deals with the energy and mass balance of one component of the greenhouse system, and attempts to relate the greenhouse behaviour to the components of these balance equations.

The simplest models in this class consider only the energy balance of the greenhouse air. An early model of this type was set out by Walker (1965) (also Walker et al, (1983)) who developed the energy balance of the greenhouse air and the equations describing the various heat fluxes contributing to the energy balance. These were used to relate the greenhouse air temperature to the input variables, solar radiation and outside air temperature.

Some authors have based their energy balances on components other than the greenhouse air. Garzoli and Blackwell (1981), in their study of the nocturnal heat loss from single skin plastic greenhouse, constructed the energy balance around the cover. They later extended this to a two cover system (Garzoli and Blackwell, 1987). Zhao et al (1985) considered the energy balance of the crop to predict night-time leaf temperatures and transpiration.

Several models of this type have been developed principally to predict the energy consumption of greenhouses. O'Flaherty et al (1973) used a simple model, and hourly temperature and wind speed records, to predict energy consumption, but ignored solar radiation. Bailey (1977) developed a model based on degree-day data corrected for solar radiation effects. White (1984) describes a model in which

hourly weather data is generated from long term monthly normals and used to solve the energy balance for each hour of a theoretical normal month. The energy input requirements are then summed over all hours for the month.

Breuer (1983) presents a model developed in the Netherlands at IMAG (Institute of Agricultural Engineering). This was used by van den Braak et al (1984) to produce cumulative frequency distributions of heat load, to test the performance of a heat pump.

Shell and Staley (1985) developed a modified form of the ASHRAE (American Society of Heating, Refrigerating and Airconditioning Engineers) steady state building heat loss model. Their model calculates the energy balance of the greenhouse, and hence the energy consumption, on a monthly basis, based on monthly solar radiation and monthly mean temperature differences. This is used as part of an economic analysis of alternative energy conservation strategies.

Recently Jolliet (1988) (also Jolliet and Munday, 1989; and Jolliet et al, 1989) developed a model which separates out the day and night time energy requirements, and accounts for the solar heat storage in the soil, as a function of potential solar energy storage lost by ventilation. This model uses the solar energy Utilisation Factor, the ratio of useful solar energy, to collected solar energy, a concept used in the analysis of solar collectors.

2.8.3 STEADY STATE MULTIPLE COMPONENT MODELS

This class of model considers the energy and mass balances of several subsystems of the greenhouse simultaneously. This results in a system of simultaneous algebraic equations which, when solved, yield the steady states of the system variables. When these steady states are found for successive time steps a quasi-steady state solution of the time response of the system results.

Businger (1963) identified many of the energy fluxes in the greenhouse and formulated a model based on the energy balances at the soil surface and the greenhouse cover. This model has been the basis for many subsequent models of this type. Kimball (1973) derived steady state energy balances for both sides of the greenhouse cover, the crop, the internal air space, six soil layers, an evaporative cooler, and a mass balance for the internal air space. The resulting set of twelve simultaneous algebraic equations was solved for the twelve unknowns, eleven temperatures and one vapour pressure.

Maher and O'Flaherty (1973), produced a similar but less detailed model, using energy balances for the cover, air and crop. This model was used to study the likely effect of evaporative cooling and polyethylene as a covering.

Kindelan (1980) developed a steady-state model of the greenhouse cover, air and crop in conjunction with a dynamic sub-model of the soil. As part of this sub-model the depth below which heat transfer was insignificant was determined.

Avissar and Mahrer (1982) (also Mahrer and Avissar, 1984) developed a similar model, with a dynamic soil sub-model. A unique feature of their model was the dynamic simulation of moisture movement within the soil profile. This was included since moisture content has a marked affect on the thermal properties of the soil. Another feature of this model is the special attention placed on realistic modelling on the stomatal functioning of the crop in response to environmental change within the greenhouse. The model was used to predict the heating and cooling requirements of glass and polyethylene covered greenhouses during the winter and summer in the coastal region of Israel.

Chandra and Albright (1980) developed a model using energy balances which included an elaborate treatment of long-wave radiation exchanges. This model was developed to estimate the energy conserving potential of thermal screens. Only conduction, convection and radiation were considered as modes of heat transfer. They decided that the effects of infiltration and condensation would be included in their future models.

Baille et al (1985) report on a nocturnal energy balance model similar to that of Kimball (1973) for testing the performance of thermal screens. The model's results were compared with experimental measurements and agreement was found to be generally good. It was decided that greater accuracy could have been achieved if condensation had of been taken into account.

Okada (1985) developed a model to analyse the effect of multi-layer thermal screens assuming: 1) steady state heat balances, 2) no latent heat flow, 3) no air infiltration, and 4) no crop. Energy balances of the cover, two screen layers, the air and the floor surface were included.

Kurata (1989) developed a greenhouse climate model for predicting the inside air temperature, canopy temperature and specific humidity of the inside air. The model consisted of heat balances for major surfaces within the house and a moisture balance for the inside air.

2.8.4 DYNAMIC MODELS

This class of model considers the time dependent energy and mass storage of each sub-system in the greenhouse. This results in systems of simultaneous differential equations, which when solved relate the time response of the system state variable to the time varying boundary values.

Takakura et al (1971) produced one of the first dynamic models of the greenhouse environment. Their model included the dynamic energy balances of the crop, air and soil, but ignored the thermal mass of the glass cover, where a steady state analysis was used. A dynamic mass balance for the greenhouse air was also included.

Kittas (1980) developed the energy and mass balance equations for the various surfaces in a greenhouse as part of a study to determine the dynamic characteristics

of the energy and mass exchange between the greenhouse air space and the exterior environment.

Van Bavel et al (1981) presented a dynamic model which was used to simulate the performance of a fluid-roof greenhouse. The results were compared to those for a conventional glass greenhouse.

Duncan et al (1981) developed a dynamic model by only considering the energy balance of the greenhouse air. The time lag of solar heat released from the soil was accounted for by introducing a third order delay of one hour into the model. This was determined by calibration experiments.

Glaub and Trezek (1981) developed the equations for a dynamic model of the greenhouse environment as part of a review of heat and mass transfer in the greenhouse environment. They developed dynamic energy balances for the inner and outer covers, air, crop, a floor slab, and a water mass balance for the air.

Ahmadi and Glockner (1982) used a dynamic model, with balances at the cover, air, crop, and four soil layers, and a water vapour balance of the air, to study the performance of inflated plastic greenhouses for Southern Canada (Ahmadi et al, 1982).

Huang and Kato (1984) developed an electrical network analogy of the energy flows in a greenhouse which included thermal capacity effects. Using this technique all energy flow equations were linearized and expressed as current flows in resistors, component temperatures were represented as voltage potentials, and thermal capacities as capacitors. For any combination of specified potentials (temperatures) the circuit could be solved using a circuit analysis program to yield the unknown potentials (temperatures) and currents (heat flows).

One of the most rigorous dynamic models of the greenhouse environment yet developed is that of Bot (1983). This model considered all components of the

system to be dynamic in nature. The system was represented using the bond graph technique, a procedure similar to the electrical network technique described above.

Arinze et al (1984) used a dynamic model solved using a Runge-Kutta predictor-corrector method to investigate greenhouses with passive and active solar heat storage. Their model considered the greenhouse cover, air crop and seven soil layers, as well as the water vapour balance of the air. Time steps of 5 and 10 minutes were used. Comparison of simulated with real data collected from a prototype greenhouse showed that the model fit was generally good (within 10% of measured temperature).

2.8.5 MODELS INCLUDING CARBON DIOXIDE

This class of model is generally dynamic with the inclusion of the carbon dioxide balance of the greenhouse airspace, and a sub-model simulating crop photosynthesis, and possibly crop growth.

Sorbie and Curry (1973) presented a dynamic energy balance model of the greenhouse which included the plant growth model of Curry (1971). The resulting system of differential equations for the energy and mass balances of the greenhouse cover, air, crop and soil layers, was solved using a program written in the CSMP (Continuous Systems Modelling Program) simulation language. The growth of lettuce in response to greenhouse environment was successfully simulated using this model.

Cooper and Fuller (1983) report a dynamic model based on the TRNSYS simulation program, a program used extensively for simulating the performance of solar energy systems (Klein et al, 1975, 1976). Energy and mass balances were developed for the greenhouse cover, air, floor, and separate growing medium. The photosynthetic rate of the crop was modelled using the model of Enoch and Sacks (1978) for a C-3 plant (spray carnations). Validation of some aspects of the model has subsequently been presented (Fuller et al, 1987).

2.9 CONCLUSIONS

The following was concluded from the preceeding review of literature:

1. A thermal screen system is generally comprised of the following component parts.

    i) thermal screen material
    ii) towing and support system
    iii) control system

2. Screening systems in greenhouses can have three functions: shading, photoperiod control and energy saving. Through the right choice of materials one can combine these functions.

3. Thermal screens are used extensively overseas and energy savings are in the order of 20-50% are reported. Controversy over their economic effectiveness limits their adoption in New Zealand.

4. Thermal screens may cause daytime shading. The following points should be considered:

    (i) daytime storage of screens can cause shading corresponding to a reduction in crop yield,
    (ii) screens should therefore be flexible in order to occupy little space when withdrawn,
    (iii) the effects of shading are minimised by placing the retracted screen on the south side of the house, beneath gutters or over pathways,
    (iv) depending on screen and house design, the reduction in light levels beneath parked screens range from 0-11%.

5. Thermal screens have been known to cause a reduction in yield and delays in harvest date.

6. In the absence of a screen the dew point (and hence the relative humidity) is controlled by the cover temperature. When a screen is installed, with occasional exceptions, the temperature of the screen is higher than the dew point. Consequently condensation on the screen is rare.

7. Non-porous curtains collect condensation dripping off the roof. The weight of the collected water can damage the screen and cable supports.

8. Because infiltration is greatly reduced, humidity beneath the curtain increases. There have been claims of both increases and decreases in related diseases.

9. Cold air descending through the open curtain in the morning can injure the crop. This can be reduced by changing the day set point one-half hour before screen opening or retracting the screen slowly to allow mixing of the air.

10. Thermal screens reduce air stratification.

11. Thermal screens reduce the volume of air to be heated. They are therefore more effective in large span houses or when pulled from gutter to gutter rather than from gutter to ridge.

12. Screens with a reflective lower surface reduce radiant loss by:

    (i) reflecting radiant energy back to the crop, and
    (ii) not absorbing radiation.

    If the lower surface absorbs little radiation however, then it can cause condensation problems. A non-reflective lower surface will rectify this.

13. The number of greenhouse models including thermel screens is limited.

14. Many of the models for predicting the greenhouse environment do not include the effects of condensation and infiltration

CHAPTER III

OBJECTIVES

The objectives for this study were:

1. To estimate the U-values of screened and non-screened greenhouses using an appropriate greenhouse model.

2. To use these U-value estimates to quantify the heating requirement of each greenhouse.

3. To compile the necessary model inputs representative of house type, locality, season, climate, and crop, cover and screen characteristics.

4. To evaluate and compare the economic feasibility of thirteen materials with thermal screening potential and rank them generically.

CHAPTER IV

THE MODEL

The chosen model was split into two phases. Phase 1 was a steady state multiple component model based on the models of Maher and O'Flaherty (1973) and Kimball (1973). Phase 1 predicted the thermodynamic state of the greenhouse environment in terms of temperatures and heat flows, under a variety of steady boundary conditions. These predictions were used to estimate the overall U-values of:

1. a glass greenhouse,
2. an *Agphane* greenhouse,
3. a twin skin *Agphane* greenhouse, and
4. 62 combinations outlined in Section 1.3.

In Phase 2 the overall U-values were used to estimate the annual auxiliary energy need of each house and screen combination. Phase 2 combined unpublished work of Wells (1989c), work by Seginer and Jenkins (1987) and part of a model by Jolliet (1988) (also Jolliet and Munday, 1989; and Jolliet et al, 1989).

The annual auxiliary energy need of each combination was used in an internal rate of return analysis of economic feasibility.

4.1 THE PHASE 1 MODEL

Energy transfer equations, derived from conductive, convective and radiative formulae, were used to construct energy balances for locations within the greenhouse. Mass transfer equations, derived from latent heat and vapour diffusion formulae, were used to construct mass balances for locations within the greenhouse. These locations of interest were referred to as 'subsystems' of the greenhouse 'system'. The screenless greenhouse (the standard) had eight subsystems, namely: the cover, the plants, the floor, the greenhouse airspace and the four soil layers beneath the floor. The screened greenhouse had ten subsystems, namely: the cover, the thermal screen, the plants, the floor, the quiescent airspace above the screen, the greenhouse airspace below the screen and the four soil layers beneath the floor.

Two major efforts were made to simplify Phase 1. Firstly, each subsystem was assumed to have reached a stable condition known as 'steady state'. Steady state conditions prevail when the amount of energy or mass stored within a subsystem remains static. In other words the flow of energy to and from each subsystem equates. Similarly, the flow of mass to and from each subsystem equates. It follows that at steady state a subsystem's inflow and outflow equations sum to zero, hence forming energy and mass balances. For example, the energy (heat) balance for a steady state plant subsystem during the day comprises five energy transfer equations, each one describing energy absorbed (ie. an inflow) or lost (ie. an outflow) from the plant subsystem. The inflows are:

i) the radiation gain from warmer surfaces,
ii) the convective gain from warm greenhouse air, and
iii) the absorbed solar radiation.

The outflows are:

i) radiation to cooler objects, and
ii) latent heat associated with transpiration.

The second simplification was that of modelling the standard and screened systems as a series of non-overlapping horizontal layers (see Figures 4.1 and 4.2). The cover, thermal screen, floor, and soil layer subsystems were modelled as single continuous layers whereas the plant subsystem was modelled as a number of horizontal, broken layers.

The units of each transfer equation were standardised to W per m^2 of floor area (Wm^{-2}floor) and g per s per m^2 of floor ($gs^{-1}m^{-2}$floor) to facilitate comparison between subsystems.

As the cover and plant subsystems did not share the flat, horizontal geometry of the floor, variables known as the **cover area index** (CAI) and **leaf area index** (LAI) were introduced to adjust the cover and plant equations accordingly. The CAI, defined as 'the area of cover per unit floor area', that is:

$$CAI = \frac{Area\ of\ cover}{Area\ of\ floor}$$

converts cover heat and mass transfer units of Wm^{-2}cover and $gs^{-1}m^{-2}$cover to Wm^{-2}floor and $gs^{-1}m^{-2}$floor respectively.

The magnitude of the CAI caters for architectural variation such as roof slope and wall height. Figure 4.3 shows three hypothetical greenhouse cover designs each with a CAI of 1.6. In this instance, multiplying the predicted transfers by 1.6 will produce cover heat and mass transfer with units of Wm^{-2}floor and $gs^{-1}m^{-2}$floor respectively.

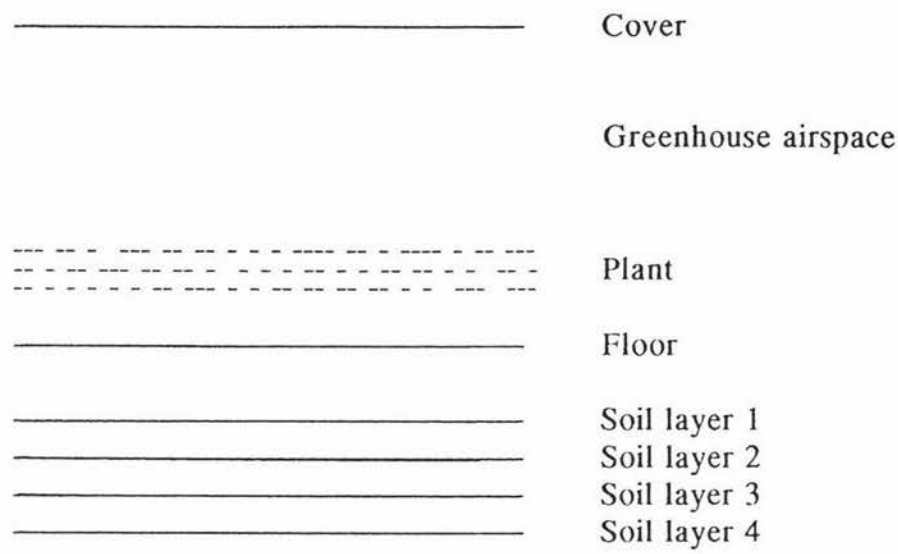

Figure 4.1 **Simplified representation of the standard greenhouse.**

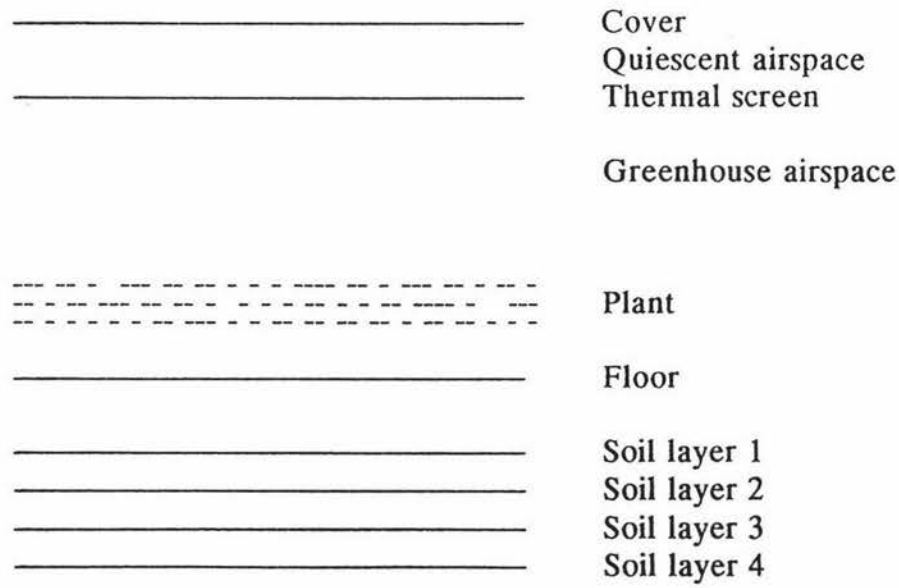

Figure 4.2 **Simplified representation of the screened greenhouse.**

a) A detached even span gable greenhouse.

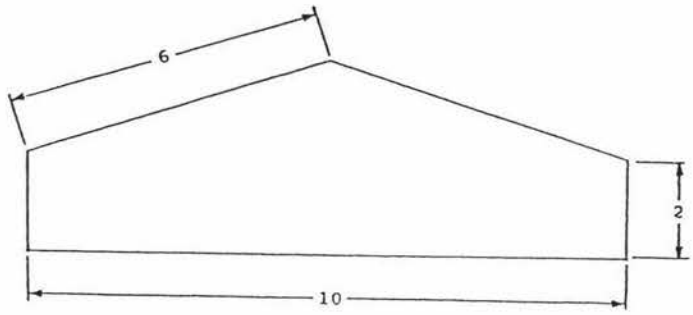

$$CAI = \frac{\text{Area of cover}}{\text{Area of floor}} = \frac{length \times (2+6+6+2)}{length \times 10} = 1.6$$

b) A multi-span greenhouse.

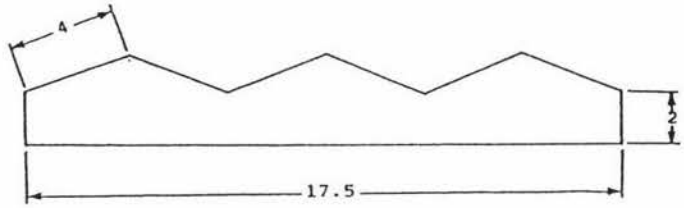

$$CAI = \frac{\text{Area of cover}}{\text{Area of floor}} = \frac{length \times (2+4+4+4+4+4+4+2)}{length \times 17.5} = 1.6$$

c) A tunnel greenhouse (paraboloid design).

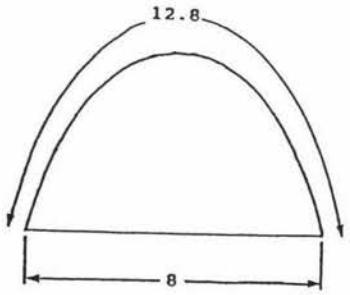

$$CAI = \frac{\text{Area of cover}}{\text{Area of floor}} = \frac{length \times 12.8}{length \times 8} = 1.6$$

Figure 4.3 Three cover shapes with a CAI of 1.6.

The plant subsystem on the other hand comprises randomly arranged leaves, varying in size, shape, and density. A variable known as the LAI, defined as 'the plan leaf area per unit floor area', that is:

$$LAI = \frac{Area\ of\ leaf}{Area\ of\ floor}$$

was introduced to convert the crop's heat and mass transfer from units of Wm^{-2}leaf and $gs^{-1}m^{-2}$leaf to Wm^{-2}floor and $gs^{-1}m^{-2}$floor respectively. Hence variation in heat and mass transfer resulting from leaf orientation, crop type, age and planting density are catered for. The LAI for the crop shown in Figure 4.4 is 2.1.

LAI considers only one side of the leaf. As a result, transfers associated with the plant subsystem are doubled to account for exchange from both upper and lower leaf cuticles. The transfer in Figure 4.4 is therefore two times the initial prediction ie. 4.2 .

The standard greenhouse consisted of eight energy balances (for the cover, crop, floor, greenhouse airspace and four soil layers) and one mass balance (for the greenhouse airspace). The standard balances, and the equations which form them, are defined in Section 4.1.1. The screened greenhouse consisted of ten balances (for the cover, quiescent airspace, thermal screen, crop, floor, greenhouse airspace and the four soil layers) and two of them mass balances (for the quiescent and greenhouse airspaces). The screened balances, and the equations which form them, are defined in Section 4.1.2.

Each balance contained three types of equation governing inputs; parameters, known variables (independent variables) and unknown variables (dependent variables). Parameters were usually constants although some changed with respect to known variables. The values assigned to the parameters and independent variables are given in Appendix 4.

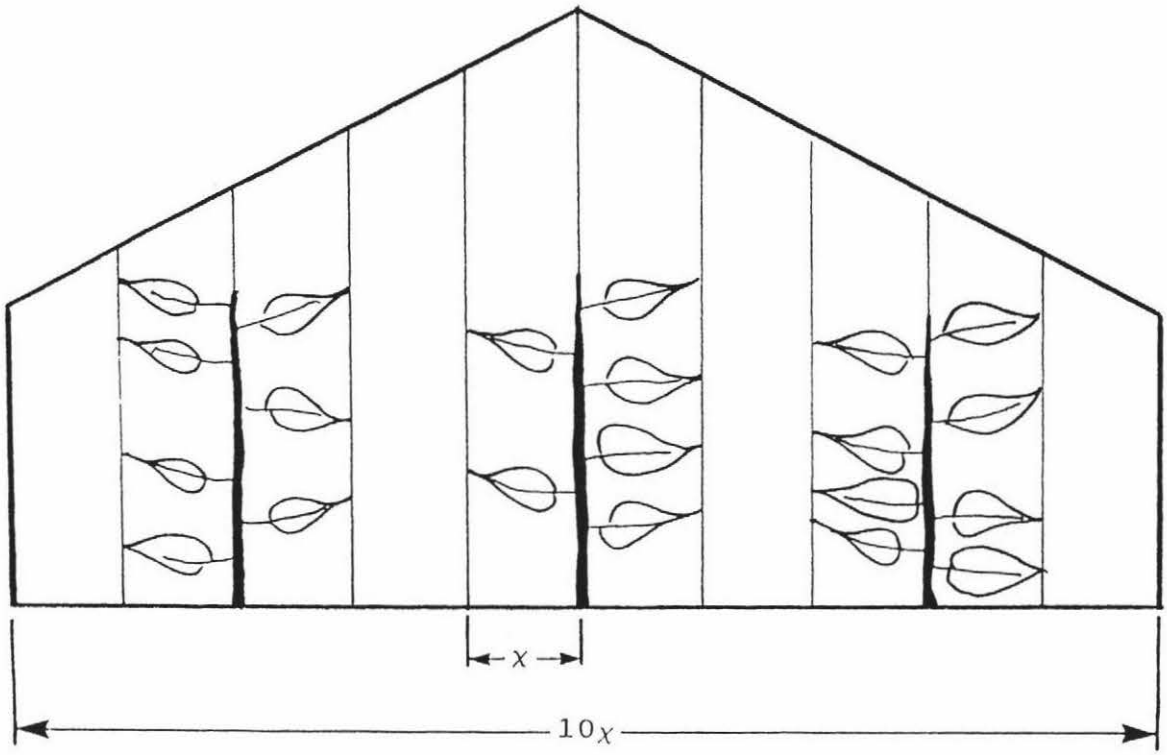

$$LAI = \frac{Area\ of\ leaf}{Area\ of\ floor}$$
$$= \frac{length \times (7\chi + 6\chi + 8\chi)}{length \times 10\chi}$$
$$= 2.1$$

Figure 4.4 A system with a LAI of 2.1.

The standard had nine dependent variables: cover temperature, plant temperature, floor temperature, airspace wet bulb temperature, four soil layer temperatures, and the amount of heating or cooling required to hold the house airspace at a predetermined set point (see Table 4.1a). The screened greenhouse had twelve dependent variables: cover temperature, thermal screen temperature, plant temperature, floor temperature, quiescent airspace wet and dry bulb temperatures, greenhouse airspace wet bulb temperature, four soil layer temperatures and the heating or cooling required to hold the house airspace at a predetermined set point (see Table 4.1b).

Table 4.1a Dependent variables for the standard greenhouse.

Name	Symbol
Cover temperature	T_c
Plant temperature	T_p
Floor temperature	T_f
Soil layer 1. temperature	T_{s1}
Soil layer 2. temperature	T_{s2}
Soil layer 3. temperature	T_{s3}
Soil layer 4. temperature	T_{s4}
Airspace wetbulb temperature	T_{aw}
Heating or Cooling to bring airspace to the Set Point in $Wm^{-2}{}_{floor}$	AUX

Table 4.1b Dependent variables for the screened greenhouse.

Name	Symbol
Cover temperature	T_c
Screen temperature	T_s
Plant temperature	T_p
Floor temperature	T_f
Soil layer 1. temperature	T_{s1}
Soil layer 2. temperature	T_{s2}
Soil layer 3. temperature	T_{s3}
Soil layer 4. temperature	T_{s4}
Quiescent airspace temperature	T_q
Quiescent airspace wetbulb temperature	T_{qw}
Airspace wetbulb temperature	T_{aw}
Heating or Cooling to bring airspace to the Set Point in $Wm^{-2}{}_{floor}$	AUX

The balance equations were organised into two categories; a series of standard balances, and a series of screened balances. Solving each series simultaneously by matrix inversion ($X=A^{-1}B$, where A^{-1} is the inverse matrix of A) established the value of each dependent variable. This process served to simulate the thermodynamic state of the greenhouse.

Matrix inversion involved separating each balance into its known and unknown components, arranging them into the form $AX=B$, where A, X and B are matrices. Matrix A was a square matrix having the order 9x9 and 12x12 for the standard and screened situations respectively. X and B were of the order 9x1 for the standard and 12x1 for the screened house.

The A matrix contained the parameters and known variables associated with dependent variables. For example, all first column entries of A belonged to the dependent variable in the first row of X; all second column entries of A belonged to the unknown variable in the second row of X; and so on.

The X matrix contained arabic entries representative of the dependent variables. The B matrix contained numerical entries representative of the parameters and the known variables not associated with the dependent variables.

A^{-1} may be calculated using several numerical techniques; most are iterative and slow. With a SYMPHONY spreadsheet however, A^{-1} was calculated in a matter of seconds. The same spreadsheet was used to multiply A^{-1} by B to solve for X.

The heating or cooling requirement in Wm^{-2}floor was one the dependent variables solved for on the X matrix. Dividing this term by the inside and outside temperature difference produced the instantaneous U-value in $Wm^{-2}floor^{\circ}K^{-1}$.

The instantaneous U-value is the U-value for a minute point in time. As time elapses, environmental conditions and crop characteristics change. As a result the parameters and known variables responsible for describing the environment and

crop constantly change causing variation in successive instantaneous U-values. Instantaneous U-values are therefore not accurate indicators of actual U-values. The latter describes heat exchange as a whole rather than for an instance in time.

A fair estimate of the actual U-value was obtained by running Phase 1 for thirty two different crop and climate situations. These situations arose by varying parameters and known variables denotative of different crop and climate regimes. The simulated instantaneous U-value was noted for each situation. The actual U-value was assumed to be the average of these thirty two instantaneous values.

The thirty two different crop and climatic situations resulted from crossing the following combinations: (1) LAI=1 or 5, ie: a young crop Vs an established crop; (2) cloud factor=0 or 1, ie: no cloud Vs full cloud cover; (3) RH_{out}=90% or 60% ie: high and low outside relative humidities; (4) T_s=13 or 20°C, ie: variation in greenhouse heating set point temperature; and (5) T_o=5 or 10°C, ie: variation in outside temperature.

Note that T_o was kept relatively low, the reason being that it reduced the likelihood of the model to predict ventilation. Avoiding ventilation increased the accuracy of the U-value prediction because heat was dissipated through the covering material only and not through cover openings.

4.1.1 PHASE 1 EQUATIONS FOR THE STANDARD GREENHOUSE

This section defines the energy and mass balance equations for the standard greenhouse. Equation derivations are given in Appendix 3 and equation parameters and independent variables are given in Appendix 4.

4.1.1.1 Greenhouse cover energy balance

The energy balance for the cover is given by:

$$P_c + N_c + R_c + H_{ac} - H_{co} - L_{ca} = 0 \qquad (4.1a)$$

where the PAR absorbed by the cover is:

$$P_c = S_P\alpha_{cP} + S_P\tau_{cP}\rho_{pP}\alpha_{cP} + S_P\tau_{cP}\tau^2_{pP}\rho_{fP}\alpha_{cP} \qquad (4.1b)$$

The NIR absorbed by the cover is:

$$N_c = S_N\alpha_{cN} + S_N\tau_{cN}\rho_{pN}\alpha_{cN} + S_N\tau_{cN}\tau^2_{pN}\rho_{fN}\alpha_{cN} \qquad (4.1c)$$

The net FIR absorbed by the cover is:

$$\begin{aligned} R_c = {} & 4.6\alpha_{cF}(T_{sky} - T_c)(1 + \tau_{cF}\rho_{pF} + \tau_{cF}\tau^2_{pF}\rho_{fF}) \\ & + 5.4\alpha_{cF}(T_p - T_c)(1 + \rho_{cF}\rho_{pF} + \rho_{cF}\tau^2_{pF}\rho_{fF} - \rho_{fF}\tau^2_{pF}) \\ & + 5.4_{cF}(T_p - T_f)(\rho_{fF}\tau_{pF} - \tau_{pF} - \tau_{pF}\rho_{cF}\rho_{pF}) \end{aligned} \qquad (4.1d)$$

The convection from the inside air to the cover is:

$$H_{ac} = CAI\, h_{ca}(T_a - T_c) \qquad (4.1e)$$

The convection from the cover to the outside air is:

$$H_{co} = CAI\, h_{co}(T_c - T_o) \qquad (4.1f)$$

The latent heat lost to the inside air is:

$$L_{ca} = CAI\, E_{ac}\left[\frac{\delta(T_c - T_{aw})}{\gamma} + (T_a - T_{aw})\right] \qquad (4.1g)$$

4.1.1.2 Plant energy balance

The energy balance for the plant is given by:

$$P_p + N_p + R_p - H_{pa} - L_{pa} = 0 \qquad (4.2a)$$

where the PAR absorbed by the plant is:

$$P_p = S_P\tau_{cP}\alpha_{pP} + S_P\tau_{cP}\tau_{pP}\rho_{fP}\alpha_{pP} + S_P\tau_{cP}\rho_{pP}\rho_{cP}\alpha_{pP} \quad (4.2b)$$

The NIR absorbed by the plant is:

$$N_p = S_N\tau_{cN}\alpha_{pN} + S_N\tau_{cN}\tau_{pN}\rho_{fN}\alpha_{pN} + S_N\tau_{cN}\rho_{pN}\rho_{cN}\alpha_{pN} \quad (4.2c)$$

The net FIR absorbed by the plant is:

$$\begin{aligned} R_p = {} & 4.6\alpha_{pF}(T_{sky} - T_c)[\tau_{cF}(1 + \rho_{pF}\rho_{cF} + \tau_{pF}\rho_{fF})] \\ & + 5.4\alpha_{pF}(T_c - T_p)[\rho_{cF}\rho_{pP}(1 - \rho_{cF}) + 1 - \rho_{cF} + \tau_{pF}\rho_{fF}] \\ & + 5.4_{pF}(T_f - T_p)[\tau_{pF}\rho_{cF}(1 + \rho_{cF}\rho_{pF} + \tau_{pF}\rho_{fF} - \rho_{fF}) + 1 - \rho_{fF}] \end{aligned} \quad (4.2d)$$

The convection to the inside air is:

$$H_{pa} = 2\,LAI\,h_{pa}(T_p - T_a) \quad (4.2e)$$

The latent heat loss to the air by transpiration is:

$$L_{pa} = 2\,LAI\,E_{ap}\left[\frac{\delta(T_p - T_{aw})}{\gamma} + (T_a - T_{aw})\right] \quad (4.2f)$$

4.1.1.3 Floor energy balance

The energy balance for the floor is given by:

$$P_f + N_f + R_f - H_{fa} + C_{1f} - L_{fa} = 0 \quad (4.3a)$$

where the PAR absorbed by the floor is:

$$P_f = S_P\tau_{cP}\tau_{pP}\alpha_{fP} \quad (4.3b)$$

The NIR absorbed by the floor is:

$$N_f = S_N\tau_{cN}\tau_{pN}\alpha_{fN} \quad (4.3c)$$

The net FIR absorbed by the floor is:

$$R_f = 4.6\alpha_{fF}(T_{sky} - T_c)[\tau_{cF}\tau_{pF}(1 + \rho_{pF}\rho_{cF})] + 5.4\alpha_{fF}(T_p - T_f)[\tau^2_{pF}\rho_{cF}(\rho_{fF} - 1 - \rho_{cF}\rho_{pF}) + 1 - \rho_{pF}] + 5.4_{fF}(T_c - T_p)[\tau_{pF}(1 + \tau_{pF}\rho_{cF} + \rho_{fF}\rho_{cF} - \rho_{cF} - \rho^2_{cF}\rho_{pF})] \quad (4.3d)$$

The convection to the inside air is:

$$H_{fa} = h_{fa}(T_f - T_a) \quad (4.3e)$$

The conduction to soil layer 1 is:

$$C_{1f} = K_1(T_1 - T_f) \quad (4.3f)$$

The latent heat loss to the inside air is:

$$L_{fa} = E_{af}\left[\frac{\delta(T_f - T_{aw})}{\gamma} + (T_a - T_{aw})\right] \quad (4.3g)$$

4.1.1.4 Soil layer 1 energy balance

The energy balance for soil layer 1 was given by:

$$C_{21} - C_{1f} = 0 \quad (4.4a)$$

where the conduction from soil layer 2 is:

$$C_{21} = K_2(T_2 - T_1) \quad (4.4b)$$

and conduction to the floor is:

$$C_{1f} = K_1(T_1 - T_f) \quad (4.4c)$$

4.1.1.5 Soil layer 2 energy balance

The energy balance for soil layer 2 is given by:

$$C_{32} - C_{21} = 0 \quad (4.5a)$$

where conduction from soil layer 3 is:

$$C_{32} = K_3 (T_3 - T_2) \qquad (4.5b)$$

and conduction to soil layer 1 is:

$$C_{21} = K_2 (T_2 - T_1) \qquad (4.5c)$$

4.1.1.6 Soil layer 3 energy balance

The energy balance for soil layer 3 is given by:

$$C_{43} - C_{32} = 0 \qquad (4.6a)$$

where conduction from soil layer 4 is:

$$C_{43} = K_4 (T_4 - T_3) \qquad (4.6b)$$

and conduction to soil layer 2 is:

$$C_{32} = K_3 (T_3 - T_2) \qquad (4.6c)$$

4.1.1.7 Soil layer 4 energy balance

The energy balance for soil layer 4 is given by:

$$C_{d4} - C_{43} = 0 \qquad (4.7a)$$

where conduction from the deep ground soil is:

$$C_{d4} = K_d (T_d - T_4) \qquad (4.7b)$$

and conduction to soil layer 3 is:

$$C_{43} = K_4 (T_4 - T_3) \qquad (4.7c)$$

4.1.1.8 Inside airspace energy balance

The energy balance for the greenhouse airspace is given by:

$$H_{pa} - H_{ac} + H_{fa} - A_{ao} + AUX - D_{ao} + L_{pa} + L_{ca} + L_{fa} = 0 \qquad (4.8a)$$

AUX symbolises the auxiliary heat required to hold the house airspace at a set temperature.

The convective heat exchange H_{pa} is defined in Section 4.1.1.2 as:

$$H_{pa} = 2\,LAI\,h_{pa}\,(T_p - T_a) \qquad (4.2e)$$

The convective heat exchange H_{ac} is defined in Section 4.1.1.1 as:

$$H_{ac} = CAI\,h_{ca}\,(T_a - T_c) \qquad (4.1e)$$

The convective heat exchange H_{fa} is defined in Section 4.1.1.3 as:

$$H_{fa} = h_{fa}\,(T_f - T_a) \qquad (4.3e)$$

The latent heat exchange L_{pa} is defined in Section 4.1.1.2 as:

$$L_{pa} = 2\,LAI\,E_{ap}\left[\frac{\delta\,(T_p - T_{aw})}{\gamma} + (T_a - T_{aw})\right] \qquad (4.2f)$$

The latent heat exchange L_{ca} is defined in Section 4.1.1.1 as:

$$L_{ca} = CAI\,E_{ac}\left[\frac{\delta\,(T_c - T_{aw})}{\gamma} + (T_a - T_{aw})\right] \qquad (4.1g)$$

The latent heat exchange L_{fa} is defined in Section 4.1.1.3 as:

$$L_{fa} = E_{af}\left[\frac{\delta\,(T_f - T_{aw})}{\gamma} + (T_a - T_{aw})\right] \qquad (4.3g)$$

The advective heat transfer is:

$$A_{ao} = \frac{\Phi_{ao}\,(\delta + \gamma)\,(T_{aw} - T_{ow})}{\gamma} \qquad (4.8b)$$

The diffusive heat transfer is:

$$D_{ao} = \mathcal{H}_v \Omega_{ao} CAI\left[\frac{(\delta + \gamma)(T_{aw} - T_{ow})}{\gamma} - (T_a - T_o)\right] \qquad (4.8c)$$

4.1.1.9 Inside airspace mass balance

The mass balance equation for the greenhouse airspace is:

$$M_{pa} + M_{ca} + M_{fa} - M_{ao} - Z_{ao} + EMF = 0 \qquad (4.9a)$$

where EMF symbolises the water vapour input from evaporative cooling, misting or fogging.

The water vapour transfer for the plants is:

$$M_{pa} = \frac{2\,LAI\,E_{ap}\left[\frac{\delta\,(T_p - T_{aw})}{\gamma} + (T_a - T_{aw})\right]}{\mathcal{L}} \qquad (4.9b)$$

The water vapour transfer for the cover is:

$$M_{ca} = \frac{CAI\,E_{ac}\left[\frac{\delta\,(T_c - T_{aw})}{\gamma} + (T_a - T_{aw})\right]}{\mathcal{L}} \qquad (4.9c)$$

The water vapour transfer for the floor is:

$$M_{fa} = \frac{E_{af}\left[\frac{\delta\,(T_f - T_{aw})}{\gamma} + (T_a - T_{aw})\right]}{\mathcal{L}} \qquad (4.9d)$$

The advective vapour transfer for the outside air is:

$$M_{ao} = \frac{\Phi_{ao}\left\{\left[\frac{(\delta + \gamma)(T_{aw} - T_{ow})}{\gamma}\right] - (T_a - T_o)\right\}}{\mathcal{L}} \qquad (4.9e)$$

The diffusive vapour transfer for the outside air is:

$$Z_{ao} = \Omega_{ao} CAI \left\{ \left[\frac{(\delta + \gamma)(T_{aw} - T_{ow})}{\gamma} \right] - (T_a - T_o) \right\} \qquad (4.9f)$$

4.1.2 PHASE 1 EQUATIONS FOR THE SCREENED GREENHOUSE

This section defines the energy and mass balance equations for the screened greenhouse. Equation derivations are given in Appendix 3 and equation parameters and independent variables are given in Appendix 4.

4.1.2.1 Greenhouse cover energy balance

The energy balance equation for the cover is given by:

$$P_c + N_c + R_c + H_{qc} - H_{co} - L_{cq} = 0 \qquad (4.10a)$$

where the PAR absorbed by the cover is:

$$P_c = S_P \alpha_{cP} + S_P \tau_{cP} \rho_{uP} \alpha_{cP} + S_P \tau_{cF} \tau^2_{sP} \rho_{pP} \alpha_{cP} \qquad (4.10b)$$

The NIR absorbed by the cover is:

$$N_c = S_N \alpha_{cN} + S_N \tau_{cN} \rho_{uN} \alpha_{cN} + S_N \tau_{cN} \tau^2_{sN} \rho_{pN} \alpha_{cN} \qquad (4.10c)$$

The net FIR absorbed by the cover is:

$$\begin{aligned} R_c = {} & 4.6 \alpha_{cF} (T_{sky} - T_c)(1 + \tau_{cF} \rho_{uF} + \tau_{cF} \tau^2_{uF} \rho_{cF} + \tau_{cF} \tau^2_{sF} \rho_{pF}) \\ & + 5.4 \alpha_{cF} (T_s - T_c) \left[1 + \rho_{cF} \rho_{uF} (1 + \rho_{cF} \rho_{uF} + \tau^2_{sF}) - \rho_{uF} - \rho_{cF} \rho^2_{uF} \right. \\ & \left. \quad - \tau^2_{sF} \rho_{pF} - \tau^2_{sF} \tau^2_{pF} \rho_{fF} \right] \\ & + 5.4 \alpha_{cF} (T_p - T_s) \left[\tau_{sF} (\rho_{cF} \rho_{uF} + \rho_{lF} \rho_{pF} - \rho_{fF} \tau^2_{pF} - \rho_{pF} - \rho_{cF} \rho_{uF} \rho_{pF}) \right] \\ & + 5.4 \alpha_{cF} (T_f - T_p) \left[\tau_{pF} \tau_{sF} (1 + \rho_{lF} \rho_{pF} + \rho_{cF} \rho_{uF} - \rho_{fF}) \right] \end{aligned} \qquad (4.10d)$$

The convection from the quiescent airspace is:

$$H_{qc} = CAI\, h_{cq} (T_q - T_c) \qquad (4.10e)$$

The convection to the outside air is defined in Section 4.1.1.1 as:

$$H_{co} = CAI\, h_{co} (T_c - T_o) \qquad (4.1f)$$

The latent heat loss to the quiescent airspace is:

$$L_{cq} = CAI\, E_{qc}\left[\frac{\delta (T_c - T_{qw})}{\gamma} + (T_q - T_{qw})\right] \qquad (4.10f)$$

4.1.2.2 Thermal screen energy balance

The energy balance for the thermal screen is given by:

$$P_s + N_s + R_s - H_{sq} + H_{as} - L_{sq} - L_{sa} = 0 \qquad (4.11a)$$

where the PAR absorbed by the screen is:

$$P_s = S_P\tau_{cP}\alpha_{uP} + S_P\tau_{cP}\rho_{uP}\rho_{cP}\alpha_{uP} + S_P\tau_{cP}\tau_{sP}\rho_{pP}\alpha_{lP} \qquad (4.11b)$$

The NIR absorbed by the screen is:

$$N_s = S_N\tau_{cN}\alpha_{uN} + S_N\tau_{cN}\rho_{uN}\rho_{cN}\alpha_{uN} + S_N\tau_{cN}\tau_{sN}\rho_{pN}\alpha_{lN} \qquad (4.11c)$$

The net FIR absorbed by the screen is:

$$\begin{aligned} R_s = {} & 4.6 (T_{sky} - T_c) \{\alpha_{uF}\tau_{cF}[1 + \rho_{uF}\rho_{cF} + \alpha_{lF} (\tau_{sF}\tau_{cF}\rho_{pF})]\} \\ & + 5.4 (T_c - T_s) \{\alpha_{uF}[1 + \rho_{uF}\rho_{cF} (1 + \rho_{uF}\rho_{cF} - \rho_{cF}) + \rho_{cF} (\rho_{pF}\tau^2_{sF} \\ & - 1)] + \alpha_{lF}[\tau_{sF}\rho_{pF} (1 - \rho_{cF}) + \tau_{sF}\tau^2_{pF}\rho_{fF}]\} \\ & + 5.4 (T_p - T_s) \{\alpha_{uF}\tau_{sF}\tau_{cF} (\rho_{lF}\rho_{pF} + 1 + \rho_{cF}\rho_{uF} - \rho_{pF}) \\ & + \alpha_{lF}[1 + \rho_{lF}\tau^2_{pF}\rho_{fF} + \rho_{pF} (\rho_{lF} + \tau^2_{sF}\rho_{cF} - 1 - \rho_{fF}\tau_{pF})]\} \\ & + 5.4 (T_f - T_p) [\alpha_{uF} (\tau_{pF}\tau_{sF}\rho_{cF} - \rho_{fF}\tau_{pF}\tau_{sF}\rho_{cF}) \\ & + \alpha_{lF} (\tau_{pF} + \tau_{pF}\rho_{lF}\rho_{pF} - \rho_{fF}\tau_{pF})] \end{aligned} \qquad (4.11d)$$

The convective heat loss to the quiescent airspace is:

$$H_{sq} = h_{sq} (T_s - T_q) \tag{4.11e}$$

The convective heat gain from the main airspace is:

$$H_{as} = h_{as} (T_a - T_s) \tag{4.11f}$$

The latent heat loss to the quiescent airspace is:

$$L_{sq} = E_{qs}\left[\frac{\delta (T_s - T_{qw})}{\gamma} + (T_q - T_{qw})\right] \tag{4.11g}$$

The latent heat loss to the main airspace is:

$$L_{sa} = E_{sa}\left[\frac{\delta (T_s - T_{aw})}{\gamma} + (T_a - T_{aw})\right] \tag{4.11h}$$

4.1.2.3 Plant energy balance

The plant energy balance equation is given by:

$$P_p + N_p + R_p - H_{pa} - L_{pa} = 0 \tag{4.12a}$$

where the PAR absorbed by the plants is:

$$P_p = S_P \tau_{cP} \tau_{sP} \alpha_{pP} \tag{4.12b}$$

The NIR absorbed by the plants is:

$$N_p = S_N \tau_{cN} \tau_{sN} \alpha_{pN} \tag{4.12c}$$

The net FIR absorbed by the plants is:

$$\begin{aligned} R_p = {} & 4.6\alpha_{pF} (T_{sky} - T_c) [\tau_{sF} \tau_{cF} (1 + \rho_{pF} \rho_{lF} + \tau_{pF} \rho_{fF} + \rho_{uF} \rho_{cF})] \\ & + 5.4\alpha_{pF} (T_s - T_p) [1 + \rho_{lF} (\rho_{pF} + \rho_{fF} \tau_{pF}^2 - 1 - \rho_{pF} \rho_{lF}) \\ & \quad + \tau_{sF}^2 (\rho_{pF} \rho_{cF} - \rho_{cF} - \rho_{cF}^2 \rho_{uF}) + \tau_{pF} \rho_{fF}] \\ & + 5.4\alpha_{pF} (T_f - T_p) (1 + \tau_{pF} \rho_{lF} + \tau_{pF} \rho_{lF}^2 \rho_{pF} + \tau_{pF} \tau_{sF}^2 \rho_{cF} - \rho_{fF}) \\ & + 5.4\alpha_{pF} (T_c - T_s) [\tau_{sF} (1 + \rho_{uF} \rho_{cF} + \rho_{pF} \rho_{lF} + \tau_{pF} \rho_{fF} \\ & \quad - \rho_{cF} - \rho_{uF} \rho_{cF}^2 \tau_{sF})] \end{aligned} \tag{4.12d}$$

The convective heat loss to the main airspace is:

$$H_{pa} = 2\,LAI\,h_{pa}\,(T_p - T_a) \tag{4.2e}$$

The latent heat loss to the air transpiration is:

$$L_{pa} = 2\,LAI\,E_{ap}\left[\frac{\delta\,(T_p - T_{aw})}{\gamma} + (T_a - T_{aw})\right] \tag{4.2f}$$

4.1.2.4 Floor energy balance

The floor energy balance equation is given by:

$$P_f + N_f + R_f - H_{fa} + C_{1F} - L_{fa} = 0 \tag{4.13a}$$

where the PAR absorbed by the floor is:

$$P_f = S_P\tau_{cP}\tau_{sP}\tau_{pP}\alpha_{fP} \tag{4.13b}$$

the NIR absorbed by the floor is:

$$N_f = S_N\tau_{cN}\tau_{sN}\tau_{pN}\alpha_{fN} \tag{4.13c}$$

The net FIR absorbed by the floor is:

$$\begin{aligned} R_f = {} & 4.6\alpha_{fF}\,(T_{sky} - T_c)\,(\tau_{cF}\tau_{sF}\tau_{pF}) \\ & + 5.4\alpha_{fF}\,(T_p - T_f)\,(1 - \rho_{pF} + \rho_{1F}\tau_{pF}^2 + \tau_{pF}^2\rho_{1F}\rho_{fF}) \\ & + 5.4\alpha_{fF}\,(T_p - T_s)\,(\tau_{pF}\rho_{1F} + \tau_{sF}\rho_{cF}\tau_{pF} + \rho_{1F}^2\rho_{pF}\tau_{pF} \\ & \quad -\tau_{pF} - \rho_{1F}\tau_{pF}\rho_{pF}) \\ & + 5.4\alpha_{fF}\,(T_c - T_s)\,(\tau_{sF}\tau_{pF} + \rho_{uF}\rho_{cF}\tau_{sF}\tau_{pF} + \tau_{sF}\rho_{pF}\rho_{1F}\tau_{pF} \\ & \quad - \tau_{sF}\tau_{pF}\rho_{cF}) \end{aligned} \tag{4.13d}$$

The conductive heat loss to the main airspace is:

$$H_{fa} = h_{fa}\,(T_f - T_a) \tag{4.3e}$$

The conductive gain from soil layer 1 is:

$$C_{1f} = K_1\,(T_1 - T_f) \tag{4.3f}$$

The latent heat loss to the main airspace is:

$$L_{fa} = E_{af}\left[\frac{\delta\,(T_f - T_{aw})}{\gamma} + (T_a - T_{aw})\right] \qquad (4.3g)$$

4.1.2.5 Soil layer 1 energy balance

The energy balance for soil layer 1 was the same as that of the standard greenhouse (see Section 4.1.1.4).

4.1.2.6 Soil layer 2 energy balance

The energy balance for soil layer 2 was the same as that of the standard greenhouse (see Section 4.1.1.5).

4.1.2.7 Soil layer 3 energy balance

The energy balance for soil layer 3 was the same as that of the standard greenhouse (see Section 4.1.1.6).

4.1.2.8 Soil layer 4 energy balance

The energy balance for soil layer 4 was the same as that of the standard greenhouse (see Section 4.1.1.7).

4.1.2.9 Quiescent airspace energy balance

The energy balance for the quiescent air space is given by:

$$H_{sq} - H_{qc} + L_{sq} + L_{cq} + A_{aq} - A_{qo} + D_{aq} - D_{qo} = 0 \qquad (4.14a)$$

where the convective heat exchange H_{sq} is defined in Section 4.1.2.2 as:

$$H_{sq} = h_{sq}\,(T_s - T_q) \qquad (4.11e)$$

The convective heat exchange H_{qc} is defined in Section 4.1.2.1 as:

$$H_{qc} = CAI\, h_{cq} (T_q - T_c) \qquad (4.10e)$$

The latent heat exchange L_{sq} is defined in Section 4.1.2.2 as:

$$L_{sq} = E_{qs}\left[\frac{\delta (T_s - T_{qw})}{\gamma} + (T_q - T_{qw})\right] \qquad (4.11g)$$

The latent heat exchange L_{cq} is defined in Section 4.1.2.1 as:

$$L_{cq} = CAI\, E_{qc}\left[\frac{\delta (T_c - T_{qw})}{\gamma} + (T_q - T_{qw})\right] \qquad (4.10f)$$

The advective heat gain from the main airspace is:

$$A_{aq} = \frac{\Phi_{aq} (\delta + \gamma) (T_{aw} + T_{qw})}{\gamma} \qquad (4.14b)$$

The advective heat loss to the outside is:

$$A_{qo} = \frac{\Phi_{qo} (\delta + \gamma) (T_{qw} + T_{ow})}{\gamma} \qquad (4.14c)$$

The diffusive heat gain from the main airspace is:

$$D_{aq} = \mathcal{H}_v \Omega_{aq}\left\{\left[\frac{(\delta + \gamma) (T_{aw} + T_{qw})}{\gamma}\right] - (T_a - T_q)\right\} \qquad (4.14d)$$

The diffusive heat loss to the outside air is:

$$D_{qo} = \mathcal{H}_v \Omega_{qo}\, CAI\left\{\left[\frac{(\delta + \gamma) (T_{qw} + T_{ow})}{\gamma}\right] - (T_q - T_o)\right\} \qquad (4.14e)$$

4.1.2.10 Greenhouse airspace energy balance

The energy balance equation for the main airspace is given by:

$$H_{pa} - H_{as} + H_{fa} + L_{pa} + L_{sa} + L_{fa} + AUX - A_{aq} - D_{aq} = 0 \qquad (4.15a)$$

Where the convective heat exchange H_{pa} is defined in Section 4.1.2.3 as:

$$H_{pa} = 2\,LAI\,h_{pa}\,(T_p - T_a) \qquad (4.2e)$$

The convective heat exchange H_{as} is defined in Section 4.1.2.2 as:

$$H_{as} = h_{as}\,(T_a - T_s) \qquad (4.11f)$$

The convective heat exchange H_{fa} is defined in Section 4.1.2.4 as:

$$H_{fa} = h_{fa}\,(T_f - T_a) \qquad (4.3e)$$

The latent heat exchange L_{pa} is defined in Section 4.1.2.3 as:

$$L_{pa} = 2\,LAI\,E_{ap}\left[\frac{\delta\,(T_p - T_{aw})}{\gamma} + (T_a - T_{aw})\right] \qquad (4.2f)$$

The latent heat exchange L_{sa} is defined in Section 4.1.2.2 as:

$$L_{sa} = E_{sa}\left[\frac{\delta\,(T_s - T_{aw})}{\gamma} + (T_a - T_{aw})\right] \qquad (4.11h)$$

The latent heat exchange L_{fa} is defined in Section 4.1.2.4 as:

$$L_{fa} = E_{af}\left[\frac{\delta\,(T_f - T_{aw})}{\gamma} + (T_a - T_{aw})\right] \qquad (4.3g)$$

The advective heat exchange A_{aq} is defined in Section 4.1.2.9 as:

$$A_{aq} = \frac{\Phi_{aq}(\delta + \gamma)\,(T_{aw} + T_{qw})}{\gamma} \qquad (4.14b)$$

The diffusive heat exchange D_{aq} is defined in Section 4.1.2.9 as:

$$D_{aq} = \mathcal{H}_v\,\Omega_{aq}\left\{\left[\frac{(\delta + \gamma)\,(T_{aw} + T_{qw})}{\gamma}\right] - (T_a - T_q)\right\} \qquad (4.14d)$$

4.1.2.11 Quiescent airspace mass balance

The mass balance equation for the quiescent airspace is given by:

$$M_{cq} + M_{sq} + M_{aq} + Z_{aq} - M_{qo} - Z_{qo} = 0 \qquad (4.16a)$$

where the water vapour exchange for the greenhouse cover is:

$$M_{cq} = \frac{CAI\,E_{qc}\left[\frac{\delta\,(T_c - T_{qw})}{\gamma} + (T_q - T_{qw})\right]}{\mathcal{L}} \qquad (4.16b)$$

The water vapour exchange for the upper surface of the screen is:

$$M_{sq} = \frac{E_{qs}\left[\frac{\delta\,(T_s - T_{qw})}{\gamma} + (T_q - T_{qw})\right]}{\mathcal{L}} \qquad (4.16c)$$

The advective water vapour exchange for the main airspace is:

$$M_{aq} = \frac{\Phi_{aq}\left[\frac{(\delta + \gamma)\,(T_{aw} - T_{qw})}{\gamma} - (T_a - T_q)\right]}{\mathcal{L}} \qquad (4.16d)$$

The diffusive vapour transfer for the main airspace is:

$$Z_{aq} = \Omega_{aq}\left\{\left[\frac{(\delta + \gamma)\,(T_{aw} + T_{qw})}{\gamma}\right] - (T_a - T_q)\right\} \qquad (4.16e)$$

The advective transfer for the outside air is:

$$M_{qo} = \Phi_{qo}\left\{\left[\frac{(\delta + \gamma)\,(T_{qw} + T_{ow})}{\gamma}\right] - (T_q - T_o)\right\} \qquad (4.16f)$$

The diffusive vapour transfer for the outside air is:

$$Z_{qo} = \Omega_{qo}\,CAI\left\{\left[\frac{(\delta + \gamma)\,(T_{qw} + T_{ow})}{\gamma}\right] - (T_q - T_o)\right\} \qquad (4.16g)$$

4.1.2.12 Greenhouse airspace mass balance

The main airspace mass balance equation is given by:

$$M_{pa} + M_{sa} + M_{fa} - M_{aq} - Z_{aq} + EMF = 0 \qquad (4.17a)$$

where the water vapour exchange for the plants is defined in Section 4.1.1.9 as:

$$M_{pa} = \frac{2\,LAI\,E_{ap}\left[\frac{\delta\,(T_p - T_{aw})}{\gamma} + (T_a - T_{aw})\right]}{\mathcal{L}} \qquad (4.9b)$$

where the water vapour exchange for the underside of the screen is:

$$M_{sa} = \frac{E_{sa}\left[\frac{\delta\,(T_s - T_{aw})}{\gamma} + (T_a - T_{aw})\right]}{\mathcal{L}} \qquad (4.17b)$$

The water vapour exchange for the floor is defined in Section 4.1.1.9 as:

$$M_{fa} = \frac{E_{af}\left[\frac{\delta\,(T_f - T_{aw})}{\gamma} + (T_a - T_{aw})\right]}{\mathcal{L}} \qquad (4.9c)$$

The advective vapour exchange for the quiescent airspace M_{aq} is defined in Section 4.1.2.11 as:

$$M_{aq} = \frac{\Phi_{aq}\left[\frac{(\delta + \gamma)\,(T_{aw} - T_{qw})}{\gamma} - (T_a - T_q)\right]}{\mathcal{L}} \qquad (4.16d)$$

The diffusive vapour exchange for the quiescent airspace Z_{aq} is defined in Section 4.1.2.11 as:

$$Z_{aq} = \Omega_{aq}\left\{\left[\frac{(\delta + \gamma)\,(T_{aw} + T_{qw})}{\gamma}\right] - (T_a - T_q)\right\} \qquad (4.16e)$$

4.2 THE PHASE 2 MODEL

Phase 2 used the U-values found in Phase 1 to calculate the annual auxiliary energy required to heat each screened and non-screened house to set points of 15°C and 20°C in Auckland and Christchurch. The approach was threefold; 1) estimate the overall energy need, 2) estimate the solar contribution to this need, and 3) find the auxiliary energy need.

4.2.1 ESTIMATING THE OVERALL ENERGY NEED

The overall energy need of a greenhouse is the sum of the day and night-time needs. The day and night-time needs were found using U-values from Phase 1 and day and night-time temperature distributions. Temperature distributions were estimated using the modified degree-day method of Wells (1989c) based on meterological data from Auckland, Wellington, Christchurch, and Invercargil.

4.2.1.1 Estimation of day and night-time temperature distribution

According to Wells (1989c) the long term temperature distribution for any day in a given month is distributed normally (Gaussian distribution). The parameters of the distribution, mean temperature and standard deviation, are functions of daily mean temperature and standard deviation, both estimated from mean maxima and minima data. The following steps outline the procedure developed by Wells (1989c) for estimating mean day and night-time temperatures under New Zealand conditions.

i) Find the mean daily maximum temperature (T_x) and mean daily minimum temperature (T_n) for each month from meterological data (see Tables 4.2a and 4.2b).

Table 4.2a T_x, T_m, and solar radiation (H) for Christchurch (from NZMS, 1980).

Month	Mean Daily Maximum (°C)	Mean Daily Minimum (°C)	Solar Radiation ($MJm^{-2}day^{-1}$)
January	21.5	11.6	21.8
February	21.1	11.6	19.5
March	19.4	10.1	13.8
April	16.9	7.4	9.7
May	13.5	4.3	6.2
June	10.8	1.8	4.9
July	10.3	1.4	5.3
August	11.6	2.5	8.1
September	14.3	4.7	12.4
October	16.9	6.8	17.9
November	18.9	8.5	21.5
December	20.6	10.6	23.3

Table 4.2b T_x, T_m, and solar radiation (H) for Auckland (from NZMS, 1980).

Month	Mean Daily Maximum (°C)	Mean Daily Minimum (°C)	Solar Radiation ($MJm^{-2}day^{-1}$)
January	23.1	15.6	24.5
February	23.5	15.8	21.5
March	22.5	14.9	16.5
April	19.8	12.6	12.1
May	16.9	9.7	8.7
June	14.7	7.8	6.9
July	14.0	6.8	8.0
August	14.7	7.7	10.2
September	15.9	9.2	14.0
October	17.5	10.8	17.7
November	19.4	12.3	22.1
December	21.4	14.1	24.6

ii) Estimate mean daily temperature (T_o) from:

$$T_o = \frac{(T_x + T_m)}{2}$$

iii) Estimate standard deviation of the temperature (S_o) from:

$$S_o = \frac{(T_x - T_m)}{2}$$

iv) The true mean night-time temperature (T_n) is:

$$T_n = 0.95T_o - 0.7$$

v) The standard deviation of night-time temperature (S_n) is given by:

$$S_n = 0.57S_o + 0.76$$

vi) The true mean daytime temperature (T_d) is:

$$T_d = 0.97T_o + 1.4$$

vii) The standard deviation of daytime temperature (S_d) is given by:

$$S_d = 0.80S_o + 0.44$$

4.2.1.2 Estimating night-time energy need

Night-time energy need was obtained using the model of Seginer and Jenkins (1987) for estimating temperature exposures (also called heating degree-days).

i) Specify the heating set point (T_{sn}).

ii) Calculate the normalised set point temperature (τ_{sn}):

$$\tau_{sn} = \frac{(T_{sn} - T_n)}{S_n}$$

iii) Calculate the normalised temperature exposure intensity (Z_n):

$$Z_n = \frac{\ln(1+\exp(\alpha\tau_{sn}))}{\alpha}$$

where $\alpha = 1.7$ approximates the integral of the normalised cumulative Gaussian distribution.

iv) Calculate the night-time temperature exposure intensity ($\oplus_n$) in °K from:

$$\oplus_n = Z_n S_n$$

v) Calculate the day length (ℓ) in hours from:

$$\ell = \frac{2w}{15}$$

where w = hour angle at sunrise

$$= \cos^{-1}(-\tan\lambda\tan\delta)$$

λ = latitude

= -43.3 for Christchurch and -37.0 for Auckland

δ = solar declination on day (d).

$$= 23.45\sin\left[360\times\frac{(280+d)}{365}\right]$$

and d = average Julian day number of month

vi) Calculate the night-time temperature exposure (X_n) in °K.s from:

$$X_n = 3600\oplus_n(24-\ell)$$

vii) The night-time energy need (E^{n}_{need}) in $Jm^{-2}day^{-1}$ is then given by:

$$E^{n}_{need} = X_n U$$

where U = the U-value for the greenhouse estimated in Phase 1 ($Wm^{-2}floor\,^{\circ}K^{-1}$)

4.2.1.3 Estimating daytime energy need

The procedure for estimating daytime energy need was similar to that given in Section 4.2.1.2.

i) Specify the heating set point (T_{sd}).

ii) Calculate the normalised set point temperature (τ_{sd}):

$$\tau_{sd} = \frac{(T_{sd} - T_d)}{S_d}$$

iii) Calculate the normalised temperature exposure intensity (Z_d):

$$Z_d = \ln \frac{(1+\exp(\alpha \tau_{sd}))}{\alpha}$$

where α = 1.7 approximates the integral of the normalised cumulative Gaussian distribution.

iv) Calculate the daytime temperature exposure intensity ($\oplus_d$) in $^{\circ}K$:

$$\oplus_d = Z_d S_d$$

v) Calculate the daytime temperature exposure (X_d) in $^{\circ}K.s$ from:

$$X_d = 3600 \oplus_d \ell$$

vi) The daytime energy need (E^d_{need}) in $Jm^{-2}day^{-1}$ is then given by:

$$E^d_{need} = X_d U$$

where U = the U-value for the greenhouse estimated in Phase 1 ($Wm^{-2}floor^{\circ}K^{-1}$).

4.2.2 ESTIMATING THE SOLAR CONTRIBUTION

Heat from the sun contributes to the thermal need of a greenhouse. Even during winter the solar contribution is an important fraction of the overall energy need.

The solar contribution was estimated using part of a model developed by Jolliet (1988) (also Jolliet and Munday, 1989; and Jolliet et al, 1989) which takes into account the solar storage of the soil as a function of potential solar storage lost by ventilation. An important parameter of this model is the mean incident global radiation, or an estimate of it. The following steps outline this model.

4.2.2.1 Solar energy collected

i) Find H, the mean monthly incident radiation on a horizontal surface at ground level in $MJm^{-2}day^{-1}$ (global radiation), from weather data (see Table 4.2a and 4.2b).

If H is not available it can by estimated from the following standard correlation using bright monthly sunshine hours:

$$H = H_o\left[0.25 + 0.54\left(\frac{n}{N}\right)\right]$$

where H_o = mean extraterrestrial daily radiation.

n = average number of hours of bright sunshine for month.

N = maximum possible number of hours of bright sunshine for month.

and where:

$$H_o = \frac{24 \times 3600 \times 1360}{\pi}\left[1 + 0.033\cos\left(\frac{360d}{365}\right)\right][\cos\lambda\cos\delta\sin w + \frac{2\pi w}{360}\sin\lambda\sin\delta]$$

The total solar energy collected by the greenhouse consists of transmitted radiation absorbed on the inside of the house (α_{trans}) and a fraction absorbed by the roof (α_{roof}). Most of the transmitted radiation gets absorbed by the soil and crop. A small portion however is reflected back to the roof. The fraction absorbed by the roof and the second reflection from the roof towards the crops must also be taken into account. To determine the energy collected in a greenhouse, account must be taken of energy collected by the lateral walls and the effect of their shadow. A single correction term ($\Delta\alpha_{lat}$), can approximate the effect by relating the differences of the incident radiation on the vertical north and south surfaces.

iii) Estimate the solar energy collected by the greenhouse E_{col} from:

$$E_{col} = \alpha_{col} H$$

where α_{col} = the greenhouse solar collection coefficient

$= \alpha_{trans} + \alpha_{roof} + \Delta\alpha_{lat}$

4.2.2.2 Useful solar energy

When solar radiation is large, part of the energy collected in the greenhouse is rejected in the form of sensible and latent heat to avoid overheating. As a result only a fraction of the collected energy is useful for heating. This useful energy is symbolised E_{use}. The Utilisation Factor (UF) is the ratio of E_{use} to E_{col} so that:

$$UF = \frac{E_{use}}{E_{col}}$$

In a greenhouse E_{use} has two components:

- the night-time contribution (E^n_{use}) resulting from soil heat storage during the day, and
- the daytime contribution (E^d_{use}) which compensates for daytime losses.

Hence:

$$E_{use} = E^n_{use} + E^d_{use}$$

E^n_{use} and E^d_{use} are ascertained as follows:

The night-time contribution: In a greenhouse not equipped with special storage devices, the upper layer of the soil (0-30cm) is the only material allowing heat accumulation. During the day solar contributions by direct soil absorption or by air heating within the greenhouse increase the average soil temperature. The heat accumulated in the soil is given up to the greenhouse during the course of the night. As a result soil stored energy becomes energy utilised for night-time heating.

Jolliet (1988) showed experimentally that there is only proportionality between soil stored energy (E^n_{use}) and E_{col} when the latter is small, that is less than $4MJm^{-2}day^{-1}$ (see Figure 4.5). Above $4MJm^{-2}day^{-1}$, soil stored energy is no longer directly dependent on incident radiation. Above this threshold saturation occurs about a fixed value, approximately $0.5MJm^{-2}day^{-1}$ in the case of chrysanthemums and about $1MJm^{-2}day^{-1}$ for tomatoes (Figure 4.5). This value depends on a number of parameters such as leaf density, mode of heating, soil quality, humidity, and heating set point temperatures. It appears that a determining factor is the leaf density: for a relatively spaced out crop (tomatoes) the soil energy is about twice that in the case of very dense vegetation (chrysanthemums). Below the $4MJm^{-2}day^{-1}$ threshold, soil storage represents between 20 and 25 % of the captured solar energy.

Over a monthly average, the daytime soil stored energy, given up at night, may be approximated by a constant. In the proposed model, the constant is made to

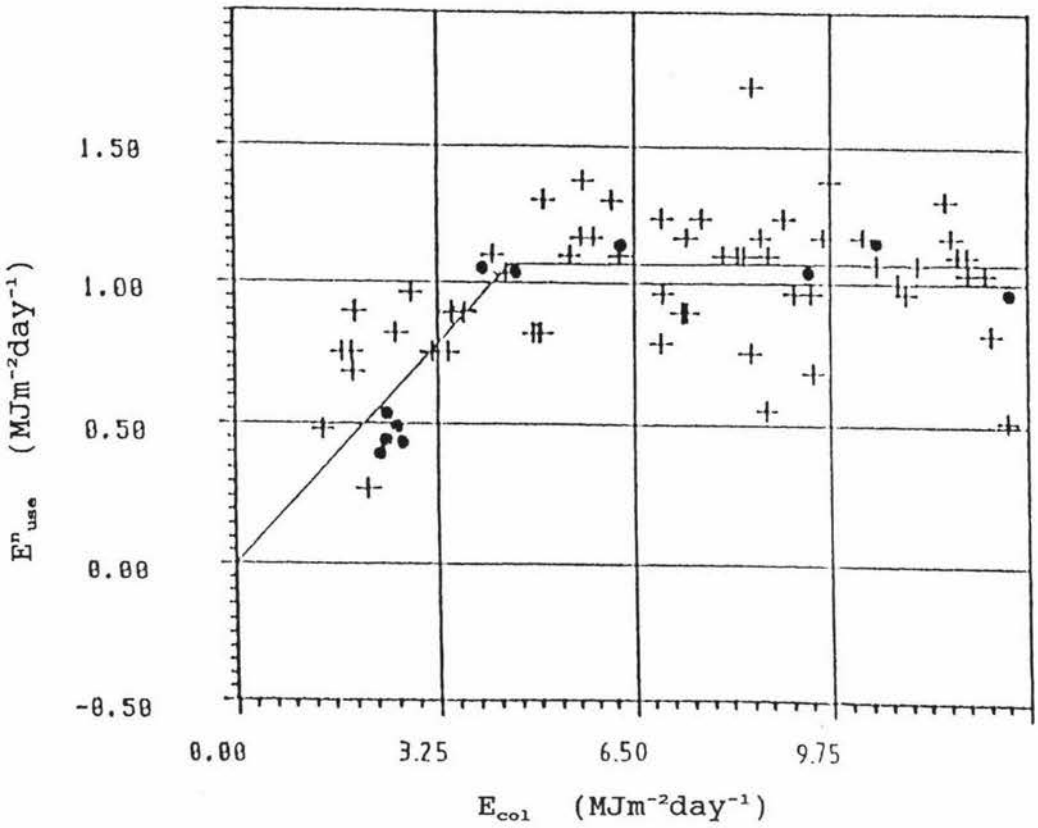

Figure 4.5 **Variation in the stored energy as a function of collected solar energy in a tomato crop. + = daily values, ● = monthly values (Jolliet, 1988).**

depend on the type of crop and heating system by means of crop density index and a coefficient related to the heating system. The stored energy however never exceeds 25% of the collected solar energy when the radiation level is low. Similarly, the energy stored during the day and given back at night cannot be greater than E^n_{need}.

iv) An estimate of the delayed contribution collected solar radiation makes to night heating (E^n_{use}) is calculated as follows in MJm^{-2}day^{-1}:

$$E^n_{use} = f_{heat}(1.5 - 0.5 f_{dens})$$

where $E^{n}_{use} \leq 0.25 E_{col}$

and $E^{n}_{col} \leq E^{n}_{need}$

f_{heat}: is the coefficient related to the heating system

= 0 for floor of low thermal inertia

= 0.8 for on the ground heating

= 1 for air or in the soil heating

and f_{dens}:is the crop density index

= 0 if there is no crop

= 1 for an average crop density (tomatoes)

= 2 for high density crops (chrysanthemums)

v) The night-time solar energy Utilisation Factor can now be found from:

$$UF^{n} = \frac{E^{n}_{use}}{E_{col}}$$

<u>The daytime contribution:</u>

vi) After deducting the daily stored energy (E^{n}_{use}), the remaining collected energy (E^{d}_{col}) is given by:

$$E^{d}_{col} = E_{col} - E^{n}_{use}$$

E^{d}_{col} can serve to heat the greenhouse during the day or is rejected via the ventilators. Note that the solar energy contributing to evapotranspiration is not directly useful for heating; thus in the proposed method the evapotranspiration energy is included in the rejected energy.

The daytime solar energy Utilisation Factor (UF_d) is defined as the ratio of E^d_{use} to E^d_{col}.

$$UF^d = \frac{E^d_{use}}{E^d_{col}}$$

As E^d_{use} serves to compensate for the daytime thermal losses, it cannot be greater than E^d_{need}. If the incident solar energy and the needs are distributed uniformly during the daytime, we have:

if $E^d_{need} > E^d_{col}$

then $E^d_{use} = E^d_{col}$

and $UF^d = 1$

On the other hand:

if $E^d_{need} < E^d_{col}$

then $E^d_{use} = E^d_{need}$

and $$UF^d = \frac{E^d_{need}}{E^d_{col}} = \frac{1}{GLR}$$

where GLR is the Gain Load Ratio (the ratio of collected solar energy to daytime need). Figure 4.6 plots the theoretical Utilisation Factor against the Gain Load Ratio (dashed line).

Neither solar contributions nor the thermal losses are in fact constant throughout the day and, therefore, the practical Utilisation Factor is less than the theoretical one. Experimental work has unfolded a more accurate relationship between UF^d and GLR.

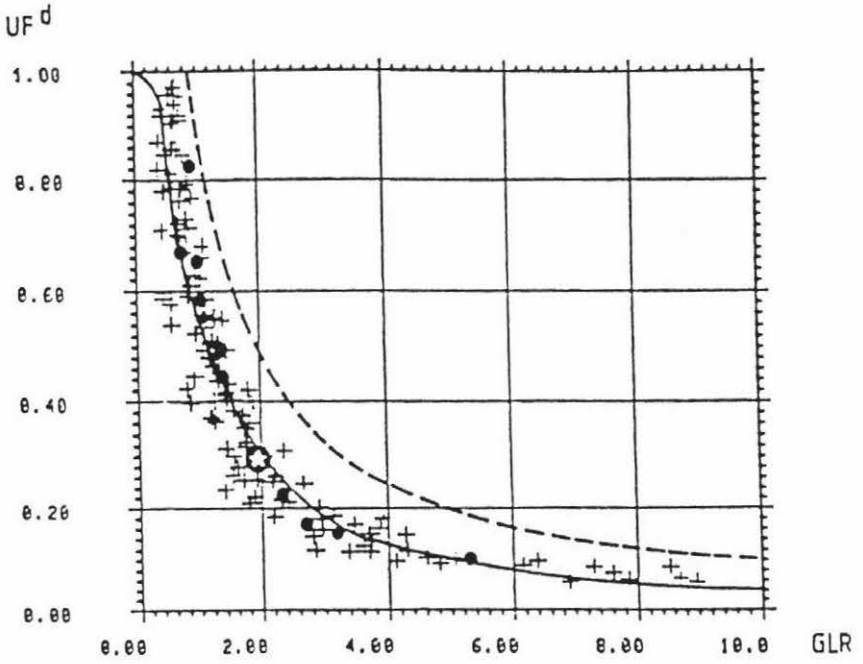

Figure 4.6 Daytime utilisation factor (UF^d) as a function of daytime GLR. Daily (+), monthly (●). ——— = fitted measurements curve; ------ = theoretical maximum. (Jolliet, 1988)

vii) An estimate of the UF^d is obtained from:

$$UF^d = 1 - \exp[-0.87\,(GLR)^{-1.31}]$$

Finally, as climatic and greenhouse factors enter into the calculation of GLR, it is assumed that the UF^d relation is independent of type of greenhouse and climate.

viii) The daytime solar energy usage (E^d_{use}) can now be calculated from:

$$E^d_{use} = E^d_{col} UF^d$$

4.2.3 AUXILIARY HEATING LOADS

The monthly auxiliary energy load may be obtained by subtracting the useful solar energy from the gross energy needs of the greenhouse.

i) The daytime auxiliary heat load (E^{d}_{aux}) is given by:

$$E^{d}_{aux} = E^{d}_{need} - E^{d}_{use}$$

ii) The night-time auxiliary heat load (E^{n}_{aux}) is given by:

$$E^{n}_{aux} = E^{n}_{need} - E^{n}_{use}$$

4.3 ECONOMIC ANALYSIS

'Internal rate of return' (IRR) is the expected rate of return 'internal' to an investment project (Fleming, 1969). The concept of IRR is similar to that of placing money in a savings or investment account which pays interest per annum. This is the market rate of interest or the external rate of return (ERR).

IRR can be used to measure the economic feasibility of an investment project. A negative IRR symbolises an investment loss while a positive value symbolises a gain. If IRR exceeds the market rate of interest, the investment is worth undertaking. On the other hand if the IRR is less than the market rate of interest, the investment should not be undertaken (Dunnett, 1987).

IRR describes what the method sets out to determine. Its alternative name, the 'discounted cash flow', describes how it works. 'Cash flow' refers to the flow of income and/or expenditure over a period of time. 'Discounted' means the discounting of future sums of money by their appropriate factors. The method equates the present worth of the costs of a proposed scheme with the present worth of the estimated net cash flow, over a study period which is usually the economic life of the scheme (Lu, 1969).

The IRR of each combination outlined in Section 1.3 was calculated by equating the extra investment of each screen installation to the present worth of the annual

savings in heating expenditure over a period of time approximately equal to the economic life of the screen, that is:

$$\textit{Extra Investment of Thermal Screen} = \textit{Annual Savings in Heat Expenditure} \times \left[\frac{(1+i)^{n}-1}{i(1+i)^{n}}\right]$$

where n = approximate economic life of thermal screen (years)

i = IRR (%)

A SYMPHONY spreadsheet was used to conduct the IRR analysis.

Heating expenditure is a function of the auxiliary energy load calculated in Phase 2 of the model and fuel type. As a result the IRR was investigated for five common fuel types. IRRs in Christchurch were calculated using coal, diesel, electricity and L.P.G. (liquified petroleum gas) as fuels, whereas coal, diesel, electricity and natural gas were the fuel types used in the Auckland analysis.

4.3.1 SCREEN AND FUEL COSTS

Table 4.3 **Economic life, screen cost, and complete cost (screen material + labour + fittings + hardware) in 1990 dollars. †**

Screen Type	Econ. Life (yrs) *	Screen Cost ($/m²)	Complete Cost ($/m²) ‡		Complete Cost ($/house)	
			300m² House	1000m² House	300m² House	1000m² House
LS 13	6	4.15	13.15	11.15	3,945	11,150
LS 15	6	5.00	14.00	12.00	4,200	12,000
LS 18	6	5.40	14.40	12.40	4,320	12,400
LS 18F	6	5.40	14.40	12.40	4,320	12,400
Marix	3	1.20	10.20	8.20	3,060	8,200
Clr.PE	4	0.60	9.60	7.60	2,880	7,600
Blk.PE	4	0.45	9.45	7.45	2,835	7,450
Infran	4	0.75	9.75	7.75	2,925	7,750
Infsol	4	2.50	11.50	9.50	3,450	9,500
Dura.f	4	2.25	11.25	9.25	3,375	9,250
Dura.t	4	2.40	11.40	9.40	3,420	9,400
Hyplyt	7	5.85	14.85	12.85	4,455	12,850
Agphan	4	2.10	11.10	9.10	3,330	9,100

† Prices are GST inclusive and were obtained from a number of reputable New Zealand greenhouse manufacturers and plastic film distributors.

‡ Complete cost ≡ capital cost of the screen installation
≡'the extra investment'

* Economic life obtained from supplier information.

Table 4.4 Fuels: cost (in 1990 dollars), calorific value and efficiency in 1990.

Fuel Type	Cost/Unit (including cartage)	Calorific Value	Combustion Efficiency (%)
Coal	$200/t (H)	23.6MJ/kg (*)	70 (*)
Diesel	$0.60/l (BP)	37.6 MJ/l (*)	75 (*)
Electricity	Day rate: 4.68¢/MJ Night rate: 1.06¢/MJ (CP)		100
LPG	$0.87/kg (BP)	50MJ/kg (BP)	80 (A)
Natural Gas	0.9¢/MJ (PNGD)	42.1 MJ/m^3 (*)	80 (*)

Information Sources: (H) Huntly Premium Grade.
(BP) BP Head Office, Auckland.
(CP) Central Power, Palmerston North.
(PNGD) Palmerston North Gas Dept.
(*) Lamb, (1980).
(A) Assumed.

4.3.2 FUEL USE AND COST CALCULATIONS

The following calculations were used to ascertain fuel use and cost:

4.3.2.1 Diesel

For the diesel heated houses:

$$Fuel\ usage = \frac{Tot.\ Ann.\ Heat\ Load}{Cal.\ value \times Efficiency}$$

where calorific values and efficiencies were given in Table 4.4.

$$Cost = Fuel\ usage \times Fuel\ price$$

where fuel price was given in Table 4.4.

4.3.2.2 Coal

For the coal heated houses usage and cost were calculated using the formulae given in Section 4.3.2.1.

4.3.2.3 Electricity

For electrically heated houses:

$$Total\ electicity\ cost = daytime\ cost + night\text{-}time\ cost$$

where $daytime\ cost = daytime\ aux.\ heat\ load \times day\ rate$

and $nighttime\ cost = nighttime\ aux.\ heat\ load \times night\ rate$

The day and night rates are given in Table 4.4.

4.3.2.4 Natural Gas

For natural gas heated houses:

$$Total\ gas\ cost = \frac{Tol.\ Ann.\ Heat\ Load \times Gas\ cost}{Efficiency}$$

where gas cost and efficiency were given in Table 4.4.

4.3.2.5 L.P.G.

For L.P.G. heated houses:

$$Fuel\ usage = \frac{Tot.\ Ann.\ Heat\ Load}{Cal.\ value \times Efficiency}$$

where calorific value and efficiency were given in Table 4.4.

$$Cost = Fuel\ usage \times Fuel\ price$$

where the L.P.G. price was given in Table 4.4.

CHAPTER V

RESULTS AND OBSERVATIONS

5.1 PHASE 1 RESULTS

Table 5.1 summarises the findings of Phase 1 of the model. The U-values in Table 5.1 are average values. They were obtained by running Phase 1 of the model for the thirty two crop and climate combinations outlined in Section 4.1 and averaging the thirty two instantaneous values that resulted. To all intents and purposes these average values were assumed estimates of actual U-values.

It should be noted that the U-values in Table 5.1 have units of $Wm^{-2}floor^{\circ}K^{-1}$. They therefore describe the amount of heat dissipated through an area of cover above $1m^2$ of floor for a $1^{\circ}K$ temperature difference, rather than the amount of heat dissipated through $1m^2$ of cover for a $1^{\circ}K$ temperature difference.

From Table 5.1 the *Agphane* covered greenhouse (CAI=1.6) has an average U-value of $11.2Wm^{-2}floor^{\circ}K^{-1}$, the glass covered house (CAI=1.2) has an average U-value $9.9Wm^{-2}floor^{\circ}K^{-1}$, and the twin skin *Agphane* house (CAI=1.6) has an average value of $9.2Wm^{-2}floor^{\circ}K^{-1}$. It follows that the single skin *Agphane* house loses the most heat per m^2 of floor and the twin skin *Agphane* house loses the least.

Table 5.1 highlights a significant reduction in U-value by thermal screening. Once again the single skin *Agphane* house loses the most heat per m^2 of floor and the twin skin *Agphane* house loses the least.

Table 5.1 Average U-values in $Wm^{-2}floor^{\circ}K^{-1}$ for screen and cover combinations.

Screen	Cover		
	Glass	*Agphane*	Double *Agphane*
No Screen	9.9	11.2	9.2
LS 13	6.2	6.5	5.8
LS 15	5.8	6.1	5.4
LS 18	5.4	5.6	5.0
LS 18F	5.5	5.7	5.1
Marix	6.1	6.5	5.7
Clear PE	5.2	5.6	4.9
Black PE	3.9	4.3	3.7
Infrane	4.5	4.9	4.3
Infrasol	4.7	5.2	4.5
Durafilm	4.8	5.2	4.5
Duratherm	4.0	4.5	3.9
Hyperlyte	3.7	4.1	3.6
Agphane	4.6	5.1	4.4

From Table 5.1 the thirteen screens can be ranked in order of ability to reduce U-value as follows:

Hyperlyte
Black PE
Duratherm
Infrane
Agphane
Infrasol
Durafilm
Clear PE
LS 18
LS 18F
LS 15
Marix
LS 13

5.2 PHASE 2 RESULTS

In the tables which follow cover type is abbreviated as follows:

G = Glass
A = *Agphane*
D.A = Double *Agphane*

5.2.1 ANNUAL HEATING LOADS

Tables 5.2a and 5.2b give annual auxiliary day and night-time heat loads and the total annual auxiliary heat loads, for forty two screen and cover combinations at set points of 15°C and 20°C, in Auckland and Christchurch respectively. The annual total was the sum of the annual daytime and annual night-time loads.

The annual daytime loads in Tables 5.2a and 5.2b were obtained by summing monthly daytime auxiliary heat loads. These monthly loads were in turn calculated by entering monthly meterological data (from Tables 4.2a and 4.2b) and U-values (from Phase 1) into the daytime equations of the Phase 2 model. The annual night-time loads in Tables 5.2a and 5.2b were obtained using a similar procedure.

The following observations were made from Tables 5.2a and 5.2b.

1. As expected, total annual heat loads at the 20°C set point were greater than those at the 15°C set point.

2. As expected, total annual heat loads were greater in Christchurch than Auckland.

3. In a non-screened house, annual night-time loads were over twice the annual daytime loads for both locations.

4. Thermal screening had no affect on daytime load but greatly reduced night-time loads.

5. In comparison to Auckland, annual night-time loads in Christchurch made up a greater proportion of the total heat load.

6. Heat loads were the least in double *Agphane* houses and greatest in single *Agphane* houses.

Table 5.2a Annual auxiliary heating loads for Auckland in MJm^{-2}floor.

Screen Type	Cov. Type	T_a = 15°C			T_a = 20°C		
		Day	Nght.	Tot.	Day	Nght.	Tot.
None	G	88	201	289	292	733	1026
	A	98	251	349	336	872	1209
	D.A	73	174	247	275	660	935
LS 13	G	88	68	156	292	353	645
	A	98	78	176	336	382	719
	D.A	73	55	128	275	314	589
LS 15	G	88	55	143	292	314	607
	A	98	64	162	336	344	680
	D.A	73	44	117	275	276	551
LS 18	G	88	44	132	292	276	568
	A	98	49	147	336	295	631
	D.G	73	34	107	275	237	512
LS 18F	G	88	46	135	292	285	578
	A	98	52	149	336	305	641
	D.A	73	36	109	275	247	521
Marix	G	88	64	152	292	344	636
	A	98	78	176	336	382	719
	D.A	73	52	125	275	305	580
Clr.PE	G	88	39	127	292	256	548
	A	98	49	147	336	295	631
	D.A	73	31	104	275	227	502
Blk.PE	G	88	7	95	292	137	429
	A	98	16	114	336	172	508
	D.A	73	4	77	275	120	395
Infran	G	88	21	110	292	190	482
	A	98	31	129	336	227	564
	D.A	73	16	89	275	172	447
Infsol	G	88	26	115	292	208	500
	A	98	39	136	336	256	593
	D.A	73	21	94	275	190	465
Dura.f	G	88	29	117	292	218	510
	A	98	39	136	336	256	593
	D.A	73	21	94	275	190	465
Dura.t	G	88	9	97	292	145	437
	A	98	21	119	336	190	526
	D.A	73	7	80	275	137	412
Hyplyt	G	88	4	92	292	120	413
	A	98	11	109	336	154	490
	D.A	73	3	76	275	112	387
Agphn.	G	88	24	112	292	199	491
	A	98	36	134	336	147	583
	D.A	73	19	92	275	181	456

Table 5.2b Annual auxiliary heating loads for Christchurch in MJm^{-2}floor.

Screen Type	Cov. Type	T_a = 15°C			T_a = 20°C		
		Day	Nght.	Tot.	Day	Nght.	Tot.
None	G	203	592	796	483	1255	1738
	A	242	702	944	551	1463	2013
	D.A	190	532	722	448	1143	1591
LS 13	G	203	289	492	483	663	1146
	A	242	312	554	551	705	1256
	D.A	190	241	431	448	600	1047
LS 15	G	203	256	460	483	600	1082
	A	242	280	522	551	648	1198
	D.A	190	224	414	448	536	983
LS 18	G	203	224	428	483	536	1019
	A	242	240	482	551	568	1119
	D.A	190	182	372	448	474	921
LS 18F	G	203	232	436	483	552	1034
	A	242	248	490	551	584	1134
	D.A	190	202	392	448	489	936
Marix	G	203	280	484	483	648	1130
	A	242	312	554	551	705	1256
	D.A	190	248	438	448	584	1031
Clr.PE	G	203	209	413	483	504	987
	A	242	240	482	551	568	1119
	D.A	190	187	377	448	459	906
Blk.PE	G	203	119	322	483	332	815
	A	242	146	387	551	370	920
	D.A	190	105	295	448	281	728
Infran	G	203	159	363	483	399	882
	A	242	187	429	551	459	1009
	D.A	190	146	336	448	370	817
Infsol	G	203	173	376	483	429	912
	A	242	209	451	551	504	1055
	D.A	190	102	292	448	399	847
Dura.f	G	203	180	383	483	444	927
	A	242	209	451	551	504	1054
	D.A	190	102	292	448	399	847
Dura.t	G	203	125	329	483	325	808
	A	242	159	401	551	399	950
	D.A	190	76	266	448	332	780
Hyplyt	G	203	105	308	483	281	764
	A	242	132	374	551	340	891
	D.A	190	85	275	448	268	715
Agphn	G	203	166	370	483	414	897
	A	242	202	443	551	489	1040
	D.A	190	140	330	448	385	832

5.2.2 FUEL USAGE AND COST

This section summarises the amount of fuel used to heat each house and screen combination, and the associated cost. The results are organised into the following tables:

Table 5.3a Auckland and Diesel
Table 5.3b Auckland and Coal
Table 5.3c Auckland and Electricity
Table 5.3d Auckland and Natural Gas

Table 5.4a Christchurch and Diesel
Table 5.4b Christchurch and Coal
Table 5.4c Christchurch and Electricity
Table 5.4d Christchurch and L.P.G.

5.2.2.1 Diesel

Example: Using Table 5.2a calculate the annual diesel usage and annual diesel cost for a glass covered, non-screened greenhouse in Auckland at a set point of 15°C.

$$\begin{aligned} \textit{Fuel usage} &= \frac{\textit{Tot. Ann. Heat Load}}{\textit{Cal. value} \times \textit{Efficiency}} \\ &= \frac{289\ MJ/m^2}{37.62\ MJ/l \times 0.75} \\ &\approx 10.24\ l/m^2 \end{aligned}$$

$$\begin{aligned} \textit{Cost} &= \textit{Fuel usage} \times \textit{Fuel price} \\ &= 10.24\ l/m^2 \times 0.60\ \$/l \\ &\approx 6.14\ \$/m^2 \end{aligned}$$

5.2.2.2 Coal

Example: Using Table 5.2b calculate the annual coal usage and the annual associated cost for an *Agphane* covered, *Marix* screened, house in Christchurch at a set point of 20°C.

$$\text{Fuel usage} = \frac{\text{Tot. Ann. Heat Load}}{\text{Cal. value} \times \text{Efficiency}}$$
$$= \frac{1256\ MJ/m^2}{23.26\ MJ/kg \times 0.70}$$
$$\approx 77.12\ kg/m^2$$

$$\text{Cost} = \text{Fuel usage} \times \text{Fuel price}$$
$$= 77.12\ kg/m^2 \times 0.20\ \$/kg$$
$$\approx 15.42\ \$/m^2$$

5.2.2.3 Electricity

Daytime costs (ie. the cost in the absence of a screen, or when the screen is withdrawn) are given in Tables (5.i) and (5.ii) below.

Table 5.i Daytime electricity heating costs (in $/m²) for Auckland greenhouses at set points of 15°C and 20°C.

Cov. Type	T_a=15°C	T_a=20°C
G	4.14	13.70
A	4.57	15.77
D.A	3.46	12.89

Table 5.ii Daytime electricity heating costs (in $/m²) for Christchurch greenhouses at set points of 15°C and 20°C.

Cov. Type	T_a=15°C	T_a=20°C
G	9.54	22.65
A	11.33	25.83
D.A	8.91	21.00

Example: Using Table 5.2a calculate the annual electricity cost for a glass covered, *Infrane* screened house in Auckland at 20°C.

$$\begin{aligned} \textit{daytime cost} &= \textit{daytime aux. heat load} \times \textit{day rate} \\ &= 292\ MJ/m^2 \times 0.0469\ \$/MJ \\ &= 13.70\ \$/m^2 \end{aligned}$$

$$\begin{aligned} \textit{nighttime cost} &= \textit{nighttime aux. heat load} \times \textit{night rate} \\ &= 190\ MJ/m^2 \times 0.0106\ \$/MJ \\ &= 2.02\ \$/m^2 \end{aligned}$$

Therefore:

$$\begin{aligned} \textit{Total electricity cost} &= 13.70\ \$/m^2 + 2.02\ \$/m^2 \\ &= 15.72\ \$/m^2 \end{aligned}$$

5.2.2.4 Natural Gas

Example: Using Table 5.2a calculate the annual natural gas cost for a twin *Agphane* covered, *Durafilm* screened house in Auckland at 20°C.

$$\begin{aligned} \textit{Total gas cost} &= \frac{\textit{Tot. Ann. Heat Load} \times \textit{Gas cost}}{\textit{Efficiency}} \\ &= \frac{465\ MJ/m^2 \times 0.009\ \$/MJ}{0.80} \\ &= 5.23\ \$/m^2 \end{aligned}$$

5.2.2.5 L.P.G.

Example: Using Table 5.2b calculate the L.P.G. usage and associated cost for a non-screened glass covered house in Christchurch at 15°C set point.

$$\begin{aligned} \textit{Fuel usage} &= \frac{\textit{Tot. Ann. Heat Load}}{\textit{Cal. value} \times \textit{Efficiency}} \\ &= \frac{796\ MJ/m^2}{50\ MJ/kg \times 0.80} \\ &\approx 19.89\ kg/m^2 \end{aligned}$$

$$\begin{aligned} \textit{Cost} &= \textit{Fuel usage} \times \textit{Fuel price} \\ &= 19.89\ kg/m^2 \times 0.867\ \$/kg \\ &\approx 17.25\ \$/m^2 \end{aligned}$$

The following observations were made from Tables 5.3a-5.4d:

1. As expected, the annual fuel cost was greater at 20°C than at 15°C.

2. As expected, the annual cost in Christchurch was greater than that in Auckland for the same fuel.

3. As expected, the annual cost was less when a house had a thermal screen.

4. As expected, the annual cost was greatest for single *Agphane* covered houses and least for double *Agphane* houses.

5. The following rank of fuel efficiency was established for heating non-screened houses in Auckland. The fuel with the lowest $\$/m^2$ features at the top.

   Natural Gas
   Coal
   Electricity and Diesel

6. The following rank of fuel efficiency was established for heating non-screened houses in Christchurch. The fuel with the lowest $\$/m^2$ features at the top.

   Coal
   Electricity
   Diesel
   L.P.G.

7. For heating screened houses in Auckland the fuels can be ranked in the following order where the lowest $\$/m^2$ fuel features at the top.

Natural Gas
Coal
Diesel
Electricity

8. For heating screened houses in Christchurch the fuels can be ranked in the following order where the lowest $\$/m^2$ fuel features at the top.

Coal
Diesel
L.P.G.
Electricity

Table 5.3a Diesel usage (in l/m^2) and cost (in $\$/m^2$) for screened and non-screened greenhouses in Auckland at set points of 15°C and 20°C.

Screen Type	Cov. Type	T_a = 15°C		T_a = 20°C	
		l/m^2	$\$/m^2$	l/m^2	$\$/m^2$
None	G	10.24	6.14	36.35	21.81
	A	12.36	7.41	42.83	25.70
	D.A	8.77	5.26	33.12	19.87
LS 13	G	5.52	3.31	22.88	13.73
	A	6.23	3.74	25.47	15.28
	D.A	4.53	2.72	20.89	12.53
LS 15	G	5.07	3.04	21.50	12.90
	A	5.73	3.44	24.10	14.46
	D.A	4.15	2.49	19.51	11.71
LS 18	G	4.69	2.81	20.13	12.08
	A	5.19	3.12	22.38	13.43
	D.A	3.79	2.27	18.14	10.88
LS 18F	G	4.78	2.87	20.47	12.28
	A	5.29	3.17	22.72	13.63
	D.A	3.88	2.33	18.48	11.09
Marix	G	5.40	3.24	22.53	13.52
	A	6.23	3.74	25.47	15.28
	D.A	4.42	2.65	20.54	12.33
Clr.PE	G	4.51	2.70	19.44	11.66
	A	5.19	3.12	22.38	13.43
	D.A	3.70	2.22	17.80	10.68
Blk.PE	G	3.37	2.02	15.21	9.12
	A	4.03	2.42	18.02	10.81
	D.A	2.73	1.64	14.01	8.41
Infran	G	3.88	2.33	17.09	10.26
	A	4.57	2.74	19.97	11.98
	D.A	3.17	1.90	15.84	9.51
Infsol	G	4.06	2.44	17.74	10.64
	A	4.84	2.90	21.00	12.60
	D.A	3.34	2.01	16.48	9.89
Dura.f	G	4.15	2.49	18.06	10.84
	A	4.84	2.90	21.00	12.60
	D.A	3.34	2.01	16.48	9.89
Dura.t	G	3.44	2.06	15.50	9.30
	A	4.21	2.53	18.66	11.20
	D.A	2.83	1.70	14.60	8.76
Hyplyt	G	3.27	1.96	14.64	8.77
	A	3.86	2.31	17.38	10.43
	D.A	2.69	1.62	13.72	8.23
Agphn	G	3.97	2.38	17.42	10.45
	A	4.75	2.85	20.66	12.40
	D.A	3.25	1.95	16.16	9.70

Table 5.3b Coal usage (in kg/m²) and cost (in $/m²) for screened and non-screened greenhouses in Auckland at set points of 15°C and 20°C.

Screen Type	Cov. Type	15°		20°C	
		$/m²	$/m²	kg/m²	$/m²
None	G	17.74	3.55	62.99	12.60
	A	21.41	4.28	74.22	14.84
	D.A	15.19	3.04	57.40	11.48
LS 13	G	9.57	1.91	39.64	7.93
	A	10.80	2.16	44.14	8.83
	D.A	7.85	1.57	36.19	7.24
LS 15	G	8.78	1.76	37.25	7.45
	A	9.92	1.98	41.76	8.35
	D.A	7.19	1.44	33.81	6.76
LS 18	G	8.12	1.62	34.87	6.97
	A	9.00	1.80	38.78	7.76
	D.A	6.57	1.31	31.43	6.29
LS 18F	G	8.27	1.65	35.47	7.09
	A	9.16	1.83	39.37	7.87
	D.A	6.72	1.34	32.03	6.41
Marix	G	9.36	1.87	39.04	7.81
	A	10.80	2.16	44.14	8.83
	D.A	7.66	1.53	35.60	7.12
Clr.PE	G	7.81	1.56	33.68	6.74
	A	9.00	1.80	38.78	7.76
	D.A	6.41	1.28	30.84	6.17
Blk.PE	G	5.84	1.17	26.35	5.27
	A	6.99	1.40	31.22	6.24
	D.A	4.73	0.95	24.28	4.86
Infran	G	6.73	1.35	29.62	5.92
	A	7.92	1.58	34.61	6.92
	D.A	5.49	1.10	27.45	5.49
Infsol	G	7.04	1.41	30.74	6.15
	A	8.38	1.68	36.40	7.28
	D.A	5.79	1.16	28.56	5.71
Dura.f	G	7.19	1.44	31.30	6.26
	A	8.38	1.68	36.40	7.28
	D.A	5.79	1.16	28.56	5.71
Dura.t	G	5.96	1.19	26.87	5.37
	A	7.30	1.46	32.33	6.47
	D.A	4.90	0.98	25.29	5.06
Hyplyt	G	5.66	1.13	25.34	5.07
	A	6.68	1.34	30.11	6.02
	D.A	4.67	0.93	23.77	4.75
Agphn	G	6.88	1.38	30.18	6.04
	A	8.23	1.65	35.80	7.16
	D.A	5.64	1.13	28.01	5.60

Table 5.3c Electricity cost (in $/m²) for screened and non-screened greenhouses in Auckland at set points of 15°C and 20°C.

Screen Type	Cov. Type	15°C		20°C	
		Night	Total	Night	Total
None	G	2.13	6.27	7.77	21.48
	A	2.66	7.24	9.25	25.02
	D.A	1.85	5.27	6.99	19.89
LS 13	G	0.72	4.86	3.74	17.45
	A	0.83	5.40	4.05	19.83
	D.A	0.58	4.01	3.33	16.23
LS 15	G	0.58	4.72	3.33	17.04
	A	0.68	5.25	3.64	19.41
	D.A	0.47	3.89	2.92	15.82
LS 18	G	0.47	4.61	2.92	16.62
	A	0.52	5.09	3.13	18.90
	D.A	0.36	3.79	2.51	15.40
LS 18F	G	0.49	4.63	3.03	16.73
	A	0.55	5.12	3.23	19.00
	D.A	0.39	3.81	2.61	15.51
Marix	G	0.68	4.82	3.64	17.34
	A	0.83	5.40	4.05	19.83
	D.A	0.55	3.97	4.23	16.12
Clr.PE	G	0.41	4.55	2.72	16.42
	A	0.52	5.09	3.13	18.90
	D.A	0.33	3.76	2.40	15.30
Blk.PE	G	0.07	4.21	1.45	15.15
	A	0.17	4.75	1.82	17.60
	D.A	0.04	4.47	1.28	14.17
Infran	G	0.23	4.36	2.02	15.72
	A	0.33	4.91	2.41	18.18
	D.A	0.17	3.60	1.82	14.72
Infsol	G	0.28	4.42	2.21	15.91
	A	0.41	4.99	2.72	18.49
	D.A	0.23	3.65	2.02	14.91
Dura.f	G	0.31	4.44	2.31	16.01
	A	0.41	4.99	2.72	18.49
	D.A	0.23	3.65	2.02	14.91
Dura.t	G	0.09	2.23	1.54	15.24
	A	0.23	4.80	2.02	17.79
	D.A	0.07	3.50	1.45	14.34
Hyplyt	G	0.04	4.18	1.28	14.98
	A	0.12	4.69	1.63	17.41
	D.A	0.03	3.46	1.19	14.08
Agphn	G	0.25	3.39	2.11	15.82
	A	0.39	4.96	2.61	18.39
	D.A	0.20	3.63	1.92	14.81

Table 5.3d Natural gas cost (in $/m^2) for screened and non-screened greenhouses in Auckland at set points of 15°C and 20°C.

Screen Type	Cov. Type	15°C $/m²	20°C $/m²
None	G	3.25	11.54
	A	3.92	13.60
	D.A	2.78	10.51
LS 13	G	1.75	7.26
	A	1.98	8.09
	D.A	1.44	6.63
LS 15	G	1.61	6.82
	A	1.82	7.65
	D.A	1.32	6.19
LS 18	G	1.49	6.39
	A	1.65	7.10
	D.A	1.20	5.76
LS 18F	G	1.52	6.50
	A	1.68	7.21
	D.A	1.23	5.87
Marix	G	1.71	7.15
	A	1.98	8.09
	D.A	1.40	6.52
Clr.PE	G	1.43	6.17
	A	1.65	7.10
	D.A	1.17	5.65
Blk.PE	G	1.07	4.83
	A	1.28	5.72
	D.A	0.87	4.45
Infran	G	1.23	5.43
	A	1.45	6.34
	D.A	1.00	5.03
Infsol	G	1.29	5.63
	A	1.54	6.67
	D.A	1.06	5.23
Dura.f	G	1.32	5.73
	A	1.54	6.67
	D.A	1.06	5.23
Durat.	G	1.09	4.92
	A	1.34	5.92
	D.A	0.90	4.63
Hyplyt	G	1.04	4.64
	A	1.22	5.52
	D.A	0.86	4.35
Agphan	G	1.26	5.53
	A	1.51	6.56
	D.A	1.03	5.13

Table 5.4a **Diesel usage (in l/m^2) and cost (in $\$/m^2$) for screened and non-screened greenhouses in Christchurch at set points of 15°C and 20°C.**

Screen Type	Cov. Type	15°C		20°C	
		l/m^2	$\$/m^2$	l/m^2	$\$/m^2$
None	G	28.20	16.92	61.59	36.95
	A	33.46	22.08	71.35	42.81
	D.A	25.59	15.35	56.38	33.83
LS 13	G	17.44	10.46	40.62	24.37
	A	19.63	11.78	44.50	26.70
	D.A	15.29	9.17	37.12	22.27
LS 15	G	16.30	9.78	38.36	23.02
	A	18.51	11.10	42.46	25.48
	D.A	14.69	8.81	34.85	20.91
LS 18	G	15.16	9.10	36.10	21.66
	A	17.09	10.25	39.65	23.79
	D.A	13.19	7.91	32.65	19.59
LS 18F	G	15.45	9.27	36.66	22.00
	A	17.37	10.42	40.20	24.12
	D.A	13.88	8.33	33.18	19.91
Marix	G	17.15	10.29	40.06	24.04
	A	19.63	11.78	44.50	26.70
	D.A	15.54	9.32	36.55	21.93
Clr.PE	G	14.63	8.78	34.97	20.98
	A	17.09	10.25	39.65	23.79
	D.A	13.36	8.02	32.13	19.28
Blk.PE	G	11.41	6.85	28.89	17.33
	A	13.73	8.24	32.62	19.57
	D.A	10.46	6.27	25.82	15.49
Infran	G	12.86	7.71	31.27	18.76
	A	15.19	9.11	35.77	21.46
	D.A	11.90	7.14	28.97	17.38
Infrsol	G	13.34	8.00	32.32	19.39
	A	15.99	9.59	32.37	22.42
	D.A	10.35	6.21	30.02	18.01
Dura.f	G	13.58	8.15	32.85	19.71
	A	15.99	9.59	37.37	22.42
	D.A	10.35	6.21	30.02	18.01
Dura.t	G	11.65	6.99	28.64	17.18
	A	14.22	8.53	33.67	20.20
	D.A	9.44	5.66	27.64	16.59
Hyplyt	G	10.93	6.56	27.06	16.24
	A	13.25	7.95	31.57	18.94
	D.A	9.76	5.85	25.35	15.21
Agphan	G	13.10	7.86	31.79	19.08
	A	15.72	9.43	36.83	22.10
	D.A	11.68	7.01	29.50	17.70

Table 5.4b **Coal usage (in kg/m²) and cost (in $/m²) for screened and non-screened greenhouses in Christchurch at set points of 15°C and 20°C.**

Screen Type	Cov. Type	15°C		20°C	
		kg/m²	$/m²	kg/m²	$/m²
None	G	48.87	9.77	106.73	21.35
	A	57.98	11.60	123.65	24.73
	D.A	44.35	8.87	97.69	19.54
LS 13	G	30.22	6.04	70.39	14.08
	A	34.01	6.80	77.12	15.42
	D.A	26.50	5.30	64.32	12.86
LS 15	G	28.24	5.65	66.48	13.30
	A	32.07	6.41	73.59	14.72
	D.A	25.45	5.09	60.39	12.08
LS 18	G	26.27	5.25	62.55	12.51
	A	29.61	5.92	68.71	13.74
	D.A	22.85	4.57	56.58	11.32
LS 18F	G	26.77	5.35	63.54	12.71
	A	30.10	6.02	69.66	13.93
	D.A	24.06	4.81	57.50	11.50
Marix	G	29.71	5.94	69.43	13.89
	A	34.01	6.80	77.12	15.42
	D.A	26.93	5.39	63.34	12.67
Clr.PE	G	25.35	5.07	60.59	12.12
	A	29.61	5.92	68.71	13.74
	D.A	23.15	4.63	55.67	11.13
Blk.PE	G	19.77	3.95	50.07	10.01
	A	23.80	4.76	56.52	11.30
	D.A	18.12	3.62	44.74	8.95
Infran	G	22.28	4.46	54.19	10.84
	A	26.32	5.26	61.99	12.40
	D.A	20.62	4.12	50.20	10.04
Infsol	G	23.11	4.62	56.01	11.20
	A	27.71	5.54	64.75	12.95
	D.A	17.94	3.59	52.03	10.41
Dura.f	G	23.53	4.71	56.92	11.38
	A	27.71	5.54	64.75	12.95
	D.A	17.94	3.59	52.03	10.41
Dura.t	G	20.19	4.04	49.63	9.93
	A	24.63	4.93	58.35	11.67
	D.A	16.36	3.27	47.90	9.58
Hyplyt	G	18.94	3.79	46.09	9.38
	A	22.96	4.59	54.70	10.94
	D.A	16.91	3.38	43.94	8.79
Agphan	G	22.69	4.54	55.10	11.02
	A	27.23	5.45	63.82	12.76
	D.A	20.25	4.05	51.11	10.22

Table 5.4c **Electricity cost (in $/m²) for screened and non-screened greenhouses in Christchurch at set points of 15°C and 20°C.**

Screen Type	Cov. Type	15°C		20°C	
		Night	Total	Night	Total
None	G	6.28	15.81	13.30	35.95
	A	7.45	18.78	15.50	41.33
	D.A	5.64	14.55	12.12	33.11
LS 13	G	3.06	12.60	7.03	29.68
	A	3.31	14.64	7.47	33.30
	D.A	2.56	11.47	6.36	27.35
LS 15	G	2.72	12.25	6.36	29.00
	A	2.97	14.31	6.86	32.69
	D.A	2.38	11.29	5.68	26.67
LS 18	G	2.38	11.92	5.68	28.32
	A	2.55	13.88	6.02	31.85
	D.A	1.93	10.84	5.02	26.02
LS 18F	G	2.46	12.00	5.85	28.49
	A	2.63	13.97	6.19	32.01
	D.A	2.14	11.05	5.18	26.17
Marix	G	2.97	12.51	6.86	29.51
	A	3.31	14.64	7.47	33.30
	D.A	2.63	11.55	6.19	27.18
Clr.PE	G	2.22	11.76	5.34	27.99
	A	2.55	13.88	6.02	31.85
	D.A	1.98	10.89	4.86	25.86
Blk.PE	G	1.26	10.79	3.52	26.17
	A	1.54	12.88	3.92	29.74
	D.A	1.11	10.02	2.98	23.97
Infran	G	1.69	11.23	4.23	26.88
	A	1.98	13.32	4.86	30.69
	D.A	1.54	10.46	3.92	24.92
Infsol	G	1.83	11.37	4.55	27.19
	A	2.22	13.56	5.34	31.16
	D.A	1.08	9.99	4.23	25.23
Dura.f	G	1.91	11.44	4.71	27.35
	A	2.22	13.56	5.34	31.16
	D.A	1.08	9.99	4.23	25.23
Dura.t	G	1.33	10.87	3.45	26.09
	A	1.69	13.02	4.23	30.06
	D.A	0.81	9.72	3.52	24.52
Hyplyt	G	1.11	10.65	2.98	25.62
	A	1.40	12.74	3.60	29.43
	D.A	0.90	9.82	2.84	23.83
Agphan	G	1.76	11.30	4.39	27.04
	A	2.14	13.47	5.18	31.00
	D.A	1.48	10.39	4.08	25.07

Table 5.4d L.P.G. usage (in kg/m²) and cost (in $/m²) for screened and non-screened greenhouses in Christchurch at set points of 15°C and 20°C.

Screen Type	Cov. Type	15°C		20°C	
		kg/m²	$/m²	kg/m²	$/m²
None	G	19.89	17.25	43.44	37.67
	A	23.60	20.46	50.33	43.64
	D.A	18.05	15.65	39.77	34.48
LS 13	G	12.30	10.67	28.65	24.84
	A	13.85	12.00	31.39	27.22
	D.A	10.79	9.35	26.18	22.70
LS 15	G	11.49	9.97	27.06	23.46
	A	13.05	11.32	29.95	25.97
	D.A	10.36	8.98	24.58	21.31
LS 18	G	10.69	9.27	25.46	22.08
	A	12.05	10.45	27.97	24.25
	D.A	9.30	8.06	23.03	19.97
LS 18F	G	10.90	9.45	25.86	22.42
	A	12.25	10.62	28.35	24.58
	D.A	9.79	8.49	23.40	20.29
Marix	G	12.10	10.49	28.26	24.50
	A	13.85	12.00	31.39	27.22
	D.A	10.96	9.50	25.78	22.35
Clr.PE	G	10.32	8.95	24.66	21.38
	A	12.05	10.45	27.97	24.25
	D.A	9.42	8.17	22.66	19.65
Blk.PE	G	8.05	6.98	20.38	17.67
	A	9.69	8.40	23.01	19.95
	D.A	7.38	6.39	18.21	15.79
Infran	G	9.07	7.86	22.06	19.12
	A	10.71	9.29	25.23	21.88
	D.A	8.39	7.28	20.44	17.72
Infsol	G	9.41	8.16	22.80	19.77
	A	11.28	9.78	26.36	22.85
	D.A	7.30	6.33	21.18	18.36
Dura.f	G	9.58	8.30	23.17	20.09
	A	11.28	9.78	26.36	22.85
	D.A	7.30	6.33	21.18	18.36
Dura.t	G	8.22	7.13	20.20	17.52
	A	10.03	8.69	23.75	20.59
	D.A	6.66	5.77	19.50	16.91
Hyplyt	G	7.71	6.68	19.09	16.55
	A	9.35	8.10	22.27	19.30
	D.A	6.88	5.97	17.88	15.51
Agphan	G	9.24	8.01	22.43	19.44
	A	11.09	9.61	25.98	22.52
	D.A	8.24	7.15	20.81	18.04

Table 5.5a AHC, AS, and IRR of 300m² and 1000m² screened greenhouses in Auckland, for diesel heating, at T_s=15°C.

Scrn	Cov	AHC ($)		AS ($)		IRR	
		300m²	1000m²	300m²	1000m²	300m²	1000m²
LS13	G	994	3,313	849	2,829	0.08	0.14
	A		3,738		3,675		0.24
	D.A		2,717		2,543		0.10
LS15	G	912	3,040	931	3,102	0.09	0.13
	A		3,436		3,977		0.24
	D.A		2,488		2,772		0.10
LS18	G	843	2,812	999	3,331	0.10	0.16
	A		3,116		4,298		0.26
	D.A		2,274		2,986		0.12
L18F	G	860	2,865	983	3,277	0.10	0.15
	A		3,172		4,242		0.25
	D.A		2,328		2,932		0.11
Marx	G	972	3,239	871	2,903	-0.08	0.04
	A		3,738		3,675		0.16
	D.A		2,652		2,609		-0.02
ClPE	G	811	2,705	1,031	3,438	0.16	0.29
	A		3,116		4,298		0.43
	D.A		2,221		3,039		0.22
BkPE	G	606	2,021	1,236	4,121	0.27	0.41
	A		2,420		4,994		0.56
	D.A		1,636		3,624		0.33
Infn	G	699	2,330	1,144	3,813	0.21	0.34
	A		2,741		4,672		0.48
	D.A		1,899		3,361		0.26
Insl	G	731	2,437	1,112	3,705	0.11	0.22
	A		2,902		4,512		0.32
	D.A		2,006		3,254		0.14
Dufm	G	747	2,490	1,096	3,652	0.11	0.21
	A		2,902		4,512		0.33
	D.A		2,006		3,254		0.15
Dthm	G	619	2,062	1,224	4,080	0.16	0.26
	A		2,527		4,887		0.37
	D.A		1,698		3,562		0.19
Hylt	G	588	1,959	1,255	4,183	0.20	0.26
	A		2,313		5,100		0.35
	D.A		1,616		3,644		0.21
Agph	G	715	2,384	1,128	3,759	0.13	0.24
	A		2,848		4,565		0.35
	D.A		1,953		3,307		0.14

Table 5.5b AHC, AS, and IRR of 300m² and 1000m² screened greenhouses in Auckland, for coal heating, at T_s=15°C.

Scrn	Cov	AHC ($)		AS ($)		IRR	
		300m²	1000m²	300m²	1000m²	300m²	1000m²
LS13	G	574	1,914	490	1,634	-0.08	-0.03
	A		2,159		2,123		0.04
	D.A		1,570		1,469		-0.06
LS15	G	527	1,756	538	1,792	-0.07	-0.03
	A		1,985		2,297		0.04
	D.A		1,437		1,601		-0.06
LS18	G	487	1,624	577	1,924	-0.06	-0.02
	A		1,800		2,483		0.06
	D.A		1,313		1,725		-0.05
L18F	G	496	1,655	568	1,893	-0.06	-0.03
	A		1,832		2,450		0.05
	D.A		1,345		1,694		-0.05
Marx	G	561	1,871	503	1,677	-0.28	-0.21
	A		2,159		1,123		-0.12
	D.A		1,532		1,507		-0.25
ClPE	G	469	1,562	596	1,986	-0.07	0.02
	A		1,800		2,483		0.12
	D.A		1,283		1,756		-0.02
BkPE	G	350	1,167	714	2,381	0.01	0.11
	A		1,398		2,885		0.20
	D.A		945		2,093		0.05
Infn	G	404	1,346	661	2,202	-0.04	0.05
	A		1,583		2,699		0.15
	D.A		1,097		1,941		0.00
Insl	G	422	1,408	642	2,140	-0.11	-0.04
	A		1,676		2,606		0.04
	D.A		1,159		1,879		-0.09
Dufm	G	431	1,438	633	2,110	-0.11	-0.04
	A		1,676		2,606		0.05
	D.A		1,159		1,879		-0.08
Dthm	G	357	1,191	707	2,357	-0.07	0.00
	A		1,459		2,823		0.08
	D.A		981		2,058		-0.05
Hylt	G	340	1,132	725	2,416	0.03	0.07
	A		1,336		2,946		0.13
	D.A		934		2,105		0.04
Agph	G	413	1,377	651	2,171	-0.09	-0.02
	A		1,645		2,637		0.06
	D.A		1,128		1,910		-0.07

Table 5.5c AHC, AS, and IRR of 300m² and 1000m² screened greenhouses in Auckland, for electrical heating, at T_a=15°C.

Scrn	Cov	AHC ($)		AS ($)		IRR	
		300m²	1000m²	300m²	1000m²	300m²	1000m²
LS13	G	1,457	4,855	423	1,410	-0.11	-0.08
	A		5,403		1,832		0.00
	D.A		4,006		1,268		-0.10
LS15	G	1,416	4,719	464	1,546	-0.11	-0.07
	A		5,253		1,983		0.00
	D.A		3,893		1,382		-0.10
LS18	G	1,382	4,605	498	1,660	-0.10	-0.06
	A		5,093		2,142		0.01
	D.A		3,786		1,489		-0.09
L18F	G	1,390	4,632	490	1,634	-0.10	-0.06
	A		5,121		2,114		0.01
	D.A		3,813		1,462		-0.09
Marx	G	1,446	4,818	434	1,447	-0.33	-0.26
	A		5,403		1,832		-0.21
	D.A		3,974		1,300		-0.29
ClPE	G	1,366	4,552	514	1,714	-0.12	-0.04
	A		5,093		2,142		0.05
	D.A		3,759		1,515		-0.08
BkPE	G	1,263	4,211	616	2,054	-0.06	0.04
	A		4,746		2,489		0.13
	D.A		3,468		1,807		-0.01
Infn	G	1,309	4,365	570	1,901	-0.09	-0.01
	A		4,906		2,329		0.08
	D.A		3,599		1,675		-0.08
Insl	G	1,326	4,419	554	1,847	-0.16	-0.09
	A		4,986		2,249		-0.02
	D.A		3,652		1,622		-0.14
Dufm	G	1,333	4,445	546	1,821	-0.15	-0.09
	A		4,986		2,249		-0.01
	D.A		3,652		1,622		-0.13
Dthm	G	1,269	4,232	610	2,034	-0.13	-0.06
	A		4,799		2,436		0.01
	D.A		3,498		1,776		-0.10
Hylt	G	1,254	4,180	626	2,085	0.00	0.03
	A		4,693		2,542		0.09
	D.A		3,458		1,816		0.00
Agph	G	1,318	4,392	526	1,874	-0.14	-0.07
	A		4,960		2,276		0.00
	D.A		3,626		1,649		-0.12

Table 5.5d AHC, AS, and IRR 300m² and 1000m² of screened greenhouses in Auckland, for natural gas heating, at T_i=15°C.

Scrn	Cov	AHC ($)		AS ($)		IRR	
		300m²	1000m²	300m²	1000m²	300m²	1000m²
LS13	G	526	1,753	449	1,497	-0.10	-0.06
	A		1,978		1,944		0.01
	D.A		1,437		1,345		-0.09
LS15	G	483	1,608	492	1,641	-0.09	-0.05
	A		1,818		2,104		0.01
	D.A		1,316		1,466		-0.08
LS18	G	446	1,487	529	1,762	-0.08	-0.04
	A		1,648		2,274		0.03
	D.A		1,203		1,580		-0.07
L18F	G	455	1,516	520	1,734	-0.09	-0.05
	A		1,678		2,244		0.02
	D.A		1,232		1,551		-0.08
Marx	G	514	1,714	461	1,536	-0.31	-0.24
	A		1,978		1,944		-0.15
	D.A		1,403		1,380		-0.28
ClPE	G	429	1,431	546	1,819	-0.11	-0.02
	A		1,648		2,274		0.08
	D.A		1,175		1,608		-0.06
BkPE	G	321	1,069	654	2,180	0.01	0.07
	A		1,280		2,642		0.15
	D.A		866		1,917		0.01
Infn	G	370	1,232	605	2,017	-0.07	0.02
	A		1,450		2,472		0.11
	D.A		1,005		1,778		-0.03
Insl	G	387	1,289	588	1,960	-0.14	-0.07
	A		1,535		2,387		0.00
	D.A		1,061		1,721		-0.12
Dufm	G	395	1,317	580	1,932	-0.13	-0.07
	A		1,535		2,387		0.01
	D.A		1,061		1,721		-0.11
Dthm	G	327	1,091	648	2,159	-0.10	-0.03
	A		1,337		2,585		0.04
	D.A		898		1,885		-0.08
Hylt	G	311	1,036	664	2,213	0.01	0.05
	A		1,234		2,698		0.11
	D.A		855		1,928		0.01
Agph	G	378	1,261	597	1,988	-0.12	-0.05
	A		1,507		2,415		0.02
	D.A		1,033		1,750		-0.10

Table 5.6a AHC, AS, and IRR of 300m² and 1000m² screened greenhouses in Auckland, for diesel heating, at T_s=20°C.

Scrn	Cov	AHC ($)		AS ($)		IRR	
		300m²	1000m²	300m²	1000m²	300m²	1000m²
LS13	G	4,118	13,726	2,425	8,084	0.58	0.69
	A		15,283		10,416		0.92
	D.A		12,532		7,343		0.62
LS15	G	3,870	12,899	2,673	8,911	0.60	0.71
	A		14,457		11,242		0.92
	D.A		11,708		8,167		0.65
LS18	G	3,623	12,075	2,920	9,735	0.64	0.75
	A		13,426		12,273		0.97
	D.A		10,884		8,991		0.69
L18F	G	3,685	12,282	2,858	9,528	0.62	0.74
	A		13,633		12,066		0.95
	D.A		11,089		8,785		0.68
Marx	G	4,056	13,519	2,487	8,291	0.62	0.85
	A		15,283		10,416		1.14
	D.A		12,327		7,548		0.74
ClPE	G	3,499	11,663	3,044	10,147	0.99	1.29
	A		13,426		12,273		1.57
	D.A		10,677		9,197		1.16
BkPE	G	2,737	9,124	3,806	12,685	1.30	1.67
	A		10,811		14,888		1.97
	D.A		8,406		11,469		1.50
Infn	G	3,077	10,257	3,466	11,553	1.13	1.45
	A		11,983		13,716		1.74
	D.A		9,505		10,370		1.29
Insl	G	3,193	10,642	3,350	11,168	0.90	1.12
	A		12,602		13,097		1.33
	D.A		9,890		9,985		0.98
Dufm	G	3,252	10,839	3,291	10,971	0.90	1.11
	A		12,602		13,097		1.37
	D.A		9,890		9,985		1.01
Dthm	G	2,791	9,302	3,752	12,507	1.03	1.28
	A		11,196		14,504		1.50
	D.A		8,757		11,118		1.12
Hylt	G	2,632	8,774	3,911	13,036	0.87	1.01
	A		10,427		15,272		1.18
	D.A		8,230		11,645		0.89
Agph	G	3,135	10,451	3,408	11,359	0.95	1.20
	A		12,395		13,304		1.42
	D.A		9,698		10,177		1.06

Table 5.6b AHC, AS, and IRR of 300m² and 1000m² screened greenhouses in Auckland, for coal heating, at T_s=20°C.

Scrn	Cov	AHC ($)		AS ($)		IRR	
		300m²	1000m²	300m²	1000m²	300m²	1000m²
LS13	G	2,379	7,928	1,401	4,670	0.27	0.35
	A		8,828		6,017		0.49
	D.A		7,239		4,242		0.30
LS15	G	2,235	7,451	1,544	5,147	0.29	0.36
	A		8,351		6,494		0.49
	D.A		6,763		4,718		0.32
LS18	G	2,092	6,975	1,687	5,623	0.31	0.39
	A		7,755		7,090		0.53
	D.A		6,287		5,194		0.35
L18F	G	2,128	7,094	1,651	5,504	0.30	0.38
	A		7,875		6,970		0.51
	D.A		6,406		5,075		0.35
Marx	G	2,343	7,809	1,437	4,789	0.20	0.34
	A		8,828		6,017		0.52
	D.A		7,120		4,360		0.28
ClPE	G	2,021	6,737	1,758	5,861	0.49	0.67
	A		7,755		7,090		0.85
	D.A		6,168		5,313		0.59
BkPE	G	1,581	5,270	2,198	7,328	0.68	0.91
	A		6,245		8,600		1.09
	D.A		4,856		6,625		0.81
Infn	G	1,777	5,925	2,002	6,673	0.56	0.78
	A		6,922		7,923		0.95
	D.A		5,491		5,990		0.67
Insl	G	1,844	6,147	1,935	6,451	0.42	0.57
	A		7,279		7,565		0.70
	D.A		5,713		5,768		0.48
Dufm	G	1,878	6,261	1,901	6,337	0.43	0.57
	A		7,279		7,565		0.73
	D.A		5,713		5,768		0.50
Dthm	G	1,612	5,373	2,165	7,225	0.51	0.67
	A		6,467		8,378		0.81
	D.A		5,058		6,422		0.57
Hylt	G	1,520	5,068	22,59	7,530	0.47	0.56
	A		6,023		8,822		0.67
	D.A		4,754		6,727		0.49
Agph	G	1,811	6,037	1,968	6,561	0.46	0.61
	A		7,160		7,685		0.75
	D.A		5,602		5,879		0.53

Table 5.6c AHC, AS, and IRR of 300m² and 1000m² screened greenhouses in Auckland, for electrical heating, at T_a=20°C.

Scrn	Cov	AHC ($)		AS ($)		IRR	
		300m²	1000m²	300m²	1000m²	300m²	1000m²
LS13	G	5,234	17,448	1,209	4,030	0.21	0.28
	A		19,826		5,192		0.41
	D.A		16,226		3,660		0.24
LS15	G	5,111	17,036	1,333	4,442	0.22	0.29
	A		19,415		5,604		0.41
	D.A		15,815		4,071		0.25
LS18	G	4,987	16,625	1,456	4,852	0.25	0.32
	A		18,901		6,118		0.44
	D.A		15,404		4,482		0.28
L18F	G	5,018	16,728	1,425	4,749	0.24	0.31
	A		19,004		6,015		0.43
	D.A		15,507		4,379		0.27
Marx	G	5,205	17,345	1,240	4,133	0.11	0.24
	A		19,826		5,192		0.40
	D.A		16,124		3,762		0.18
ClPE	G	4,926	16,420	1,517	5,058	0.38	0.55
	A		18,901		6,118		0.71
	D.A		15,301		4,585		0.48
BkPE	G	4,546	15,154	1,897	6,323	0.56	0.76
	A		17,597		7,421		0.92
	D.A		14,169		5,717		0.67
Infn	G	4,716	15,719	1,728	5,759	0.46	0.64
	A		18,182		6,837		0.80
	D.A		14,717		5,169		0.55
Insl	G	4,773	15,911	1,670	5,567	0.33	0.46
	A		18,490		6,529		0.58
	D.A		14,909		4,977		0.38
Dufm	G	8,403	16,009	1,641	5,469	0.33	0.46
	A		18,490		6,529		0.60
	D.A		14,909		4,977		0.40
Dthm	G	4,573	15,243	1,870	6,235	0.41	0.55
	A		17,789		7,230		0.67
	D.A		14,344		5,542		0.46
Hylt	G	4,494	14,979	1,949	6,498	0.39	0.47
	A		17,406		7,613		0.57
	D.A		14,081		5,805		0.41
Agph	G	4,745	15,815	1,699	5,662	0.36	0.50
	A		18,387		6,631		0.62
	D.A		14,813		5,073		0.42

Table 5.6d AHC, AS, and IRR of 300m² and 1000m² screened greenhouses in Auckland, for natural gas heating, at T_s=20°C.

Scrn	Cov	AHC ($)		AS ($)		IRR	
		300m²	1000m²	300m²	1000m²	300m²	1000m²
LS13	G	2,178	7,261	1,283	4,277	0.23	0.31
	A		8,085		5,511		0.44
	D.A		6,630		3,885		0.26
LS15	G	2,047	6,824	1,414	4,714	0.25	0.32
	A		7,648		5,947		0.44
	D.A		6,194		4,321		0.28
LS18	G	1,916	6,388	1,545	5,150	0.27	0.35
	A		7,103		6,493		0.47
	D.A		5,758		4,757		0.31
L18F	G	1,949	6,498	1,512	5,040	0.26	0.33
	A		7,212		6,384		0.46
	D.A		5,867		4,648		0.30
Marx	G	2,146	7,152	1,316	4,386	0.13	0.28
	A		8,085		5,511		0.45
	D.A		6,521		3,993		0.22
ClPE	G	1,851	6,170	1,610	5,368	0.43	0.60
	A		7,103		6,493		0.77
	D.A		5,649		4,866		0.52
BkPE	G	1,448	4,827	2,013	6,711	0.60	0.82
	A		5,720		7,876		0.99
	D.A		4,447		6,067		0.72
Infn	G	1,628	5,426	1,834	6,112	0.50	0.69
	A		6,340		7,256		0.86
	D.A		5,029		5,486		0.60
Insl	G	1,689	5,630	1,772	5,908	0.37	0.50
	A		6,667		6,929		0.62
	D.A		5,232		5,283		0.42
Dufm	G	1,720	5,734	1,741	5,804	0.37	0.50
	A		6,667		6,929		0.65
	D.A		5,232		5,283		0.43
Dthm	G	1,476	4,921	1,985	6,617	0.45	0.59
	A		5,923		7,673		0.72
	D.A		4,633		5,882		0.50
Hylt	G	1,392	4,642	2,069	6,897	0.43	0.51
	A		5,516		8,079		0.60
	D.A		4,354		6,161		0.44
Agph	G	1,659	5,529	1,803	6,009	0.40	0.54
	A		6,558		7,038		0.68
	D.A		5,130		5,384		0.46

Table 5.7a AHC, AS, and IRR of 300m² and 1000m² screened greenhouses in Christchurch, for diesel heating, at T_a=15°C.

Scrn	Cov	AHC ($)		AS ($)		IRR	
		300m²	1000m²	300m²	1000m²	300m²	1000m²
LS13	G	3,139	10,464	1,937	6,456	0.44	0.54
	A		11,777		8,300		0.72
	D.A		9,174		6,181		0.51
LS15	G	2,933	9,778	2,143	7,142	0.46	0.55
	A		11,104		8,973		0.72
	D.A		8,813		6,542		0.50
LS18	G	2,729	9,096	2,347	7,823	0.49	0.59
	A		10,253		9,824		0.76
	D.A		7,912		7,443		0.56
L18F	G	2,780	9,268	2,296	7,652	0.48	0.58
	A		10,423		9,654		0.75
	D.A		8,331		7,024		0.52
Marx	G	3,087	10,289	1,989	6,631	0.43	0.62
	A		11,777		8,300		0.85
	D.A		9,324		6,031		0.53
ClPE	G	2,634	8,778	2,442	8,141	0.76	1.00
	A		10,253		9,824		1.25
	D.A		8,015		7,339		0.89
BkPE	G	2,054	6,847	3,022	10,073	1.00	1.30
	A		8,239		11,838		1.56
	D.A		6,274		9,081		1.16
Infn	G	2,314	7,714	2,762	9,206	0.87	1.13
	A		9,114		10,963		1.37
	D.A		7,140		8,215		0.99
Insl	G	2,401	8,002	2,675	8,917	0.68	0.86
	A		9,594		10,483		1.04
	D.A		6,211		9,144		0.89
Dufm	G	2,444	8,148	2,632	8,772	0.68	0.87
	A		9,594		10,483		1.07
	D.A		6,211		9,144		0.92
Dthm	G	2,097	6,990	2,979	9,929	0.79	0.98
	A		8,529		11,547		1.17
	D.A		5,664		9,690		0.96
Hylt	G	1,967	6,557	3,109	10,363	0.68	0.79
	A		7,951		12,126		0.93
	D.A		5,855		9,500		0.72
Agph	G	2,357	7,858	2,718	9,062	0.72	0.92
	A		9,429		10,647		1.11
	D.A		7,010		8,345		0.84

Table 5.7b AHC, AS, and IRR of 300m² and 1000m² screened greenhouses in Christchurch, for coal heating, at T_a=15°C.

Scrn	Cov	AHC ($)		AS ($)		IRR	
		300m²	1000m²	300m²	1000m²	300m²	1000m²
LS13	G	1,813	6,044	1,119	3,729	0.18	0.24
	A		6,803		4,794		0.36
	D.A		5,299		3,570		0.22
LS15	G	1,694	5,648	1,238	4,125	0.19	0.26
	A		6,414		5,183		0.37
	D.A		5,091		3,779		0.22
LS18	G	1,576	5,254	1,356	4,519	0.22	0.28
	A		5,299		5,675		0.40
	D.A		4,570		4,300		0.26
L18F	G	1,606	5,353	1,326	4,420	0.21	0.27
	A		6,020		5,577		0.39
	D.A		4,812		4,057		0.24
Marx	G	1,783	5,943	1,149	3,830	0.06	0.19
	A		6,803		4,794		0.34
	D.A		5,386		3,484		0.13
ClPE	G	1,521	5,071	1,411	4,703	0.34	0.49
	A		5,922		5,675		0.64
	D.A		4,630		4,240		0.42
BkPE	G	1,186	3,955	1,746	5,818	0.49	0.68
	A		4,759		6,838		0.84
	D.A		3,624		5,246		0.60
Infn	G	1,337	4,456	1,595	5,317	0.41	0.57
	A		5,265		6,332		0.73
	D.A		4,124		4,745		0.49
Insl	G	1,387	4,622	1,545	5,151	0.28	0.40
	A		5,542		6,055		0.52
	D.A		3,588		5,282		0.42
Dufm	G	1,412	4,706	1,520	5,067	0.29	0.41
	A		5,542		6,055		0.54
	D.A		3,588		5,282		0.44
Dthm	G	1,211	4,038	1,721	5,735	0.35	0.48
	A		4,927		6,670		0.60
	D.A		3,272		5,597		0.47
Hylt	G	1,136	3,787	1,796	5,986	0.36	0.43
	A		4,592		7,005		0.52
	D.A		3,382		5,488		0.38
Agph	G	1,362	4,539	1,570	5,234	0.31	0.44
	A		5,447		6,150		0.56
	D.A		4,049		4,820		0.39

Table 5.7c AHC, AS, and IRR of 300m² and 1000m² screened greenhouses in Christchurch, for electrical heating, at T_s=15°C.

Scrn	Cov	AHC ($)		AS ($)		IRR	
		300m²	1000m²	300m²	1000m²	300m²	1000m²
LS13	G	3,779	12,597	965	3,218	0.12	0.18
	A		14,643		4,137		0.29
	D.A		11,471		3,081		0.17
LS15	G	3,676	12,255	1,068	3,560	0.13	0.19
	A		14,308		4,473		0.29
	D.A		11,291		3,261		0.16
LS18	G	3,575	11,915	1,170	3,900	0.16	0.22
	A		13,884		4,897		0.32
	D.A		10,841		3,710		0.20
L18F	G	3,600	12,001	1,144	3,814	0.15	0.21
	A		13,968		4,812		0.31
	D.A		11,050		3,501		0.18
Marx	G	3,753	12,510	992	3,305	-0.05	0.10
	A		14,643		4,137		0.24
	D.A		11,545		3,006		0.05
ClPE	G	3,527	11,757	1,217	4,058	0.25	0.39
	A		13,884		4,897		0.52
	D.A		10,893		3,658		0.33
BkPE	G	3,238	10,794	1,506	5,021	0.39	0.56
	A		12,880		5,901		0.70
	D.A		10,025		4,527		0.48
Infn	G	3,368	11,226	1,377	4,589	0.31	0.46
	A		13,316		5,465		0.60
	D.A		10,457		4,095		0.38
Insl	G	3,411	11,370	1,333	4,445	0.20	0.31
	A		13,555		5,225		0.41
	D.A		9,994		4,558		0.32
Dufm	G	3,433	11,442	1,312	4,372	0.20	0.31
	A		13,555		5,225		0.43
	D.A		9,994		4,558		0.34
Dthm	G	3,260	10,866	1,485	4,949	0.26	0.38
	A		13,025		5,756		0.49
	D.A		9,721		4,830		0.37
Hylt	G	3,195	10,649	1,550	5,165	0.29	0.35
	A		12,736		6,045		0.43
	D.A		9,816		4,735		0.31
Agph	G	3,389	11,298	1,355	4,517	0.23	0.34
	A		13,473		5,307		0.45
	D.A		10,392		4,160		0.29

Table 5.7d AHC, AS, and IRR of 300m² and 1000m² screened greenhouses in Christchurch, for L.P.G. heating, at T_s=15°C.

Scrn	Cov	AHC ($)		AS ($)		IRR	
		300m²	1000m²	300m²	1000m²	300m²	1000m²
LS13	G	3,200	10,665	1,974	6,580	0.45	0.55
	A		12,004		8,460		0.73
	D.A		9,351		6,300		0.52
LS15	G	2,990	9,966	2,184	7,279	0.47	0.57
	A		11,318		9,146		0.73
	D.A		8,983		6,668		0.51
LS18	G	2,781	9,272	2,392	7,974	0.51	0.61
	A		10,450		10,013		0.78
	D.A		8,064		7,587		0.57
L18F	G	2,834	9,446	2,340	7,799	0.49	0.59
	A		10,623		9,840		0.77
	D.A		8,491		7,160		0.53
Marx	G	3,146	10,487	2,028	6,759	0.44	0.64
	A		12,004		8,460		0.88
	D.A		9,504		6,147		0.55
ClPE	G	2,684	8,948	2,489	8,298	0.78	1.03
	A		10,450		10,013		1.27
	D.A		8,170		7,481		0.91
BkPE	G	2,094	6,978	3,080	10,267	1.02	1.33
	A		8,398		12,066		1.59
	D.A		6,394		9,256		1.19
Infn	G	2,359	7,863	2,815	9,383	0.88	1.15
	A		9,290		11,174		1.40
	D.A		7,278		8,373		1.01
Insl	G	2,447	8,157	2,727	9,089	0.69	0.88
	A		9,779		10,685		1.06
	D.A		6,331		9,320		0.91
Dufm	G	2,491	8,305	2,682	8,941	0.70	0.89
	A		9,779		10,685		1.10
	D.A		6,331		9,320		0.94
Dthm	G	2,138	7,125	3,036	10,120	0.80	1.01
	A		8,694		11,770		1.20
	D.A		5,774		9,877		0.98
Hylt	G	2,005	6,683	3,169	10,562	0.69	0.81
	A		8,104		12,360		0.95
	D.A		5,968		9,683		0.74
Agph	G	2,403	8,009	2,771	9,236	0.74	0.94
	A		9,611		10,853		1.13
	D.A		7,145		8,506		0.86

The following observations were made from Tables 5.5a-5.7d:

1. IRR of thermal screens was greatest in the single skin *Agphane* house, mediocre in the glass houses and lowest in the double skin houses.

2. The IRR of thermal screens were greater in 1000m^2 glasshouses than in 300m^2 glasshouses.

3. The IRR of thermal screens were greater at the 20°C set point than at 15°C.

4. The IRR of thermal screens were greater in Christchurch than those in Auckland.

5. In Auckland at both set points, IRR for screens were greatest when diesel was the heating fuel. The IRR for screens with coal, electricity and natural gas were similar in magnitude.

6. In Christchurch at the 15°C set point, IRR for screens were greatest with diesel and L.P.G. Electricity and coal both had lower IRR.

7. In each test Black PE had the highest IRR and *Marix* the lowest. Although a middle order was not so clearly defined, *Infrane*, *Hyperlyte*, *Duratherm* and Clear PE were consistently characterised by relatively high IRR.

CHAPTER VI

DISCUSSION

To be a wise investment, the IRR for a thermal screen must exceed the ERR of alternate money making ventures. To all intents and purposes this study assumed the grower did not have to borrow to finance screen installation, and that an interest rate of 20% was available with bank investment accounts. As a result, thermal screen, cover, location, and set point combinations with IRRs less than 20% are not recommended.

To ascertain the feasibility of each combination an investment feasibility classification system was introduced based on the following IRR categories:

E	= exceptional investment	(IRR above 99%)
V	= very profitable investment	(IRR of 70%-99%)
P	= profitable investment	(IRR of 40%-69%)
W	= worthwhile investment	(IRR of 20%-39%)
B	= bad investment	(IRR of 0%-19%)
L	= loss	(IRR below 0%)

Tables 6.1a-6.1c were constructed in accordance to these categories.

It should be noted that an ERR less than or greater than 20% promotes a shift in investment category. For example an ERR of 15% will cause many modelled combinations to ascend to more profitable categories. On the other hand an ERR of 25% will cause combinations to fall into less profitable categories.

Table 6.1a Investment feasibility of thermal screens in Auckland at 15°C.

Scrn	Cov	Diesel		Coal		Electric.		Nat. Gas	
		300	1000	300	1000	300	1000	300	1000
LS13	G	B	B	L	L	L	L	L	L
	A		W		B		B		B
	D.A		B		L		L		L
LS15	G	B	B	L	L	L	L	L	L
	A		W		B		B		B
	D.A		B		L		L		L
LS18	G	B	B	L	L	L	L	L	L
	A		W		B		B		B
	D.A		B		L		L		L
L18F	G	B	B	L	L	L	L	L	L
	A		W		B		B		B
	D.A		B		L		L		L
Marx	G	L	B	L	L	L	L	L	L
	A		B		L		L		L
	D.A		L		L		L		L
ClPE	G	B	W	L	B	L	L	L	L
	A		P		B		B		B
	D.A		W		L		L		L
BlPE	G	W	P	B	B	L	B	B	B
	A		P		W		B		B
	D.A		W		B		L		B
Infn	G	W	W	L	B	L	L	L	B
	A		P		B		B		B
	D.A		W		B		L		L
Insl	G	B	W	L	L	L	L	L	L
	A		W		B		L		B
	D.A		B		L		L		L
Dufm	G	B	W	L	L	L	L	L	L
	A		W		B		L		B
	D.A		B		L		L		L
Dthm	G	B	W	L	B	L	L	L	L
	A		W		B		B		B
	D.A		B		L		L		L
Hylt	G	W	W	B	B	B	B	B	B
	A		W		B		B		B
	D.A		W		B		B		B
Agph	G	B	W	L	L	L	L	L	L
	A		W		B		B		B
	D.A		B		L		L		L

Table 6.1b Investment feasibility of thermal screens in Auckland at 20°C.

Scrn	Cov	Diesel		Coal		Electric.		Nat. Gas	
		300	1000	300	1000	300	1000	300	1000
LS13	G	P	P	W	W	W	W	W	W
	A		V		P		P		P
	D.A		P		W		W		W
LS15	G	P	V	W	W	W	W	W	W
	A		V		P		P		P
	D.A		P		W		W		W
LS18	G	P	V	W	W	W	W	W	W
	A		V		P		P		P
	D.A		P		W		W		W
L18F	G	P	V	W	W	W	W	W	W
	A		V		P		P		P
	D.A		P		W		W		W
Marx	G	P	V	W	W	B	W	B	W
	A		E		P		P		P
	D.A		V		W		W		W
ClPE	G	V	E	P	P	W	P	P	P
	A		E		V		V		V
	D.A		E		P		P		P
BlPE	G	E	E	P	V	P	V	P	V
	A		E		E		V		V
	D.A		E		V		V		V
Infn	G	E	E	P	V	P	P	P	P
	A		E		V		V		V
	D.A		E		P		P		P
Insl	G	V	E	P	P	W	P	W	P
	A		E		V		P		P
	D.A		V		P		W		P
Dufm	G	V	E	P	P	W	P	W	P
	A		E		V		P		P
	D.A		E		P		P		P
Dthm	G	E	E	P	P	P	P	P	P
	A		E		V		P		V
	D.A		E		P		P		P
Hylt	G	V	E	P	P	W	P	P	P
	A		E		P		P		P
	D.A		V		P		P		P
Agph	G	V	E	P	P	W	P	P	P
	A		E		V		P		P
	D.A		E		P		P		P

Table 6.1c Investment feasibility of thermal screens in Christchurch at 15°C.

Scrn	Cov	Diesel		Coal		Electric.		L.P.G.	
		300	1000	300	1000	300	1000	300	1000
LS13	G	P	P	B	W	B	B	P	P
	A		V		W		W		V
	D.A		P		W		B		P
LS15	G	P	P	B	W	B	B	P	P
	A		V		W		W		V
	D.A		P		W		B		P
LS18	G	P	P	W	W	B	W	P	P
	A		V		P		W		V
	D.A		P		W		W		P
L18F	G	P	P	W	W	B	W	P	P
	A		V		W		W		V
	D.A		P		W		B		P
Marx	G	P	P	B	B	L	B	P	P
	A		V		W		W		V
	D.A		P		B		B		P
ClPE	G	V	E	W	P	W	W	V	E
	A		E		P		P		E
	D.A		V		P		W		V
BlPE	G	E	E	P	P	W	P	E	V
	A		E		V		V		V
	D.A		E		P		P		V
Infn	G	V	E	P	P	W	P	V	V
	A		E		V		P		V
	D.A		V		P		W		V
Insl	G	P	V	W	P	W	W	P	V
	A		E		P		P		E
	D.A		V		P		W		V
Dufm	G	P	V	W	P	W	W	V	V
	A		E		P		P		E
	D.A		V		P		W		V
Dthm	G	V	V	W	P	W	W	V	E
	A		E		P		P		E
	D.A		V		P		W		V
Hylt	G	P	V	W	P	W	W	P	V
	A		V		P		P		V
	D.A		V		W		W		V
Agph	G	V	V	W	P	W	W	V	V
	A		E		P		P		E
	D.A		V		W		W		V

6.1 SCREEN TYPE

To a grower contemplating thermal screening, information regarding the expected returns of each available system is important.

In Section 5.1 the thirteen screens were ranked according to their ability to reduce U-value. *Hyperlyte*, Black PE, and *Duratherm* were the top three in this list.

As a result a greenhouse screened with *Hyperlyte* will have:

- the lowest annual heat load (see Tables 5.2a and 5.2b),
- the lowest fuel use and cost figures (see Tables 5.3a-5.4d),
- the lowest annual heat cost (see Tables 5.5a-5.7d) and
- the highest annual savings in heating expenditure (see Tables 5.5a-5.7d).

Although this may seem a reasonable system for accessing the worth of thermal screens, it does not take account of screen cost and screen life, both of which affect the economic feasibility of the investment. An IRR assessment takes into account fuel savings, capital cost, screen life and facilitates a comparison with returns of alternate investment options (eg. bank investments). To have a high IRR the screen must have at least one of the following qualities:

1. high annual fuel savings,
2. low capital cost, or
3. long economic life.

In Table 6.1a, for 300m^2 houses heated with diesel, Black PE, *Infrane* and *Hyperlyte* stand out as the better investments. Each has a W investment (ie. IRR 20-39 %). In Table 6.1b however, keeping with 300m^2 houses heated with diesel, Black PE, *Infrane* and *Duratherm* were the better investments. Each has an E investment (ie. IRR above 99 %). *Hyperlyte* is no longer in the leading category but has slipped to a V investment (ie. IRR 70-99 %). In Table 6.1c, again keeping with

300m² houses heated with diesel, Black PE stands alone as the best investment. Clear PE, *Infrane*, *Duratherm* and *Agphane* are in the second most economic category, and *Hyperlyte* offers one of the lowest pay offs. *Hyperlyte* therefore dropped from a leading investment in Auckland at 15°C, with diesel heating, to a poor investment in Christchurch at 15°C with diesel heating.

Using Tables 6.5a-6.7d the following categorisation of IRR rankings was put together. The thermal screen with the highest IRR (found by averaging the IRR of all three cover types and house sizes) features at the top.

Auckland at 15°C	Auckland at 20°C	Christchch. at 15°C
Black PE	Black PE	Black PE
Hyperlyte	*Infrane*	*Infrane*
Infrane	Clear PE	Clear PE
Clear PE	*Duratherm*	*Duratherm*
Duratherm	*Agphane*	*Agphane*
Agphane	*Infrasol*	*Durafilm*
LS 18	*Durafilm*	*Infrasol*
LS 18F	*Hyperlyte*	*Hyperlyte*
Durafilm	*LS 18*	*LS 18*
Infrasol	*LS 18F*	*LS 18F*
LS 15	*LS 15*	*LS 15*
LS 13	*Marix*	*LS 13*
Marix	*LS 13*	*Marix*

Of the thirteen materials tested, Black PE cost the least at \$0.45/m² (see Table 4.3). This together with its very low U-value caused it to rank above the others in each situation. *Hyperlyte* recorded the lowest U-value and had the longest economic life of 7 years (see Table 4.3). When the T_o T_s temperature difference was low (ie. Auckland at 15°C), *Hyperlyte* ranked highly. However as the temperature difference increased, as a result of high T_s and/or low T_o, *Hyperlyte* was displaced from the top order due to its expense (\$5.85/m²). Materials such as Clear PE, with moderate U-value and low cost, and *Duratherm* with it's low U-value and moderate cost, moved up in rank.

Black PE, *Infrane*, Clear PE, *Duratherm*, and *Agphane* each had economic lives of 4 years and U-values between 4.3 and 5.6$Wm^{-2}{}^{\circ}K^{-1}$. The main factor setting them apart was cost. *Infrane* and Clear PE cost \$0.75/m^2 and \$0.60/m^2 respectively while *Duratherm* and *Agphane* cost \$2.40/m^2 and \$2.10/m^2 respectively.

The IRR for thermal screens at the 20°C set point exceeded those of the 15°C set point. The IRR for thermal screens in Christchurch exceeded those of Auckland. As most screens in Christchurch at 15°C had IRR in excess of 70%, investigating their worth at 20°C was considered unnecessary.

During a hot day temperatures within the greenhouse may become dangerously high. If ventilation is insufficient plants may wilt or suffer sun scorch. An unfortunate shortcoming of the model was that assessing the shade value of each screen was beyond the scope of the study. If included, the LS range of permeable screens, which are commonly installed for crop shading, would have ranked much higher.

Photoperiodic crops such as chrysanthemums initiate flowers in response to short days. Short days may be mimicked by drawing a blackout cover over the crop at dawn or dusk. As Black PE is completely opaque to visible radiation it was the only material with photoperiodic potential.

An advantage of the LS screens and *Marix* is their permeability. In contrast to plastic film screens permeable materials reduce problems associated with condensation and humidity such as disease outbreak and water droplet damage. Such issues were also beyond the scope of the study. Had the model addressed these issues the LS screens and *Marix* would have ranked much higher.

6.2 SECONDARY ISSUES

6.2.1 COVER TYPE

An *Agphane* cover transmits thermal radiation. In this study it was shown to have a long wave transmission of 0.37. Double layer covers transmit less thermal radiation than single layer covers as twice the resistance is encounted. A twin *Agphane* cover is therefore more effective as a thermal barrier than a single *Agphane* cover. Glass on the other hand is opaque to thermal radiation. When used as a greenhouse cover however, heat escapes through loose construction and unsealed glazing gaps.

In Table 5.1 the *Agphane* covered greenhouse (CAI=1.6) had an average U-value of 11.2$Wm^{-2}floor^{\circ}K^{-1}$, the glass covered house (CAI=1.2) had an average U-value 9.9$Wm^{-2}floor^{\circ}K^{-1}$, and the twin skin *Agphane* house (CAI=1.6) had an average value of 9.2$Wm^{-2}floor^{\circ}K^{-1}$. As a result the single skin *Agphane* house would lose the most heat per m^2 of floor and the twin skin *Agphane* house would lose the least. Table 5.1 suggests that thermal screening reduces the U-value of *Agphane*, double *Agphane*, and glass covered houses by up to 65 %.

Greenhouses which are naturally heat conservative have low heating costs. This is seen in Tables 5.3a-5.4d where *Agphane* covered houses were the most expensive to heat, followed by glass, followed by double *Agphane* covered houses. As a thermal screen is effectively a heat saving device it follows they are more suited to houses that readily lose heat. This is seen in Tables 5.5a-5.7d where *Agphane* covered houses gave the highest IRR and the double *Agphane* covered houses gave the least.

IRRs for thermal screens were consistently higher in single *Agphane* houses followed by glass houses, and then double *Agphane*. In Table 6.1a-6.1c the investment feasibility is highest in single *Agphane* houses and least in double *Agphane* houses no matter what location set point or screen type.

6.2.2 GREENHOUSE SIZE

Economy of scale is a well known economic theory which explains why the outlay on a commodity decreases proportionally as more is purchased. As Table 4.3 suggests there is no exception to this theory when it comes to installing a thermal screen in a $300m^2$ or $1000m^2$ glasshouse.

On a per m^2 basis it costs less to install a screen in a $1000m^2$ house than a $300m^2$ house. The reason for this being items such as the control and drive system cost the same irrespective of size. The results demonstrate economy of scale as the IRR of thermal screens in $1000m^2$ glass houses were consistently higher than those in $300m^2$ glass houses (see Tables 5.5a-5.7d).

6.2.3 SET POINT

Set point temperature has a marked influence on thermal screen feasibility. The greater the set point the greater the heating cost as more fuel is required to meet the set point. Screen feasibility increases as fuel use increases. The results illustrate this point as the IRR in Tables 5.5a-5.5d (Auckland at $15^{\circ}C$) are lower than those in Tables 5.6a-5.6d (Auckland at $20^{\circ}C$).

6.2.4 LOCATION

The T_a T_o temperature difference is naturally greater in Christchurch compared with Auckland. The driving force for heat loss through the cover is therefore greater in Christchurch. Because of this more is gained by thermal screening in Christchurch. Tables 6.1a and 6.1c illustrate this as investment feasibilities in Christchurch are at least two categories above those in Auckland.

6.2.5 FUEL TYPE

In Auckland at both set points, the use of thermal screens with diesel heating provides the most feasible investment. At 15°C thermal screening with diesel gives B and W feasibilities. This compares to coal, electricity and natural gas, all of which are one investment category lower than diesel. At 20°C the diesel and thermal screen combinations gives P and V feasibilities. Coal, electricity and natural gas are once again one investment category lower.

In Christchurch at 15°C diesel and L.P.G. offer mainly E and V investments. Electricity and coal are slightly less feasible with predominately W and P investments.

CHAPTER VII

SUMMARY AND CONCLUSIONS

A greenhouse grower has several options when it comes to conserving heating fuel. Deciding which option to choose can be complicated and goes beyond simple advantage and disadvantage comparisons. Decision making agents based on economic criteria are useful as they consider the grower's cash flow. This study evaluated the heat saving potential of thermal screens in New Zealand using IRR as an economic criterion.

The principle objectives of this study involved the development of a mathematical model to evaluate the economic feasibility of thermal screens as heat savers. Thirteen materials with thermal screen potential were investigated within glass, *Agphane*, and twin skin *Agphane* greenhouses, at heating set points of 15°C and 20°C, in Auckland and Christchurch when diesel, coal, electricity, natural gas and L.P.G. were heating fuels.

The model was split into two parts; Phase 1, Phase 2, together with an IRR analysis. In Phase 1 the U-values of screened and unscreened greenhouses were simulated by solving heat and mass balances simultaneously. Along with meterological data for Auckland and Christchurch, the U-values served as inputs

to Phase 2. Phase 2 of the model found the annual auxiliary heat load of each screened greenhouse together with the load of its identical non-screened counterpart. Using these loads the heat saving of each combination was collated based on current fuel prices. An IRR analysis was conducted using:

1) monetary savings from thermal screens,
2) screen installation cost, and
3) screen economic life.

Practical problems associated with impermeable screens can have significant affects on plant productivity and hence the economic performance of the greenhouse system. It is also apparent that thermal screens have shade cloth value or may double as photoperiodic screens. Since these issues were beyond the scope of the study it is impossible to make an overall screen recommendation. Nevertheless the contribution this study makes to the energy saving performance of thermal screens in New Zealand is considerable.

The following conclusions were drawn from this study:

1) For a 15°C set point in Auckland the top five thermal screen materials, listed in order of feasibility as heat savers, were Black PE, *Infrane*, *Hyperlyte*, Clear PE and *Duratherm*. The top five materials for a 20°C set point in Auckland were Black PE, *Infrane*, and Clear PE, *Duratherm*, and *Agphane*. The top five in Christchurch at 15°C were Black PE, *Infrane*, Clear PE, *Duratherm*, and *Agphane*. It would be fairly safe assuming this order held for Christchurch at 20°C.

2) Greenhouses with heat retentive coverings (eg. twin skin structures), offer lower returns with thermal screens in comparison to structures prone to heat loss.

3) The larger the greenhouse the greater the returns from thermal screening.

4) Justification for thermal screens increase with set point temperature.

5) Justification for thermal screens increase as climatic conditions become cooler.

6) Returns from thermal screens in Auckland are the greatest when diesel is used as the heating fuel.

7) Returns from thermal screens in Christchurch are the greatest when diesel and L.P.G. are used as heating fuels.

CHAPTER VIII

RECOMMENDATIONS FOR FUTURE RESEARCH

The main limitation in this study was that economic feasibility was assessed solely in terms of heat savings. The analysis did not evaluate thermal screens as shade or photoperiod covers nor did it examine intangible issues such as unwanted shade, head room, positioning of plant support systems, and ease of retrofit to existing houses. Similarly the study did not penalise impermeable screens for inevitable product damage by harmful moisture tolerant organisms and the cost of sprays necessary to combat them.

The aim of future research should be to develop a method for evaluating such intangible issues, incorporating them with the heat saving results of this study to produce an overall ranking system. Only then will the absolute economic feasibility of thermal screens be known.

REFERENCES

Albright, L.D. (1983). New Double Layer Thermal Curtain Reduces Fuel Waste. *American Nurserymen.* **158** (10): 81-85.

Andrews, J.G. and McLone, R.R. (1976). *Mathematical Modelling.* Butterworths, London.

Arinze, E.A., Schoenau, G.J. and Besant, R.W. (1984). A Dynamic Thermal Performance Simulation Model of an Energy Conserving Greenhouse with Thermal Storage. *Trans. A.S.A.E.* **27** (2): 508-519.

Arinze, E.A., Schoenau, G.J. and Besant, R. W. (1986). Experimental and Computer Performance Evaluation of a Movable Thermal Insulation for Energy Conservation in Greenhouses. *J. Agric. Engng. Res.* **34** (1): 97-113.

Avissar, R. and Mahrer, Y. (1982). Verification Study of a Numerical Greenhouse Microclimate Model. *Trans. A.S.A.E.* **25** (6): 1711-1719.

Badger, P.C. and Poole, H.A. (1979). *Conserving Energy in Ohio Greenhouses.* Extension Bulletin 651. Ohio Department of Energy. Ohio State University. Ohio.

Bailey, B.J. and Winspear, K.W. (1975). Reducing the Heat Requirements of a Glasshouse. *Acta Hort.* **51**: 19-28.

Bailey, B.J. (1977). The Calculation of Glasshouse Fuel Requirements Using

Degree-day Data Corrected for Solar Heat Gain. Dept. Note DN/G/798/04013, Natn. Inst. Agric. Engng. Silsoe, England.

Bailey, B.J. and Cotton, R.F. (1977). Reducing Glasshouse Heat Losses with Reflective Thermal Screens. Dept. Note DN/G/797/04013, Natn. Inst. Agric. Engng. Silsoe, England. (unpub.)

Bailey, B.J. (1978a). Heat Conservation in Glasshouses with Aluminised Thermal Screens. *Acta Hort.* **76**: 275-278.

Bailey, B.J. (1978b). *Applications of Plastics Screens in Glasshouse Environmental Control.* British Agricultural and Horticultural Plastics Association Conference: Advances in the use of Plastics in Agriculture, Horticulture and Produce Distribution. Silsoe, England.

Bailey, B.J. (1978c). Glasshouse Thermal Screens: Air Flow Through Permeable Materials. Dept. Note DN/G/859/04013, Natn. Inst. Agric. Engng. Silsoe, England. (unpub.)

Bailey, B.J. (1979a). Energy Conservation in Glasshouses using Thermal Screens. In: *Energy for Industry.* (Ed. P.W. O'Calloghan). Pergaman Press, England.

Bailey, B.J. (1979b). Glasshouse Thermal Screen Development Farm Project, First Season: Heat Consumption and Environment. Dept. Note DN/G/981/04013, Natn. Inst. Agric. Engng. Silsoe, England. (unpub.)

Bailey, B.J. and Cotton, R.F. (1980). Glasshouse Thermal Screens: Influence of Single and Double Screens on Heat Loss and Crop Environment. Dept. Note DN/G/982/04013, Natn. Inst. Agric. Engng. Silsoe, England. (unpub.)

Bailey, B.J. (1981a). The Reduction of Thermal Radiation in Glasshouses by Thermal Screens. *J. Agric. Engng. Res.* **26**: 215-224.

Bailey, B.J. (1981b). The Evaluation of Thermal Screens in Glasshouses on Commercial Nurseries. *Acta Hort.* **115**: 663-670.

Bailey, B.J. (1981c). Experiences with Thermal Screens in Glasshouses on Commercial Nurseries in England. *Plasticulture.* **50**: 13-22.

Baille, A., Aries, F., Baille, M. and Laury, J.C. (1985). Influence of Thermal Screen Optical Properties on Heat Losses and Microclimate of Greenhouses. *Acta Hort.* **174**: 111-118.

Bot, G.P.A. (1983). *Greenhouse Climate: From Physical Processes to a Dynamic Model.* Ph.D. Thesis. Agricultural University, Wageningen. :240pp.

Breuer, J.J.G. (1983). *Computer Model of Energy Requirements in Greenhouses.* (2nd Edition) Part 1. A Guide. Report No. 49. I.M.A.G. Wageningen. :72pp. [In Dutch].

Breuer, D.R. (1985a). *Energy in New Zealand Greenhouses.* New Zealand Energy Research and Development Committee, Interim Report. Contract 3255. Auckland, New Zealand.

Breuer, D.R. (1985b). *Energy in New Zealand Greenhouses.* New Zealand Energy Research and Development Committee, (Report No. 120). University of Auckland, New Zealand.

Burit, E.S., Cattell, P.R. and Nesbit, S.M. (1978). *Glasshouses: Heating and Ventilation.* (Unpublished dissertation). Lincoln College, New Zealand.

Businger, J.A. (1963). The Glasshouse (Greenhouse) Climate. In: *Physics of Plant Environment. (Ed. W.R. Van Wijk)* North Holland Publishing Co., Amsterdam.

Chandra, P. and Albright, L.D. (1980). Analytical Determination of the Effect on Greenhouse Heating Requirement of Using Night Curtains. *Trans. A.S.A.E.* 23 (4): 994-1000.

Chapman, A.J. (1974). *Heat Transfer.* (3rd Edit.). MacMillan Publishing Co. Inc., U.S.A.

Cooper, P.I. and Fuller, R.J. (1983). A Transient Model of the Interaction between Crop, Environment and Greenhouse Structure for Predicting Crop Yield and Energy Consumption. *J. Agric. Engng. Res.* 28: 401-417.

Curry, R.B. (1971). Dynamic Simulation of Plant Growth. I. Development of a Model. *Trans. A.S.A.E.* 14 (5): 946-949, 959.

Dartiguepeyrou, R. (1986). EVA for Cladding Plastic Structures. What to choose? *Plasticulture.* 70: 19-26.

Davis, P.F. (1984). A Technique of Adaptive Control of the Temperature in a Greenhouse Using Ventilator Adjustments. *J. Agri. Engng. Res.* 29: 241-248.

Dawson, J.R. and Winspear, K.W. (1976). The Reduction of Glasshouse Heat Losses by Internal Blinds. *J. Agric. Engng Res.* 21 (4): 431-436.

Dossat, R.J. (1981). *Principles of Refrigeration.* (2nd Edit.). John Wiley & Sons, New York.

Duffie, J.A. and Beckman, W.A. (1980). *Solar Engineering of Thermal Processes.* John Wiley & Sons, Canada.

Duncan, G.A., Loewer, O.J., Jr. and Colliver, D.G. (1981). Simulation of Energy Flows in a Greenhouse: Magnitudes and Conservation Potential.

Trans. A.S.A.E. **24** (4): 1014- 1021.

Dunnett, A. (1987). *Understanding the Economy.* (2nd Edit.) Longman Inc., New York.

Enoch, H.Z. and Sacks, J.M. (1978). An Emperical Model of CO_2 Exchange at a C3 Plant in Relation to Light, CO_2 Concentration and Temperature. *Photosynthetica.* 12: 150-157.

Faber, L. (1990). Pers. Comm. Faber Glasshouses Waiuku Ltd. Waiuku, New Zealand.

Fleming, M. (1969). *Introduction to Economic Analysis.* George Allen and Unwin Ltd, London.

Fuller, R.J., Sides, R. and Blackwell, J. (1984). A Thermal Screen System for Energy Conservation. *Agriculture Engineering Australia.* ***13*** (2): 13-18.

Fuller, R.J., Meyer, C.P. and Sale, P.J.M. (1987). Validation of a Dynamic Model for Predicting Energy Use in Greenhouses. *J. Agric. Engng. Res.* **38** (1): 1-14.

Ganic', E.N., Hartnett, J.P. and Rohsenow, W.M. (1985). Basic Concepts of Heat Transfer. In (Ed). *Handbook of Heat Transfer Fundamentals.* (Eds. W.M. Rohsenow, J.P. Hartnett, and E.N. Ganic') (2nd Edit.). McGraw-Hill Book Company, New York.

Garzoli, K.V. and Blackwell, J. (1981). An Analysis of the Nocturnal Heatloss from a Single Skin Plastic Greenhouse. *J. Agric. Engng. Res.* **26**: 203-214.

Garzoli, K.V. and Blackwell, J. (1987). An Analysis of the Nocturnal Heatloss from a Double Skin Plastic Greenhouse. *J. Agric. Engng. Res.* **36** (2): 75-85.

Glaub, J.C. and Trezek, G.J. (1981). Heat and Mass Transfer Analysis of Greenhouses. A.S.A.E. Paper No. 81-4031.

Goudriaan, J. (1977). *Crop Micrometeorology: A Simulation Study.* Centre for Agricultural Publishing and Documentation, Netherlands.

Grange, R.I. and Hurd, R.G. (1983). Thermal Screens: Environmental and Plant Studies. *Scientia Horticulturae* **19**: 201-211.

Heatley, P.R. (1990). *Light Transmission, Heat Retention and Mechanical Strength Property Evaluation of Film Plastic Cladding Materials Available in New Zealand.* M. Hort. Sc. Thesis. Massey University. New Zealand.

Hesketh, T., Skilton, R.A. and Studman, C.J. (1986). Advanced Digital Control for New Zealand Greenhouses. *J. Agric. Engng. Res.* **34**: 207-218.

Hoore, E.R. and Morris, L.G. (1955). The Heating and Ventilation of Glasshouses. *J. Instu. Brit. Agric. Engrs.* **12**: 1-25.

Hoeflak, J.W. (1990). Pers. Comm. Managing Director of Horti. Centre Ltd. Auckland, New Zealand.

Holman, J.P. (1986). *Heat Transfer.* (6th Edit.). McGraw-Hill Book Company, New York.

Horiguchi, I., Sugaya, H. and Tani, H. (1982). The Measurement of Longwave Radiation Properties upon Plastic Films used in Greenhouses. *J. Agr. Met.* **38** (1): 9-14.

Huang, B.K. and Kato, A. (1984). Dynamic Simulation of Greenhouse Thermal Behaviour. A.S.A.E. Paper No. 84-4030.

Hurd, R.G. and Sheard, G.F. (1981). *Fuel Saving in Greenhouses.* Grower Books No.20, London.

Incropera, F.P. and DeWitt, D.P. (1985). *Fundamentals of Heat and Mass Transfer.* John Wiley & Sons, Inc., U.S.A.

Jensen, M.H. (1977). Energy Alternatives and Conservation for Greenhouses. *Hort. Science.* **12** (1): 14-24.

Jolliet, O. (1988). *A Model of Thermal Behaviour of a Horticultural Greenhouse.* Ph.D. Thesis, No. 713. Ecole Polytechnique Federale de Lausanne. Lausanne. [In French].

Jolliet, O. and Munday, G.L. (1989). A 2nd Generation Static Model of Greenhouse Energy Requirements (HORTICERN): A Comparison with Dynamic Models. *Acta Hort.* **245**: 335-346.

Jolliet, O., Gay, J.-B. and Munday, G.L. (1989). A 2nd Generation Static Model for Predicting Greenhouse Energy Inputs as an Aid for Production Planning. *Acta Hort.* **248**: 121-128.

Kano, A. and Sadler, E.J. (1985). Survey of Greenhouse Models. *J. Agric. Meteorol.* **41**: 75-81.

Kimball, B.A. (1973). Simulation of the Energy Balance of a Greenhouse. *Agric. Meteorol.* **11**: 243-260.

Kindelan, M. (1980). Dynamic Modelling of Greenhouse Environments. *Trans. A.S.A.E.* **23** (4-6): 1232-1239.

Kittas, C. (1980). *Theoretical and Experimental Contribution to the Study of the Energy Balance of Greenhouses. Application of the Analysis to Determining the Temperatures of the Cover and the Interior Air of the Greenhouse.* Ph.D. Thesis. University of Perignan. Montpellier. [In French].

Klein, S.A., Cooper, P.I., Freeman, T.L. and others (1975). A Simulation of Solar Processes and its Application. *Solar Energy.* **17**: 29-37.

Klein, S.A., Beckman, W.A., Cooper, P.I. and others (1976). *TRNSYS: A Transient Simulation Program.* Solar Energy Lab., Eng. Expt. Station Report 38. University of Wisconsin.

Lamb, J.F. (1980). *Greenhouses: Heating Alternatives.* Horticultural Produce and Practice 198, Media Services. MAF. New Zealand.

Lu, F.P.S. (1969). *Economic Decision-making for Engineers and Managers.* Whitcombe and Tombs Limited, New Zealand.

Ludvig Svensson International. (1989). Publicity Brochure. Sweden.

MacDonald, I.A. (1990). Pers. Comm. Manager of Exal Glasshouses Ltd. Christchurch, New Zealand.

Maher, M.J. and O'Flaherty, T. (1973). An Analysis of Greenhouse Climate. *J. Agric. Engng. Res.* **18**: 197-203.

Mahrer, Y. and Avissar, R. (1984). A Numerical Simulation of the Greenhouse Microclimate. *Mathematics and Computers in Simulation.* **26**: 218-228.

Marsh, L.S., Albright, L.D. and Langhans, R.W. (1984). Strategies for Controlling Greenhouse Thermal Screens. *Acta Hort.* **148**: 453-459.

Meinders, H., Vahl, H.W., and Middendorp, C.A.J. (1984). Technical Developments in Thermal Screening Systems. *Acta Hort.* **148**: 443-452.

Meyer, J. (1981). Energy Saving with Mobile Thermal Screens. *Acta Hort.* **115**: 677-684.

Monteith, J.L. and Unsworth, M.H. (1990). *Principles of Environmental Physics.* (2nd Edit.). Hodder and Stoughton Ltd, London.

Nijskens, J., Detour, J., Coutisse, S. and Nisen, A. (1984). Heat Transfer through covering Materials of Greenhouses. *Agricultural and Forest Meterology.* **33**: 193-214.

NZMS. (1980). *New Zealand Meterological Services Summary of Climatological Observations.* New Zealand Meterological Service. Wellington, New Zealand.

O'Flaherty, T., Gaffney, G.J. and Walsh, J.A. (1973). Analysis of the Temperature Control Characteristics of Heated Glasshouses Using an Analogue Computer. *J. Agric. Engng. Res.* **18**: 117-132.

Okada, M. (1985). An Analysis of Thermal Screen Effects of Greenhouse Environment by means of a Multi-layer Screen Model. *Acta Hort.* **174**: 139-144.

Rebuck, S.M., Aldrich R.A. and White, J.W. (1977). Internal Curtains for Energy Conservation in Greenhouses. *Trans. A.S.A.E.* **20** (4): 732-734.

Roberts, W.J., Mears, D.R., Simpkins, J.C. and Cipolletti, J.P. (1981). Progress in Movable Blanket Insulation Systems for Greenhouses. *Acta Hort.* **115**: 685-692.

Schockert, K. and Von Zabeltitz, C. (1980). Energy Consumption of Greenhouses. *Acta Hort.* **106**: 21-26.

Seginer, I. and Albright, L. (1980). Rational Operation of Greenhouse Thermal-curtains. *Trans. A.S.A.E.* **23** (5): 1240-1245.

Seginer, I. and Jenkins, B.M. (1987). Temperature Exposure of Greenhouses from Monthly Means of Daily Maximum and Minimum Temperatures. *J. Agric. Engng. Res.* **37**: 191-208.

Sheard, G.F. (1978). Shelter and the Effect of Wind on the Heat Loss from Greenhouses. *Acta Hort.* **76**: 357-360.

Shell, B. and Staley, L.M. (1985). Economic Analysis of Greenhouse Energy Management Techniques: A Microcumpter Spreadsheet Model. *Energy in Ag.* **4**: 331-345.

Soribe, F.I. and Curry, R.B. (1973). Simulation of Lettuce Growth in an Air-supported Plastic Greenhouse. *J. Agric. Engng. Res.* **18**: 133-140.

Strom, J.S. and Amsen, M.G. (1981). Heat Consumption Model for Greenhouse Nurseries. *Acta Hort.* **115**: 503-510.

Sturrock, J.W. (1981). Energy Conservation in the Greenhouse Industry. *New Zealand Commercial Grower.* **36** (8): 31-35.

Takakura, T., Jordan, K.A. and Boyd, L.L. (1971). Dynamic Simulation of Plant Growth and Environment in the Greenhouse. *Trans. A.S.A.E.* **14** (5): 964-971.

Tantau, H.J. (1981). Radiation Properties of Thermal Screens. *Acta Hort.* **115**: 671-675.

Taylor, G. (1990). Pers. Comm. Manager of Harford Greenhouses. Auckland, New Zealand.

Thornley, J.H.M. (1976). *Mathematical Models in Plant Physiology.* Academic Press, London.

Threlkeld, J.L. (1962). *Thermal Environmental Engineering.* (1st Ed.). Prentice-Hall Inc., New Jersey.

Udink ten Cate, A.J. (1983). *Modelling and Adaptive Control of Greenhouse Climates.* Ph.D. Thesis. Agricultural University, Wageningen, Netherlands.

van Bavel, C.H.M., Damagnez, J. and Sadler, E.J. (1981) The Fluid-roof Solar Greenhouse : Energy Budget Analysis by Simulation. *Agric. Meteorol.* **23**: 61-76.

van den Braak, N.J., Breuer, J.J.G. and Heyna, F.J. (1984). Cumulative Frequency Distribution Curves of Greenhouse Heat Requirements. *Acta Hort.* **148**: 337-344.

Walker, J.N. (1965). Predicting Temperatures in Ventilated Greenhouses. *Trans. A.S.A.E.* **8**: 445-448.

Walker, J.N., Aldrich, R.A. and Short, T.H. (1983). Quantity of Airflow for Greenhouse Structures. In: *Ventilation of Agricultural Structures.* (Eds. M.A. Hellickson and J.N. Walker). A.S.A.E. Monograph No. 6., A.S.A.E. St. Joseph. Michigan. pp 257-277.

Wells, C.M. (1989a). *Greentech 89.* Agric. Engng. Dept. Massey University, New Zealand.

Wells, C.M. (1989b). Pers. Comm. Senior Lecturer in Agric. Engng. Massey University, New Zealand.

Wells, C.M. (1989c). *Estimation of the Overall Heating Requirement of a Greenhouse.* Massey University, New Zealand. (unpub.).

Wells, C.M. (1990a). Pers. Comm. Senior Lecturer in Agric. Engng. Massey University, New Zealand.

Wells, C.M. (1990b). *Modelling the Greenhouse Climate and the Growth of Cucumbers.* Ph.D. Thesis. Massey University, New Zealand.

White, R.A.J. (1980). *Energy Conservation and Heating Problems.* Bulletin No. 139 of Electrical Development Association. Seminar for Glasshouse Owners. Blenheim, New Zealand.

White, R.A.J. (1984a). Which Film? Profit is the Aim. *Growing Today.* **1** (5): 17-23.

White, R.A.J. (1984b). *Research on Cladding and Screens for New Zealand Environment.* Levin Horticultural Research Centre. Reported at Energy in Greenhouses Workshop. University of Auckland, New Zealand.

White, R.A.J. (1984c). *Estimating Greenhouse Fuel, Water and CO_2 Consumption with Simulation Models.* Paper: 'Researchers' and Practitioners' Workshop on Energy in Greenhouses. Auckland, New Zealand.

Williams, D. (1990). Pers. Comm. Edwards & Williams Ltd. Levin, New Zealand.

Winspear, K.W. (1977). Thermal Screens save Fuel in Protected Cropping. *ARC Research Review.* **3** (1): 11-14.

Winspear, K.W. (1978). Energy and U.K. Glasshouse Crop Production. In: *Energy Conservation and Use of Renewable Energies in the Bio-Industries.* (Ed. F. Vogt) Pergamon Press, Oxford.

Young, D.J. (1990). Pers. Comm. D.J. Young Glasshouses Ltd. Auckland, New Zealand.

Zhao, J., Jenkins, B., Shaw, R.H. and Seginer, I. (1985). Heat and Water Vapour Balance of Greenhouse Plant Leaves Under Convective and Infrared Heating. A.S.A.E. Paper No. 85-4052.

APPENDICES

APPENDIX 1: HEAT TRANSFER

Incropera and De Witt (1985) define heat transfer (or, heat) as energy in transit by virtue of a temperature difference. There are three heat transfer processes referred to as modes, namely **conduction**, **convection**, and **radiation**.

A1.1 CONDUCTION

Conduction is the transfer of heat between adjacent bodies in the direction of the colder body. The conduction process takes place at a molecular level and involves the transfer of energy from more energetic to less energetic molecules. Conduction is easily visualised within gases whereby energetic molecules periodically collide with molecules of lower energy, exchanging energy and momentum. Although liquid molecules are much closer, the molecular exchange process is qualitatively similar (Ganic et al, 1985).

In solids, conduction is attributed to atomic activity in the form of lattice waves. In solids that are non-conductors of electricity, heat is transferred exclusively by lattice waves. In conducting solids, heat transfer by lattice waves is minimal, and exchange is due to the motion of free electrons, whose movement is similar to that of gaseous molecules (Incropera and De Witt, 1985).

The rate of heat transfer per unit area (the heat flux density) by conduction through a substance is directly proportional to the temperature gradient within the substance. The Fourier heat equation expresses this principle as:

$$q = -k \frac{\partial T}{\partial x} \qquad \text{(A1.1)}$$

where q = conductive heat flux density (Wm^{-2})

k = thermal conductivity ($Wm^{-1}\,^{\circ}K^{-1}$)

T = temperature ($^{\circ}K$)

x = direction of heat flow (m)

$\frac{\partial T}{\partial x}$ = temperature gradient ($^{\circ}Km^{-1}$)

The minus sign in (A1.1) indicates heat is moving in the direction of decreasing temperature.

Integrating (A1.1) across the thickness of the material gives a new property called the thermal conductance K, with units of $Wm^{-2}\,^{\circ}K^{-1}$. The heat flux density is therefore given by:

$$q = K(T_1 - T_2) \qquad \text{(A1.2)}$$

where $(T_1 - T_2)$ represents the temperature either side of the material.

Heat transfer by conduction can be reduced by placing an insulator in the heat flow path.

A1.2 CONVECTION

Heat transfer by convection occurs when warm gas or liquid moves to a cooler location. Convection incorporates two mechanisms. The first is energy transfer by random molecular motion (or diffusion) and the second is energy transfer associated with large numbers of molecules moving collectively as an aggregate. As the molecules within an aggregate retain their random motion, total convective heat transfer is the sum of the energys transported by diffusion and bulk fluid motion. It is customary to use the term convection when referring to this cumulative transport and the term advection when referring to transport solely by bulk fluid motion (Incropera and De Witt, 1985).

A temperature gradient within a fluid produces a gradient of enthalpy. The enthalpy of a substance is the amount of energy it possesses per unit mass. An enthalpy gradient within a fluid gives rise to a density gradient which in turn produces a pressure gradient. Pressure gradients cause fluids to move collectively as bulk, multi-molecule volumes, to regions of lower pressure. The energy transfer associated with this bulk motion is called advection.

As fluid enthalpy increases so too does the random motion of its molecules (Brownian Motion). Diffusive heat transfer refers to the energy transfer associated with random molecular motion. Heat transfer by diffusion is insignificant compared to advection but may become significant if a membrane or barrier is inserted within the advective flow path.

The rate of convective heat transfer from a solid surface to a fluid is described by Newton's Law of cooling which says:

$$H = h\,(T_s - T_f) \qquad \text{(A1.3)}$$

where H = convective heat flux density (Wm^{-2})

h = convective heat transfer coefficient ($Wm^{-2}\,^{\circ}K^{-1}$)

T_s = temperature of solid surface ($^{\circ}K$)

T_f = temperature of fluid ($^{\circ}K$)

The value of h depends on the type of fluid involved, the velocity of the fluid across the surface, the temperature difference between the surface and the fluid and the size, shape and orientation of the surface (Wells, 1989a).

The following criteria can be used to determine whether forced or free convection dominates:

$$\frac{\Delta TL}{u^2} < 10 \quad \text{implies forced convection} \qquad \text{(A1.4)}$$

$$\frac{\Delta TL}{u^2} > 300 \quad \text{implies free convection} \qquad \text{(A1.5)}$$

where $\Delta T = (T_s - T_f)$ = temperature difference ($^{\circ}K$)

L = characteristic dimension of object (m)

u = air speed across object (ms^{-1})

The following formulae can be used to estimate the convective heat transfer coefficient for air:

Forced Convection

$$h = 4\left(\frac{u}{L}\right)^{0.5} \quad \text{where } uL < 10 \qquad \text{(A1.6a)}$$

$$h = \frac{6\,u^{0.8}}{L^{0.2}} \quad \text{where } uL > 10 \qquad \text{(A1.6b)}$$

Free Convection

$$h = \frac{1.6\,\Delta T^{0.25}}{L} \quad \text{where } \Delta TL^3 < 10 \qquad \text{(A1.7a)}$$

$$h = 1.2\,\Delta T^{0.333} \quad \text{where } \Delta TL^3 > 10 \qquad \text{(A1.7b)}$$

(Wells, 1989a)

Heat transferred to or from a substance can bring about a change in phase as well as a change in temperature. For convenience, heat is divided into two categories, depending on what happens to the substance when it absorbs or gives up energy. Heat causing or accompaning a change in the temperature of a substance is called **sensible heat**, whereas heat causing or accompaning a change in phase of a substance is known as **latent heat** (Dossat, 1981).

Heat transfer by convection is a combination of sensible and latent heat. Sensible heat is transferred when air moves in bulk from one region to another or when water molecules diffuse from one region to another. When water evaporates, only liquid molecules with high velocities have sufficient energy to break the

intermolecular attractions and escape into the air. These molecules take with them latent heat equal to the latent heat of vaporisation (2501 $kJkg^{-1}$ at $0^{\circ}C$), and equal in magnitude to the liquids loss of sensible heat. Diffusing water vapour is therefore a carrier of latent heat as well as sensible heat and consequently evaporation of water is a powerful cooling process.

When liquid water evaporates from the underside of a greenhouse cover the airspace gains water vapour and latent heat. The water film on the other hand, having lost its most energetic molecules, suffers a drop in sensible heat equal in magnitude to the latent heat gain of air. Since the water film is in thermal contact with the cover sensible heat moves from the cover to the water film by conduction causing the cover temperature to lower. Evaporation from the cover is therefore always accompanied by a drop in cover temperature. In much the same manner, when water evaporates from the greenhouse floor the airspace gains water vapour and latent heat and the floor cools. Similarly crop transpiration is an important leaf cooling mechanism.

Condensation occurs within the greenhouse when the cover, the crop or the floor drops below the airspace dew point temperature. When this happens the airspace loses latent heat and the condensing surface gains an equal amount of sensible heat causing its temperature to increase.

Condensation therefore represents a latent heat gain to a body (a negative heat loss) and evaporation represents a latent heat loss from a body (a positive heat loss).

Ventilation and infiltration are terms used when describing convection to and from a building. Ventilation refers to deliberate air movement through controlled openings and may be forced or natural. Infiltration, also known as air leakage, is unintentional air movement through cracks and openings in the building's surface. Infiltration is more significant in glass greenhouses as warm air escapes through glazing gaps created by overlapping panes. Depending on the age and condition

of the house air will freely move through glass laps at 1 to 4 air changes/hour. This compares with 0.5 to 1 air changes/hour for a plastic film house. Heat transfer by convection can be minimised by placing barriers to the flow path to prevent the mass movement.

A1.3 RADIATION

Electromagnetic radiation, (radiation for short) is a form of energy derived from oscillating magnetic and electrostatic fields (Monteith and Unsworth, 1990). All matter with finite temperature emits radiation. This process is called radiation heat transfer. Emitted radiation, rightly termed **radiance**, is also known as **emission**, **radiated energy**, or simply **radiation**. When emitted energy arrives at a surface, the surface is said to have been irradiated, ie. received radiance. As radiated energy has wavelengths longer than solar radiation and in the infra-red range, the terms **long wave radiation** and **infra-red radiation** are often to describe radiated energy.

Radiation occurs between bodies without direct contact and without the need of an intervening transporting medium. Although radiation primarily focuses on radiance from solid surfaces, radiance is also emitted from liquids and gases.

Two theories describe the properties of radiation; the **wave theory** and **particle theory**. In the wave theory, radiation is considered to be propagated in the form of waves. Although these waves vary in wavelength, they all traverse space in a straight line at the same velocity (v). Equation (A1.8) describes the relationship that exists between wavelength, frequency, and velocity of electromagnetic radiation waves.

$$v = \lambda f \qquad \text{(A1.8)}$$

where v = velocity of light in a vacuum = 3×10^8 ms^{-1}

λ = wavelength (m)

f = frequency (s^{-1})

In the particle theory, radiation is considered to be a stream of discrete particles. Each particle is called a photon or quanta. The particle theory describes the energy possessed by radiation. A German physicist by the name of Planck showed that the energy of one photon was inversely proportional to the wavelength according to the expression:

$$E = hv \qquad \text{(A1.9)}$$

where E = energy of one photon (J)

h = Planck's constant = 6.63×10^{-34} Js^{-1}

(Monteith and Unsworth, 1990)

Figure A1.1 delineates the main spectrum of wavelengths constituting electromagnetic radiation.

Short wavelength waves such as gamma rays, X rays and ultraviolet (UV) radiation are of interest to high energy physicists and nuclear engineers. Long wavelength microwaves and radiowaves are of concern to the electrical engineer. It is the intermediate portion of the spectrum, referred to as **thermal radiation**, extending from approximately 0.1μm up to about 100μm, including a portion of the UV waveband, the entire visible waveband and all infra-red (IR) waveband, that is pertinent to heat transfer (Incropera and DeWitt, 1985).

All bodies with temperature above absolute zero emit radiation over the full electro-magnetic spectrum. The relative rate of energy emission of each wavelength depends on the temperature of the body. Figure A1.2 shows the spectral emissive power (energy per unit wavelength) of several blackbodies at

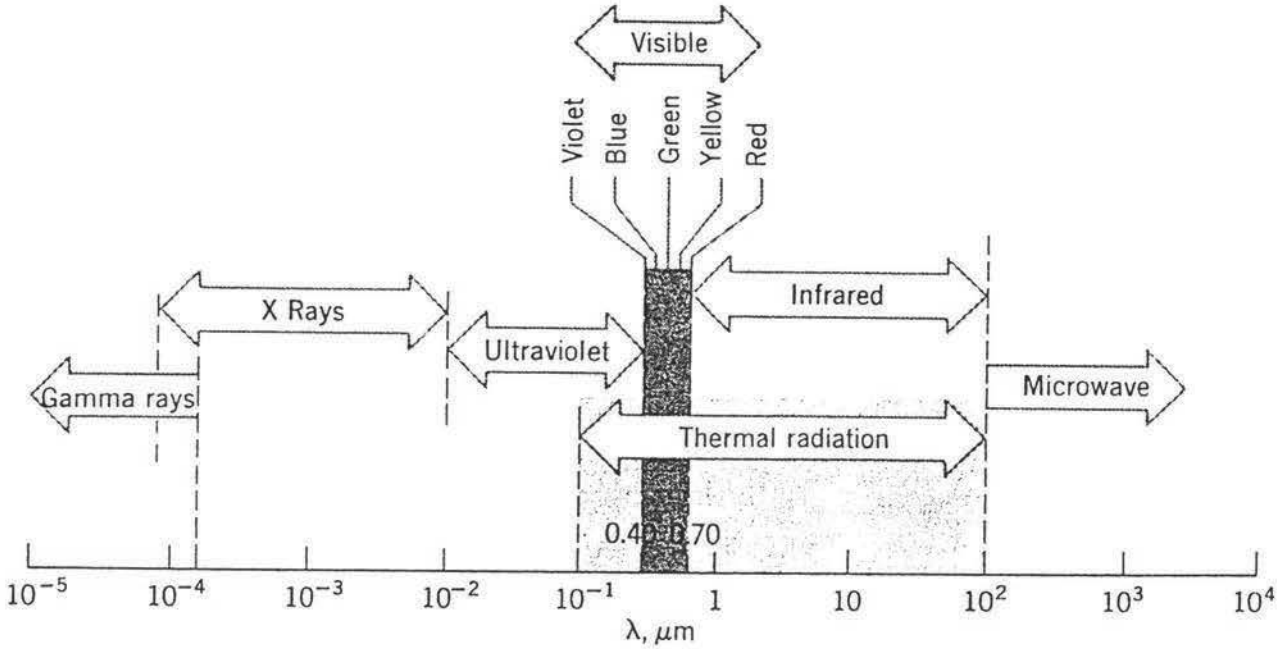

Figure A1.1 Spectrum of electromagnetic radiation (Incropera and DeWitt, 1985).

temperatures ranging from 50°K to 5,800°K. The term blackbody describes a surface which emits the maximum amount of radiance at a particular wavelength and absorbs all the irradiance falling on it. The terms **full radiator** or **perfect absorber** are therefore sometimes used instead of 'blackbody' (Wells, 1989a).

Stefan and Boltzmann showed that the total rate of radiation emission by a full radiator over all wavelengths, the total emissive power of a blackbody Eb, is proportional to the fourth power of its absolute temperature. They developed the expression:

$$Eb = \sigma T^4 \qquad \text{(A1.10)}$$

where Eb = total emissive power of a blackbody (Wm^{-2})

σ = Stefan-Boltzmann constant = 5.67×10^{-8} $Wm^{-2}\,°K^{-4}$

T = Temperature (°K)

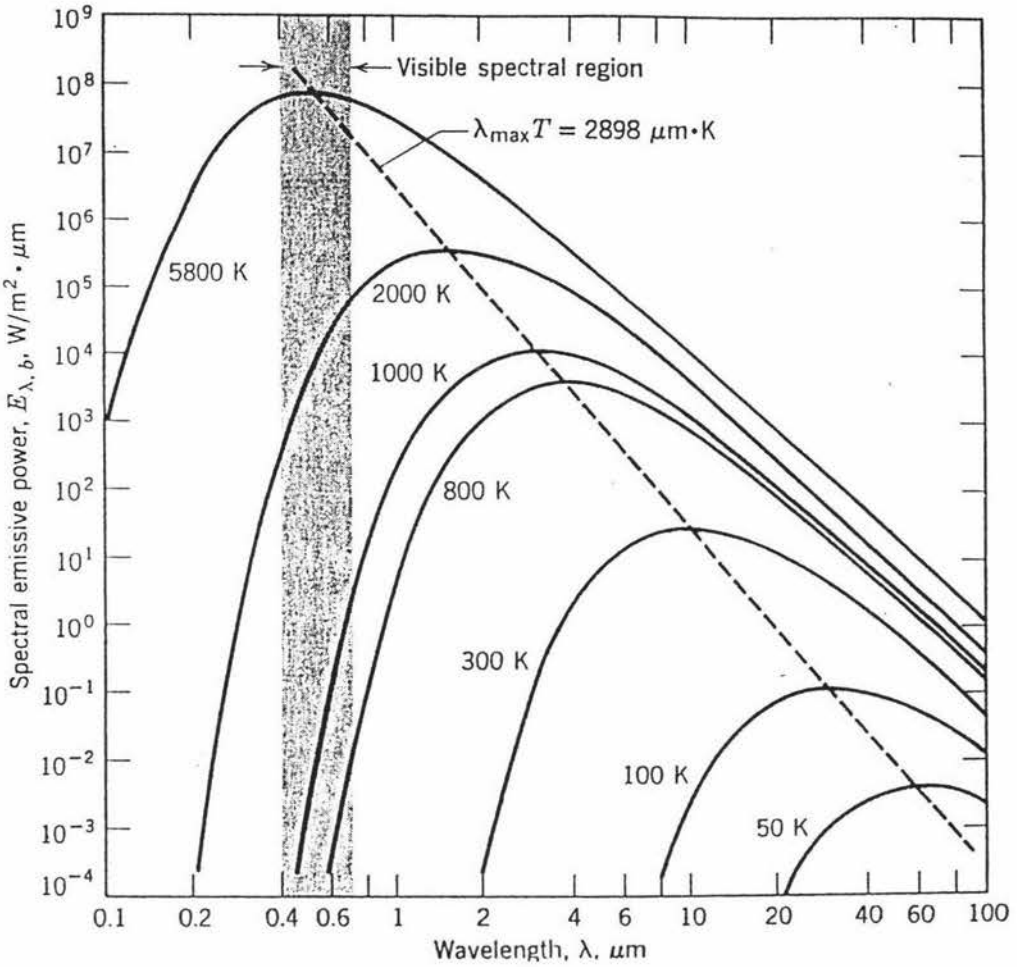

Figure A1.2 Spectral blackbody emissive power (Incropera and DeWitt, 1985).

The total emissive power of a blackbody at 300°K (approximate surface temperature of earth) is therefore:

$$Eb = 5.67 \times 10^{-8} \times 300^4$$
$$= 459\ Wm^{-2}$$

and the total emissive power at 5,800°K (surface temperature of the sun) is therefore:

$$Eb = 5.67 \times 10^{-8} \times 5,800^4$$
$$= 62.2 \times 10^6\ Wm^{-2}$$

According to Monteith and Unsworth (1990), natural surfaces (vegetation, water and soil) can usually be treated as blackbodies. The radiance emitted from these surfaces is termed **terrestrial radiation** to set it apart from shorter wavelength solar radiation emitted by the sun. It is also referred to as long wave or IR radiation.

Using special radiation functions (Holman, 1986) it can be shown that:

a. at 300°K basically all (98%) of the blackbody total emissive power is generated by radiation in the 5-75μm waveband, and
b. at 5,800°K basically all (98%) of the blackbody total emissive power is generated by radiation in the 0.25-4μm waveband.

As terrestrial surfaces are usually around 300°K, terrestrial radiance is concentrated in the 5-75μm waveband (ie. in the IR region). Similarly, the sun's radiance (solar radiation) is concentrated in the 0.25-4μm waveband (ie. some UV, all of the visible and some IR radiation). Since both sun and earth emit in the IR waveband the terms near infra-red (NIR) and far infra-red (FIR) have been coined to delineate sun sourced IR (0.7μm to about 4.5μm) from terrestrial sourced IR (4.5μm to about 100μm) respectively.

The human eye is sensitive to radiation in the 0.4μm (blue light) to 0.7μm (red light) waveband. Because photosynthesis is stimulated by radiation in the same waveband, the region from 0.4μm to 0.7μm is referred to as **photosynthetically active radiation** or PAR (Monteith and Unsworth, 1990).

At the earth's surface, solar radiation is proportioned into approximately 50% PAR and 50% NIR (Wells, 1990a).

Most objects do not act like full radiators but instead only radiate a part of what a full radiator would at the same temperature. The characteristic of a surface which determines how well it radiates is called the emissivity, ϵ.

$$\epsilon = \frac{\textit{Emissive power of real surface, Eo}}{\textit{Emissive power of a full radiator, Eb}} \qquad \text{(A1.11)}$$

$$Eo = \epsilon Eb = \epsilon \sigma T^4 \quad (Wm^{-2}) \qquad \text{(A1.12)}$$

(Wells, 1989a)

When radiation falls on a surface a fraction ρ is reflected, a fraction τ is transmitted and the remaining fraction α is absorbed (see Figure A1.3). Hence:

$$\rho + \alpha + \tau = 1$$

where the quantities, ρ, τ, and α are known as the reflectivity, transmissivity and absorptivity respectively.

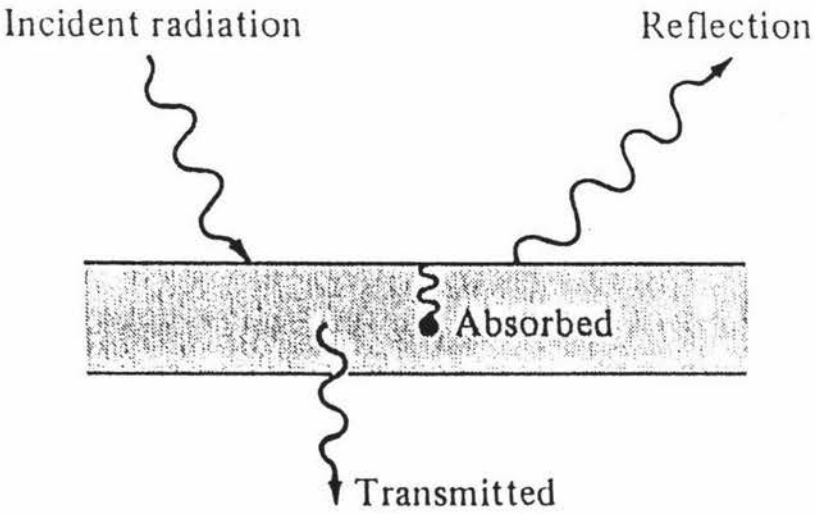

Figure A1.3 **Absorption, reflection, and transmission of radiation for a translucent medium.**

As with emissivity, the values of ρ, α and τ vary depending on wavelength. In the solar and terrestrial wavebands however, they are usually constant (Monteith and Unsworth 1990).

Most solid bodies do not transmit thermal radiation. As a result the transmissivity in some applied problems may be taken as zero. Hence:

$$\rho + \alpha = 1$$

The rate of radiative heat transfer varies with the area, temperature, and surface characteristics of the bodies involved. Based on surface characteristics an object may be rated in terms of its ability to emit radiation on a scale of zero to one (nothing emitted to everything emitted). Thus, an emissivity rating of close to one indicates the object readily emits energy. Kirchhoff's Law states that for a given wavelength of radiation $\alpha = \epsilon$ where ϵ is the emissivity (Badger and Poole, 1979).

APPENDIX 2: RADIATION SOURCES

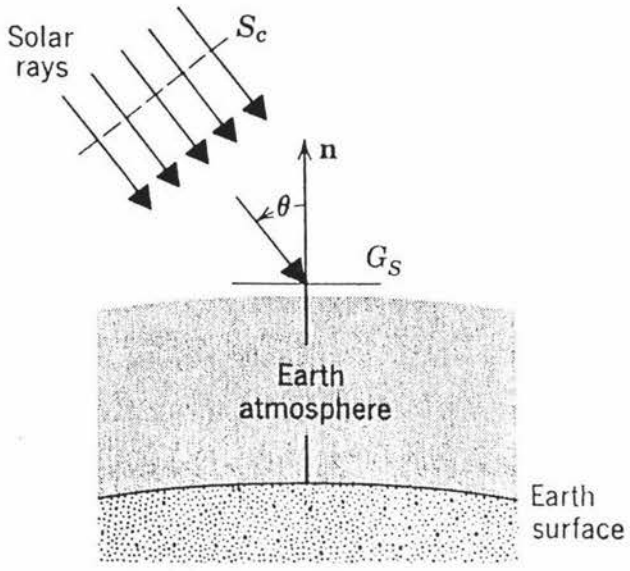

Figure A2.1 **Directional nature of solar radiation outside the earth's atmosphere (Incropera and DeWitt, 1985).**

The sun is an almost spherical radiation source 1.39 x 10^9m in diameter, located 1.50 x 10^{11}m from the earth. Its emission approximates that of a blackbody at 5,800°K. When radiation travels away from the sun its intensity decreases according to the inverse square law of illumination. In short the spectral irradiation received at the summit of the earth's atmosphere is considerably less than at the sun's surface. Similarly the irradiance received at the earth's surface is less than that at the earth's summit. For a horizontal surface outside the earth's atmosphere, solar radiation appears as a beam of nearly parallel rays that form an angle θ, the zenith angle, relative to the surface normal (Figure A2.1). The extraterrestrial solar radiation, G_s, depends on the geographic latitude, as well as the time of day and year. It can be determined from the expression:

$$G_s = Sc \,.\, F \,.\, \cos\theta \qquad \text{(A2.1)}$$

where Sc, the solar constant, is the irradiance on a surface orientated perpendicular to the solar beam. It is known to have a value of 1,353 Wm^{-2} (Duffie and Beckman, 1980). The quantity F is a small correction factor to account for the eccentricity of the earth's orbit about the sun (approximately 0.97-1.03) (Incropera and DeWitt, 1985).

A2.1 ATMOSPHERIC TRANSMISSION OF SOLAR RADIATION

As the solar beam passes through the earth's atmosphere, it is modified in quantity, quality and direction by processed of scattering, absorption and changing inclination of the sun.

Two kinds of atmospheric scattering exist; **Rayleigh Scattering** and **Mie Scattering**. Rayleigh scattering by gas molecules, in particular oxygen and nitrogen, provides an almost uniform scatter in all directions. As a result approximately half of the Rayleigh scattered radiation gets redirected back to space, whilst the remaining portion strikes the earth's surface. In contrast Mie scattering is caused by large particles suspended in the atmosphere such as water droplets (clouds), dust, salt crystals, smoke, spores, and pollen, and is concentrated in directions that are close to that of the incident rays (Incropera and DeWitt, 1981).

A third attenuation effect is attributed to the absorbing properties of ozone, oxygen, water vapour and carbondioxide (CO_2) molecules. Atmospheric ozone absorbs all solar radiation below 0.29μm (extreme ultra violet) which would otherwise be lethal to plants and animals. In the visible there is some absorption by ozone and oxygen; and in the NIR absorption is dominated by water vapour and CO_2, accounting for the deep fissures shown in Figures A2.2a and A2.2b. When the sun is low in the sky the solar beam must traverse through a large depth of atmosphere in order to reach the ground. Solar irradiance is therefore low due to increased scatter and absorption (Wells, 1989b).

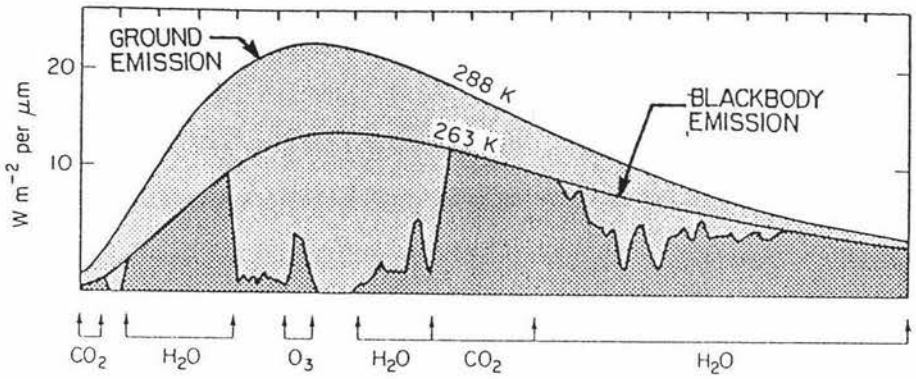

Figure A2.2a **Estimated atmospheric emission downward at the earth's surface, and ground emission upwards (Monteith and Unsworth, 1990).**

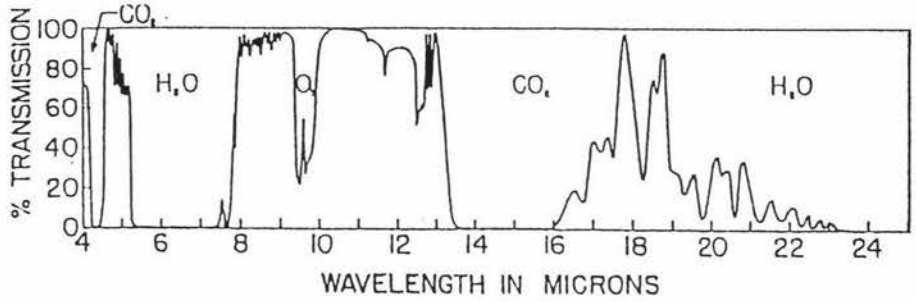

Figure A2.2b **IR transmission of the earth's atmosphere (Monteith and Unsworth, 1990).**

A2.2 SOLAR RADIATION AT THE GROUND

Because of scattering, radiation has two distinct directional properties upon reaching the ground. The portion of the radiation penetrating the atmosphere without being scattered or absorbed is termed **direct** radiation. The term **diffuse** radiation describes the scattered radiation incident on the earth's surface. The sum of the energy flux densities for direct and diffuse radiation is called **total solar radiation** or **global radiation** (Monteith and Unsworth, 1990). The diffuse contribution may vary from approximately 10% of the total solar radiation on a clear day to nearly 100% on a totally overcast day.

A2.3 EFFECT OF CLOUDS

Clouds have a marked effect on the intensity of solar radiation depending on their type and duration. Relative intensities can vary from 120% (because of reflection from large cumulus clouds when the sun shines between them) down to 5% (from multi-layered or cumulonimbus clouds)of the clear sky radiation. For days of broken or variable cloud cover typically 40 to 60% of the clear sky daily radiation is received (Wells, 1989a).

A2.4 RADIATION FROM THE ATMOSPHERE

Radiation from the atmosphere (or sky radiation), occurs at the temperature of the molecules and particles that absorb and scatter solar radiation. The emission spectrum for the sky is therefore very different to that of solar radiation. Figure A2.3a shows the approximate spectral distribution of the downward flux of atmospheric radiation at the earth's surface and the ground emission upward at 288°K. The dark grey areas show emission from atmospheric gases at 263°K (mean atmospheric temperature). The light grey area therefore shows the net loss of radiation from the earth at 288°K to a cloudless atmosphere at a uniform temperature of 263°K. Atmospheric emission is largely due to emission from CO_2 and water molecules and is concentrated in the spectral regions from 5-8μm and above 13μm.

The emissivity of the atmosphere is therefore less than unity and depends on the molecular concentrations of the atmosphere. As water vapour is the only constitute that changes concentration to any significant extent the emissivity of the atmosphere relates to the water vapour concentration. Water vapour, being a relatively heavy gas, is most prevalent in the lowest 100m of atmosphere. Its distribution within this thickness is relatively consistent. As a result the effective sky emissivity is related to the water vapour pressure of the air measured within 1 or 2 metres of the ground. Furthermore, as the vapour pressure of air closely

correlates to air temperature, sky emissivity may be defined solely in terms of air temperature to a reasonable degree of accuracy. The effective sky emissivity is given by:

$$\epsilon_{sky} = (1 - C)\,[0.72 + 0.005\,(T_o - 273)] + C\left(1 - \frac{4\Delta T}{T_o}\right) \qquad \text{(A2.2)}$$

where C = cloud fraction (C=0 for clear skies, C=1 for fully overcast)

T_o = outside air temperature ($^\circ$K)

ΔT = difference between air temperature and cloud base temperature (typically cloud base temperature = T_o - 2)

The FIR radiation emitted by the sky is therefore given by:

$$E_{sky} = \epsilon_{sky}\,\sigma\,T_o^4 = \sigma\,T_{sky}^4 \qquad (Wm^{-2}) \qquad \text{(A2.3)}$$

where T_{sky} is the apparent blackbody temperature of the sky. Hence:

$$T_{sky} = \sqrt[4]{\epsilon_{sky}\,T_o^4} \qquad \text{(A2.4)}$$

T_{sky} must therefore always be less than T_o.

For example, say the outside air temperature T_o was 20°C on an overcast day. What is the apparent blackbody temperature of the sky T_{sky}?

Using equation (A2.2):

$$\begin{aligned}\epsilon_{sky} &= (1 - C)\,[0.72 + 0.005\,(T_o - 273)] + C\left(1 - \frac{4\Delta T}{T_o}\right)\\ &= (1 - 1)\,[0.72 + 0.005\,(293 - 273)] + 1\left(1 - \frac{4\times 2}{293}\right)\\ &= 1 - \frac{8}{293}\\ &= 0.973\end{aligned}$$

therefore:

$$E_{sky} = \epsilon_{sky}\,\sigma\,T_o^4$$
$$= 0.973 \times 5.67 \times 10^{-8} \times 2934$$
$$= 406.6\ Wm^{-2}$$

and:

$$T_{sky} = \sqrt[4]{\epsilon_{sky}\,T_o^4}$$
$$= \sqrt[4]{0.937 \times 293^4}$$
$$= 271\ ^\circ K$$
$$= 18\ ^\circ C$$

A2.5 TERRESTRIAL RADIATION

Most of the radiation emitted by the earth's surface is absorbed in specific wavebands by atmospheric gases, mainly water vapour and CO_2. Figure A2.2b shows the transmission of the atmosphere to terrestrial radiation. Note the area of high transmission (low absorption/emission) in the region 8μm to 13μm. This is known as the atmospheric window.

APPENDIX 3: PHASE 1 DERIVATIONS

This section derives Phase 1 equations for the standard greenhouse. The screened greenhouse equations were derived in a similar fashion.

A3.1 COVER ENERGY BALANCE

In Section 4.1.1.1 the energy balance for the standard greenhouse cover was given as:

$$P_c + N_c + R_c + H_{ac} - H_{co} - L_{ca} = 0 \qquad (4.1a)$$

A3.1.1 Deriving the P_c equation

The P_c equation:

$$P_c = S_P\alpha_{cP} + S_P\tau_{cP}\rho_{pP}\alpha_{cP} + S_P\tau_{cP}\tau^2_{pP}\rho_{fP}\alpha_{cP} \qquad (4.1b)$$

was derived by tracing the path of an incoming S_P (solar radiation in the PAR region) beam within the system. The cover subsystem encounters this incoming S_P beam first. The cover's PAR partitioning properties, α_{cP}, ρ_{cP} and τ_{cP}, cause a percentage of the S_P to be absorbed, reflected and transmitted (see Figure A3.1). The energy associated with the S_P absorbed by the cover in Wm^{-2} is given $S_P\alpha_{cP}$. This was referred to as 1st order absorption.

The S_P transmitted through the cover ($S_P\tau_{cP}$) next encounters the plant subsystem. The PAR partitioning properties of the plant, α_{pP}, ρ_{pP} and τ_{pP}, cause a percentage of the S_P to be absorbed, reflected and transmitted. The reflected portion ($S_P\tau_{cP}\rho_{pP}$) reaches the cover only to be absorbed, reflected and transmitted once again (see Figure A3.2). The energy associated with the absorbed S_P in Wm^{-2} is $S_P\tau_{cP}\rho_{pP}\alpha_{cP}$. This term is 3rd order as the S_P has transmitted through the cover, reflected from the plant, and then been absorbed by the cover.

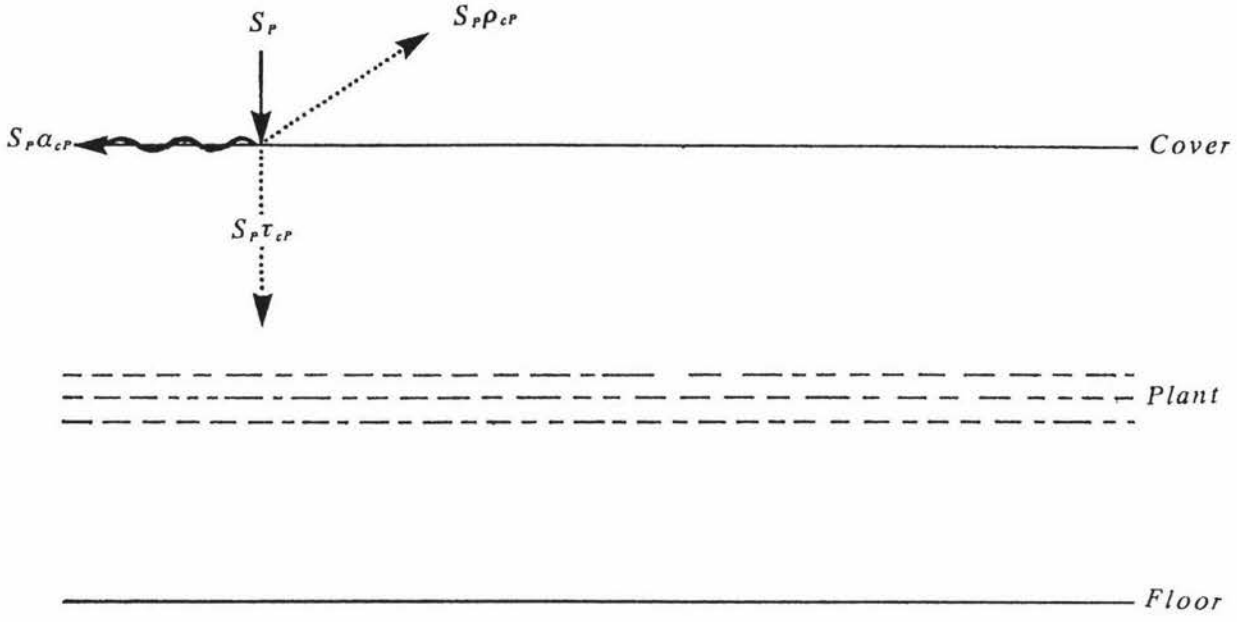

Figure A3.1 1st order PAR absorption by the cover.

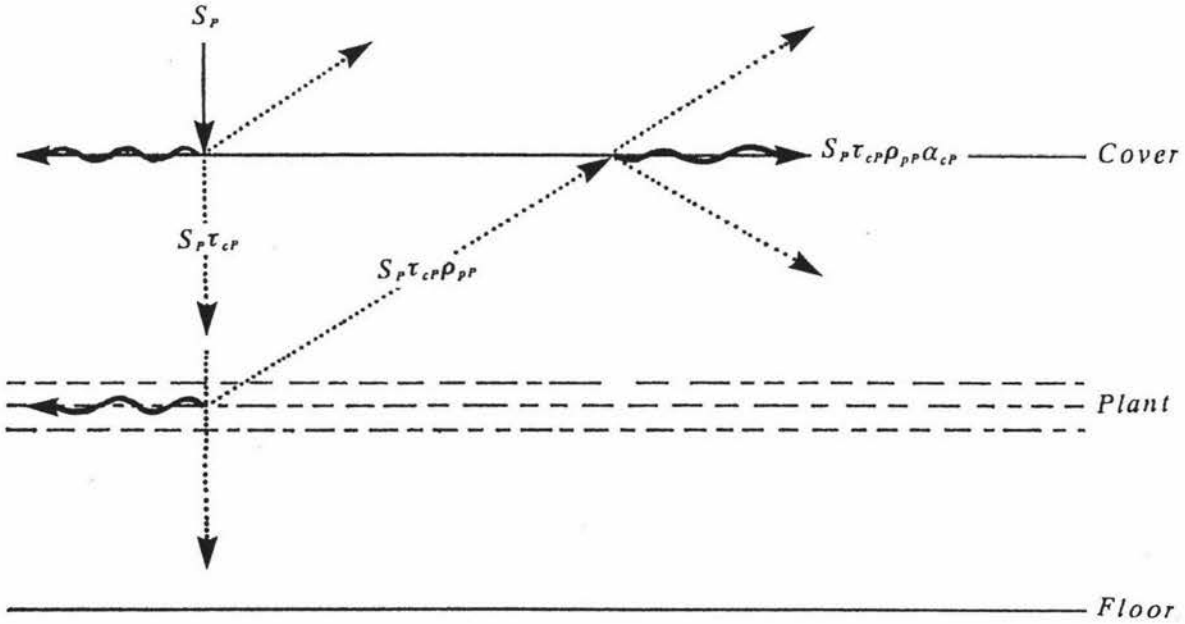

Figure A3.2 2nd order PAR absorption by the cover.

$S_P\tau_{cP}\tau_{pP}^2\rho_{fP}\alpha_{cP}$ is a 5th order term as it involves the S_P that transmitted through the cover, transmitted through the plants, reflected off the floor, transmitted back through the plants and absorbed by the underside of the cover (see Figure A3.3).

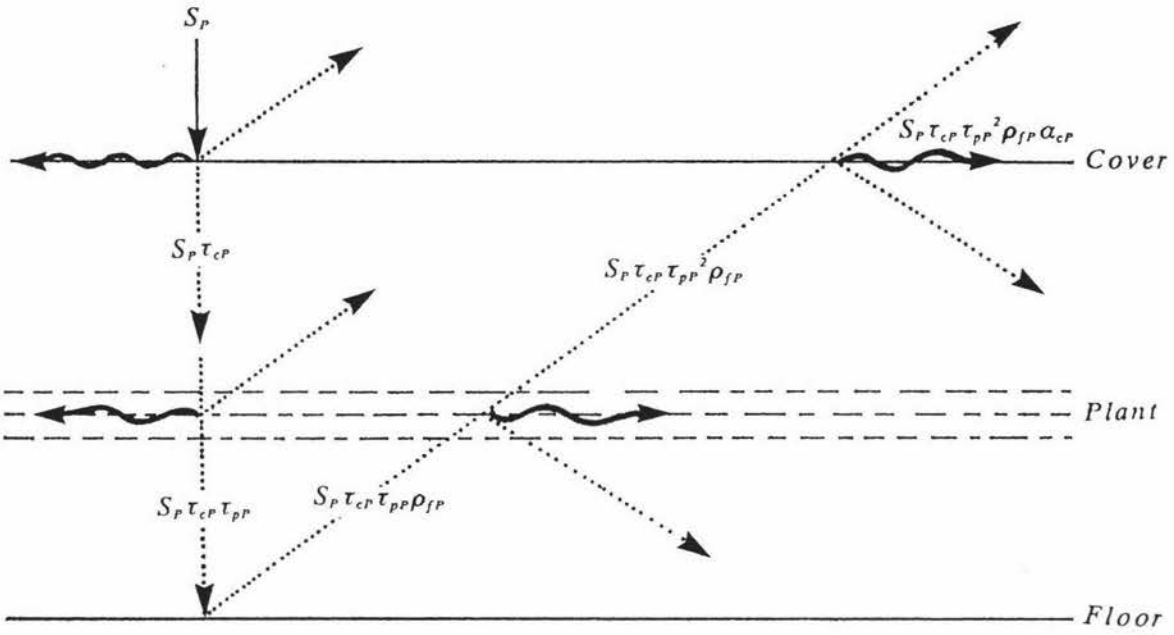

Figure A3.3 3rd order PAR absorption by the cover.

There are many other S_P paths that terminate as cover absorbed radiation. They are nevertheless 7th order or more. It is generally accepted (Wells, 1990a) that beam intensity within a greenhouse, beit PAR, NIR or FIR, is infinitesimal once its path exceeds 5th order. Consequently (4.1b) is the sum of the three most significant S_P sourced terms.

A3.1.2 Deriving the N_c equation

The N_c equation:

$$N_c = S_N\alpha_{cN} + S_N\tau_{cN}\rho_{pN}\alpha_{cN} + S_N\tau_{cN}\tau^2_{pN}\rho_{fN}\alpha_{cN} \qquad (4.1c)$$

was derived using the procedure outlinednin A3.1.1 with the exception that NIR partitioning properties were used in conjunction with solar radiation in the NIR (S_N) waveband.

A3.1.3 Deriving the R_c equation

The R_c equation:

$$R_c = 4.6\alpha_{cF}(T_{sky} - T_c)(1 + \tau_{cF}\rho_{pF} + \tau_{cF}\tau^2_{pF}\rho_{fF}) + 5.4\alpha_{cF}(T_p - T_c)(1 + \rho_{cF}\rho_{pF} + \rho_{cF}\tau^2_{pF}\rho_{fF} - \rho_{fF}\tau^2_{pF}) + 5.4_{cF}(T_p - T_f)(\rho_{fF}\tau_{pF} - \tau_{pF} - \tau_{pF}\rho_{cF}\rho_{pF}) \quad (4.1d)$$

was derived by tracing the path of a FIR beam up to the point of cover absorption using the FIR partitioning properties of the sky, cover, plant and floor.

The cover has four main sources of FIR radiation; the sky, the plant, the floor and the cover itself.

The FIR emitted by the sky was estimated by assuming it to be a blackbody with apparent temperature T_{sky}. In Appendix A2.4 the sky emission was given as:

$$E_{sky} = \sigma T^4_{sky}$$

The cover, plant, and floor are not blackbodies. Their FIR absorptivities are less than unity. The FIR emitted by the cover is therefore:

$$E_c\alpha_{cF} = \alpha_{cF}\sigma T^4_c \quad (A3.1a)$$

Similarly the FIR emitted by the plant canopy is:

$$E_p\alpha_{pF} = \alpha_{pF}\sigma T^4_p \quad (A3.1b)$$

and the FIR emitted by the floor is:

$$E_f\alpha_{fF} = \alpha_{fF}\sigma T^4_p \quad (A3.1c)$$

As $\alpha = \epsilon$ in the FIR region, α_{cF}, α_{pF} and α_{fF} are synonymous with ϵ_{cF}, ϵ_{pF} and ϵ_{pF} respectively.

R_c is derived by summing the sky, cover, plant and floor sourced FIR arriving at the cover.

Sky sourced FIR absorbed by the cover (R_{csky}), is the sum of:

- FIR emitted by the sky absorbed by the upper cover surface ($E_{sky}\alpha_{cF}$).

- FIR emitted by the sky, transmitted through the cover, reflected off the top of the plant canopy, and absorbed by the under side of the cover ($E_{sky}\tau_{cF}\rho_{pF}\alpha_{cF}$).
- FIR emitted by the sky, transmitted through the cover, transmitted through the plants, reflected off the floor, transmitted back through the plants, and absorbed by the underside of the cover ($E_{sky}\tau_{cF}\tau_{pF}^{2}\rho_{fF}\alpha_{cF}$).
- FIR emitted by the sky, transmitted through the cover, reflected off the plant canopy, reflected off the underside of the cover, reflected off the plant canopy, and absorbed by the underside of the cover ($E_{sky}\tau_{cF}\rho_{pF}^{2}\rho_{cF}\alpha_{cF}$).

Therefore:

$$R_{csky} = E_{sky}\alpha_{cF} + E_{sky}\tau_{cF}\rho_{pF}\alpha_{cF} + E_{sky}\tau_{cF}\tau_{pF}^{2}\rho_{fF}\alpha_{cF} + E_{sky}\tau_{cF}\rho_{pF}^{2}\rho_{cF}\alpha_{cF} \quad \text{(A3.2a)}$$

The **cover**, **plant** and **floor** sourced FIR absorbed by the cover, R_{cc}, R_{cp} and R_{cf} respectively, were obtained using a similar beam tracing method (see Figures A3.4, A3.5, A3.6, and A3.7).

$$R_{cc} = E_{c}\alpha_{cF}\rho_{pF}\alpha_{cF} + E_{c}\alpha_{cF}\tau_{pF}^{2}\rho_{fF}\alpha_{cF} + E_{c}\alpha_{cF}\rho_{pF}^{2}\rho_{cF}\alpha_{cF} - 2E_{c}\alpha_{cF} \quad \text{(A3.2b)}$$

$$R_{cp} = E_{p}\alpha_{pF}\alpha_{cF} + E_{p}\alpha_{pF}\rho_{cF}\rho_{pF}\alpha_{cF} + E_{p}\alpha_{pF}\rho_{fF}\tau_{pF}\alpha_{cF} + E_{p}\alpha_{pF}\rho_{pF}^{2}\rho_{cF}^{2}\alpha_{cF} + E_{p}\alpha_{pF}\rho_{fF}^{2}\rho_{pF}\tau_{pF}\alpha_{cF} + E_{p}\alpha_{pF}\rho_{cF}\tau_{pF}^{2}\rho_{fF}\alpha_{cF} + E_{p}\alpha_{pF}\rho_{fF}\tau_{pF}\rho_{cf}\rho_{pF}\alpha_{cF} \quad \text{(A3.2c)}$$

$$R_{cf} = E_{f}\alpha_{fF}\tau_{pF}\alpha_{cF} + E_{f}\alpha_{fF}\rho_{pF}\rho_{fF}\tau_{pF}\alpha_{cF} + E_{f}\alpha_{fF}\tau_{pF}\rho_{cF}\rho_{pF}\alpha_{cF} \quad \text{(A3.2d)}$$

The FIR reflectivity of plant leaves and soils is usually less than 0.05 and 0.1 respectively (Monteith and Unsworth, 1990). Consequently, when a traced FIR beam undergoes:

a) a double reflection from the plant subsystem (ie. ρ_{pF}^{2}),

b) a double reflection from the floor (ie. ρ_{fF}^{2}), or

c) a reflection from the plant and floor (ie. $\rho_{pF}\rho_{fF}$),

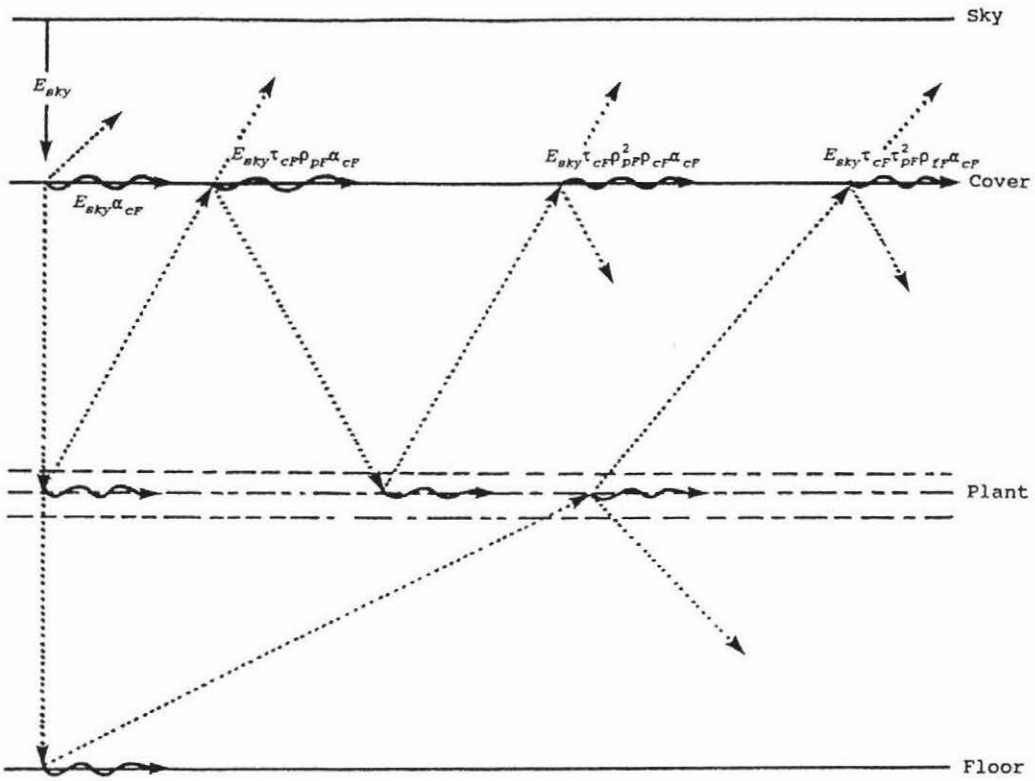

Figure A3.4 **Diagrammatic representation of equation A3.2a.**

the energy associated with the FIR is almost entirely dissipated. Consequently ρ_{pF}^2, ρ_{fF}^2, or $\rho_{pF}\rho_{fF}$ can render part of an overall energy term insignificant. Equations (A3.2a), (A3.2b), (A3.2c), and (A3.2d) therefore simplify to:

$$R_{csky} = E_{sky}(\alpha_{cF} + \tau_{cF}\rho_{pF}\alpha_{cF} + \tau_{cF}\tau_{pF}^2\rho_{fF}\alpha_{cF}) \qquad \text{(A3.3a)}$$

$$R_{cc} = E_c\alpha_{cF}(\rho_{pF}\alpha_{cF} + \tau_{pF}^2\rho_{fF}\alpha_{cF}) - 2E_c\alpha_{cF} \qquad \text{(A3.3b)}$$

$$R_{cp} = E_p\alpha_{pF}(\alpha_{cF} + \rho_{cF}\rho_{pF}\alpha_{cF} + \rho_{fF}\tau_{pF}\alpha_{cF} + \rho_{cF}\tau_{pF}^2\rho_{fF}\alpha_{cF}) \qquad \text{(A3.3c)}$$

$$R_{cf} = E_f\alpha_{fF}(\tau_{pF}\alpha_{cF} + \tau_{pF}\rho_{cF}\rho_{pF}\alpha_{cF}) \qquad \text{(A3.3d)}$$

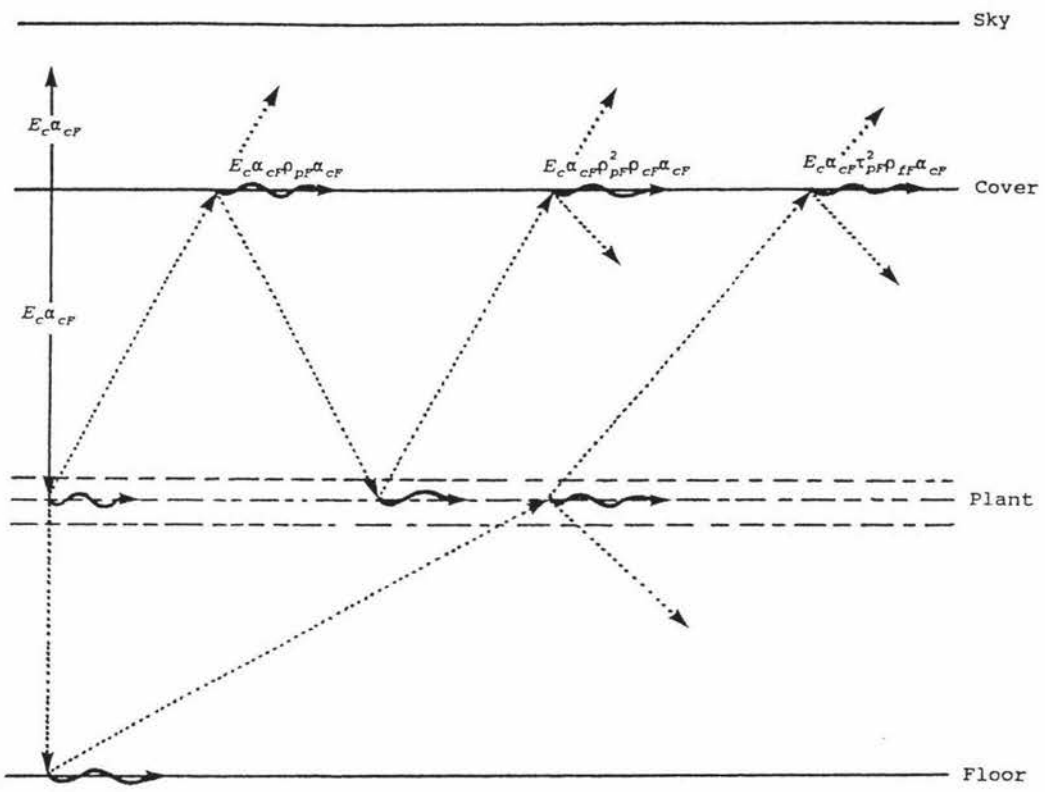

Figure A3.5 Diagrammatic representation of equation (A3.2b).

The total FIR absorbed by the cover (R_c) is therefore:

$$R_c = R_{csky} + R_{cc} + R_{cp} + R_{cf}$$

$$\begin{aligned}\rightarrow\ R_c = {} & E_{sky}(\alpha_{cF} + \tau_{cF}\rho_{pF}\alpha_{cF} + \tau_{cF}\tau_{pF}^2\rho_{fF}\alpha_{cF}) \\ & + E_c\alpha_{cF}(\rho_{pF}\alpha_{cF} + \tau_{pF}^2\rho_{fF}\alpha_{cF}) - 2E_c\alpha_{cF} \\ & + E_p\alpha_{pF}(\alpha_{cF} + \rho_{cF}\rho_{pF}\alpha_{cF} + \rho_{fF}\tau_{pF}\alpha_{cF} + \rho_{cF}\tau_{pF}^2\rho_{fF}\alpha_{cF}) \\ & + E_f\alpha_{fF}(\tau_{pF}\alpha_{cF} + \tau_{pF}\rho_{cF}\rho_{pF}\alpha_{cF})\end{aligned}$$

$$\begin{aligned}\Rightarrow\ \frac{R_c}{\alpha_{cf}} = {} & E_{sky}(1 + \tau_{cF}\rho_{pF} + \tau_{cF}\tau_{pF}^2\rho_{fF}) \\ & + E_c\alpha_{cF}(\rho_{pF} + \tau_{pF}^2\rho_{fF}) - 2E_c \\ & + E_p\alpha_{pF}(1 + \rho_{cF}\rho_{pF} + \rho_{fF}\tau_{pF} + \rho_{cF}\tau_{pF}^2\rho_{fF}) \\ & + E_f\alpha_{fF}(\tau_{pF} + \tau_{pF}\rho_{cF}\rho_{pF})\end{aligned}$$

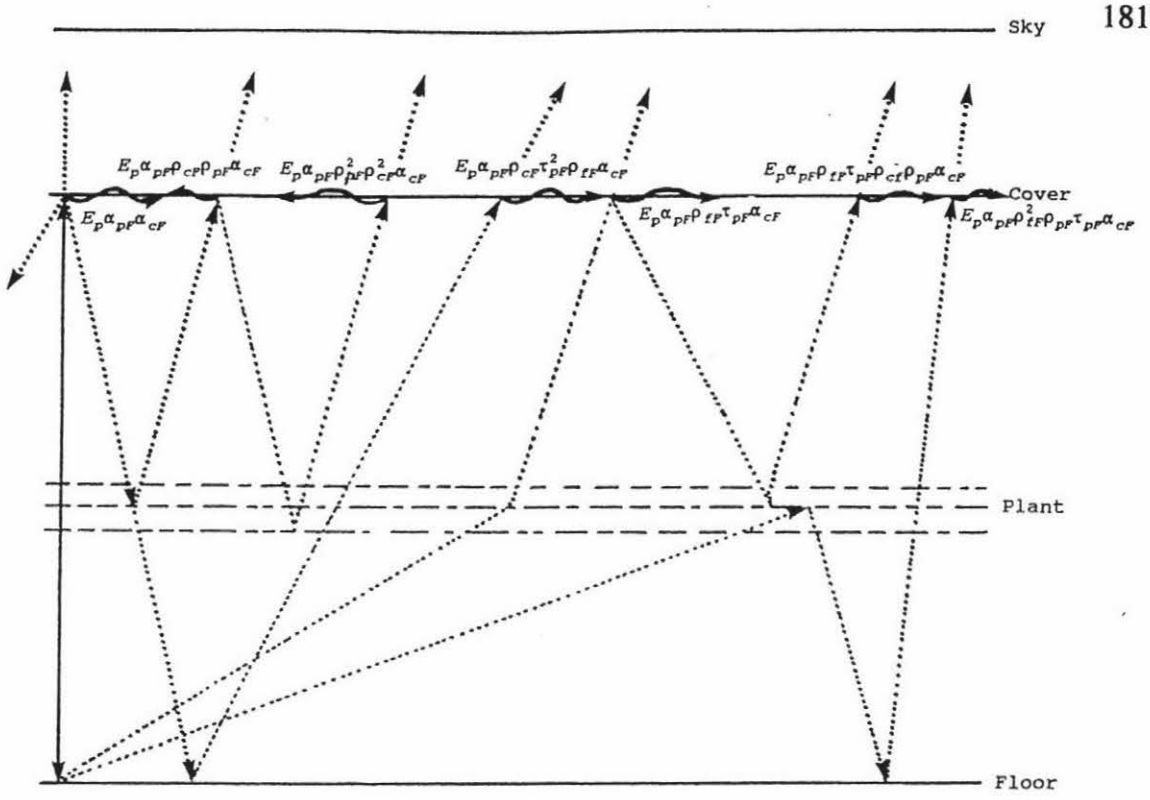

Figure A3.6 **Diagrammatic representation of equation A3.2c.**

$$\Rightarrow \frac{R_c}{\alpha_{cf}} = E_{sky}(1 + \tau_{cF}\rho_{pF} + \tau_{cF}\tau^2_{pF}\rho_{fF})$$
$$+ E_c[(1 - \tau_{cF} - \rho_{cF})(\rho_{pF} + \tau^2_{pF}\rho_{fF}) - 2]$$
$$+ E_p(1 - \tau_{pF} - \rho_{pF})(1 + \rho_{cF}\rho_{pF} + \rho_{fF}\tau_{pF} + \rho_{cF}\tau^2_{pF}\rho_{fF})$$
$$+ E_f(1 - \rho_{fF})(\tau_{pF} + \tau_{pF}\rho_{cF}\rho_{pF})$$

$$\Rightarrow \frac{R_c}{\alpha_{cf}} = E_{sky}(1 + \tau_{cF}\rho_{pF} + \tau_{cF}\tau^2_{pF}\rho_{fF})$$
$$+ E_c(\rho_{pF} + \tau^2_{pF}\rho_{fF} - \tau_{cF}\rho_{pF} - \tau^2_{pF}\rho_{fF}\tau_{cF} - \rho_{cF}\rho_{pF} - \tau^2_{pF}\rho_{fF}\rho_{cF} - 2)$$
$$+ E_p(1 + \rho_{cF}\rho_{pF} + \rho_{fF}\tau_{pF} + \rho_{cF}\tau^2_{pF}\rho_{fF} - \tau_{pF} - \tau_{pF}\rho_{cF}\rho_{pF} - \rho_{fF}\tau^2_{pF}$$
$$- \rho_{cF}\tau^3_{pF}\rho_{fF} - \rho_{pF} - \rho_{cF}\rho^2_{pF} - \rho_{fF}\tau_{pF}\rho_{pF} + \rho_{cF}\tau^2_{pF}\rho_{fF}\rho_{pF})$$
$$+ E_f(\tau_{pF} + \tau_{pF}\rho_{cF}\rho_{pF} - \tau_{pF}\rho_{fF} - \tau_{pF}\rho_{cF}\rho_{pF}\rho_{fF})$$

$$\Rightarrow \frac{R_c}{\alpha_{cf}} = (E_{sky} - E_c)(1 + \tau_{cF}\rho_{pF} + \tau_{cF}\tau^2_{pF}\rho_{fF})$$
$$+ (E_p - E_c)(1 + \rho_{cF}\rho_{pF} + \rho_{cF}\tau^2_{pF}\rho_{fF} - \rho_{pF} - \rho_{fF}\tau^2_{pF}) \qquad \text{(A3.4)}$$
$$+ (E_p - E_f)(\rho_{fF}\tau_{pF} - \tau_{pF} - \tau_{pF}\rho_{cF}\rho_{pF})$$

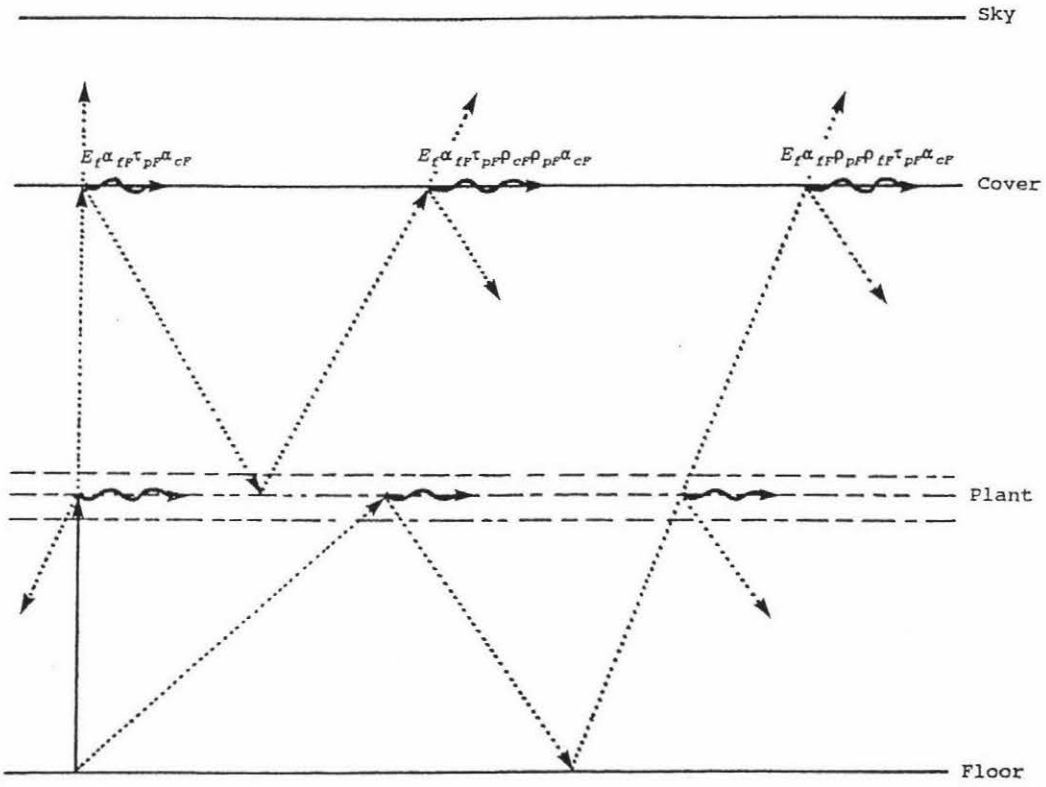

Figure A3.7 Diagrammatic representation of equation A3.2d.

It can be shown that:

$$\sigma\,(T_1^4 - T_2^4) = \sigma\,4\,Tm^3\,(T_1 - T_2) \qquad \text{(A3.5a)}$$

where $Tm \approx \dfrac{T_1 + T_2}{2}$

(A3.5a) rearranges to: $\dfrac{T_1^4 - T_2^4}{T_1 - T_2} = 4\,Tm^3$ (A3.5b)

Now:

$$\begin{aligned}\frac{T_1^4 - T_2^4}{T_1 - T_2} &= \frac{(T_1^2 - T_2^2)\,(T_1^2 + T_2^2)}{T_1 - T_2}\\ &= \frac{(T_1 + T_2)\,(T_1 - T_2)\,(T_1^2 + T_2^2)}{T_1 - T_2}\\ &= (T_1 + T_2)\,(T_1^2 + T_2^2)\\ &= T_1^3 + T_1T_2^2 + T_1^2T_2 + T_2^3\end{aligned} \qquad \text{(A3.5c)}$$

and

$$4\,Tm^3 = 4\left(\frac{T_1 + T_2}{2}\right)^3 = \frac{(T_1 + T_2)(T_1 + T_2)(T_1 + T_2)}{2} = \frac{T_1^3 + 3T_1T_2^2 + 3T_1^2T_2 + T_2^3}{2} \qquad \text{(A3.5d)}$$

Therefore (A3.5c) = (A3.5d).

$$\Rightarrow \quad T_1^3 + T_1T_2^2 + T_1^2T_2 + T_2^3 = \frac{T_1^3 + 3T_1T_2^2 + 3T_1^2T_2 + T_2^3}{2} \qquad \text{(A3.5e)}$$

$$\frac{T_1^3}{2} + \frac{T_2^3}{2} = \frac{T_1^2T_2}{2} + \frac{T_1T_2^2}{2}$$

Equation (A3.5e) only holds true when $T_1 \approx T_2 = T$

Assuming T_{sky} = mean temperature of the lower atmosphere = 263°K

and T_c = 283°K

then

$$Tm = \frac{(T_{sky} + T_c)}{2} \approx 273\ ^\circ K$$

therefore

$$(E_{sky} - E_c) = \sigma\,(T_{sky}^4 - T_c^4) = \sigma\,4\,Tm^3\,(T_{sky} - T_c) = 4.6\,(T_{sky} - T_c)$$

Assuming

$$Tm = \frac{(T_p + T_c)}{2} \approx 288\ ^\circ K$$

then

$$(E_p - E_c) = \sigma\,(T_p^4 - T_c^4) = \sigma\,4\,Tm^3\,(T_p - T_c) = 5.4\,(T_p - T_c)$$

Assuming

$$Tm = \frac{(T_p + T_f)}{2} \approx 288\ ^\circ K$$

then
$$(E_p - E_f) = \sigma (T_p^4 - T_f^4)$$
$$= \sigma 4 Tm^3 (T_p - T_f)$$
$$= 5.4 (T_p - T_f)$$

Therefore:

$$R_c = 4.6 \alpha_{cF} (T_{sky} - T_c) (1 + \tau_{cF}\rho_{pF} + \tau_{cF}\tau^2_{pF}\rho_{fF})$$
$$+ 5.4 \alpha_{cF} (T_p - T_c) (1 + \rho_{cF}\rho_{pF} + \rho_{cF}\tau^2_{pF}\rho_{fF} - \rho_{pF} - \rho_{fF}\tau^2_{pF}) \quad (A3.6)$$
$$+ 5.4 \alpha_{cF} (T_p - T_f) (\rho_{fF}\tau_{pF} - \tau_{pF} - \tau_{pF}\rho_{cF}\rho_{pF})$$

A3.1.4 Deriving the H_{ac} equation

The H_{ac} equation:

$$H_{ac} = CAI\, h_{ca} (T_a - T_c) \quad (4.1e)$$

is derived by applying Newton's cooling equation (Appendix 1) to the cover subsystem and the inside airspace.

CAI is introduced to convert H_{ac} from heat transfer per m^2 of cover to heat transfer per m^2 of floor.

A3.1.5 Deriving the H_{co} equation

The H_{co} equation:

$$H_{co} = CAI\, h_{co} (T_c - T_o) \quad (4.1f)$$

is derived from Newton's cooling equation (Appendix 1) to the cover subsystem and the outside airspace.

A3.1.6 Deriving the L_{ca} equation

The L_{ca} equation:

$$L_{ca} = CAI\, E_{ac}\left[\frac{\delta (T_c - T_{aw})}{\gamma} + (T_a - T_{aw})\right] \quad (4.1g)$$

is derived using the following methodology.

The gas equation for n moles of **perfect** or **ideal gas** is given by:

$$PV = nRT \qquad \text{(A3.7)}$$

where P = gas pressure (Pa)
V = gas volume (m^3)
n = moles of gas (mol)
R = Universal gas constant = 8.314 $Jmol^{-1}{}^{\circ}K^{-1}$

Since $n = \frac{m}{M}$ and $\rho = \frac{m}{V}$

where m = mass (g)
M = molecular mass ($gmol^{-1}$)
ρ = density of gas (gm^{-3})

then $PV = \frac{mRT}{M}$

and $$\rho = \frac{PM}{RT} \qquad \text{(A3.8)}$$

Equation (A3.8) may also be expressed as:

$$\chi = \frac{eM_v}{RT} \qquad \text{(A3.9)}$$

where χ = water vapour density or absolute humidity ($g_v m_{DA}^{-3}$)
e = water vapour pressure (Pa)

and where the subscripts $_v$ and $_{DA}$ denote water vapour and dry air respectively.

Equation (A3.9) rearranges to:

$$RT = \frac{eM_v}{\chi} \qquad \text{(A3.10)}$$

Moist air is composed of a mixture of dry air and water vapour. Applying (A3.8) to the dry air fraction:

$$\begin{aligned} \rho_{DA} &= \frac{P_{DA}M_{DA}}{RT} \\ &= \frac{(p - e)\,M_{DA}}{RT} \\ \Rightarrow \quad RT &= \frac{(p - e)\,M_{DA}}{\rho_{DA}} \end{aligned} \qquad \text{(A3.11)}$$

where p = total pressure of the moist air (Pa)

Since $p >> e$ ($e \approx 2$KPa and $P = 101.3$KPa) then (A3.11) simplifies to:

$$RT \approx \frac{p M_{DA}}{\rho_{DA}} \qquad \text{(A3.12)}$$

Combining (A3.10) and (A3.12) then:

$$\begin{aligned} \frac{eM_v}{\chi} &= \frac{p M_{DA}}{\rho_{DA}} \\ \Rightarrow \quad \chi &= \frac{e \epsilon \rho_{DA}}{p} \end{aligned} \qquad \text{(A3.13)}$$

where $\epsilon = \dfrac{M_v}{M_{DA}}$

$$= \frac{18\, g_v mol^{-1}}{29\, g_{DA} mol^{-1}}$$

$$= 0.622\, g_v g_{DA}^{-1}$$

hence $\chi^* = \dfrac{e^* \epsilon \rho_{DA}}{p}$ (A3.14)

where χ^* = saturated water vapour density ($g_v m^{-3}$)

e^* = saturated water vapour pressure (Pa)

Water vapour diffuses from regions of high water vapour density to regions of low water vapour density. The water vapour density gradient existing between the

greenhouse airspace and the region of air immediately in contact with a condensed water film on the cover surface is:

$$\chi_c^* - \chi_a = \frac{e_c^* \epsilon \rho_{DA}}{p} - \frac{e_a \epsilon \rho_{DA}}{p}$$

$$\Rightarrow \quad = \frac{\epsilon \rho_{DA}}{p} (e_c^* - e_a) \qquad \text{(A3.15)}$$

Multiplying (A3.15) by $\mathcal{L}/r_c$ converts the water vapour density gradient into a latent heat term.

$$L_{ca} = \frac{\mathcal{L} (\chi_c^* - \chi_a)}{r_c} = \frac{\mathcal{L} \epsilon \rho_{DA} (e_c^* - e_a)}{p r_c} \qquad \text{(A3.16)}$$

where L_{ca} = latent heat loss (Wm^{-2})

$\mathcal{L}$ = latent heat of vaporization of water at 20°C = $2454 Jg_v^{-1}$

r_c = resistance to water vapour diffusion from the cover surface (sm^{-1})

Equation (A3.16) therefore gives the cover latent heat loss associated with free water evaporating from its surface. A positive L_{ca} indicates evaporation from the cover and a negative L_{ca} indicates water vapour condensing on the cover.

Now γ = slope of the enthalpy lines of the psychometric chart ($Pa\,°K^{-1}$)

$= -Cp P / \mathcal{L} \epsilon$

$= -66 Pa\,°K$ (A3.17)

where Cp = specific heat capacity of dry air at 20°C = $1.01 Jg_{DA}^{-1}\,°C^{-1}$ [1]

Therefore $\frac{Cp}{\gamma} = \frac{\mathcal{L} \epsilon}{p}$

and consequently

$$L_{ca} = \frac{\rho_{DA} Cp (e_c^* - e_a)}{r_c \gamma} \qquad \text{(A3.18)}$$

---

[1] Cp varies by less than 0.5% between -20°C and 80°C. It can therefore be treated as constant (Monteith and Unsworth, 1990).

For a well designed wet bulb thermometer the slope of the wet bulb lines of the psychrometric chart correspond exactly to the slope of the enthalpy lines ($-\gamma$). The Penman-Monteith transformation may be used to decipher a relationship between adjacent air masses. The transformation is based on the slope function of a straight line, ie.

$$slope\ of\ a\ straight\ line = \frac{\Delta y}{\Delta x}$$

Using this approach then:

$$-\gamma = \frac{e^{*}_{aw} - e_a}{T_{aw} - T_a} \qquad \text{(A3.19)}$$

(See Figure A3.8)

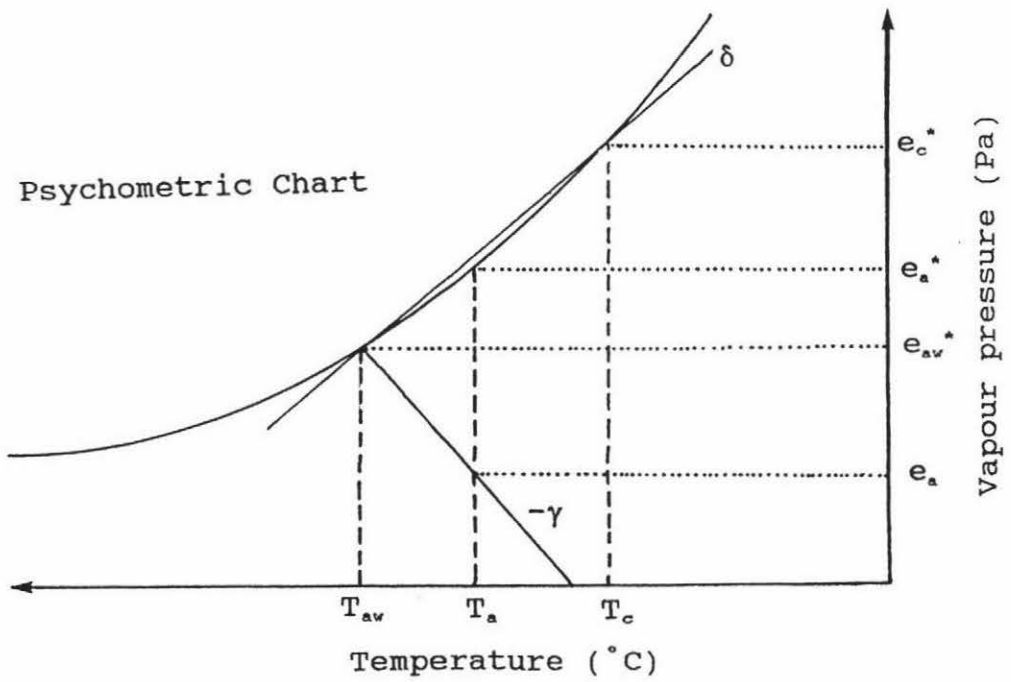

Figure A3.8 Penman-Monteith transformation I.

Therefore:

$$\begin{aligned} e^*_{aw} - e_a &= -\gamma\,(T_{aw} - T_a) \\ &= \gamma\,(T_a - T_{aw}) \\ \Rightarrow \quad e_a &= e^*_{aw} - \gamma\,(T_a - T_{aw}) \end{aligned} \qquad \text{(A3.20)}$$

Hence:

$$\begin{aligned} e^*_c - e_a &= e^*_c - [e^*_{aw} - \gamma\,(T_a - T_{aw})] \\ &= e^*_c - e^*_{aw} + \gamma\,(T_a - T_{aw}) \end{aligned} \qquad \text{(A3.21)}$$

From Figure A3.8: $\delta = \dfrac{e^*_c - e^*_{aw}}{T_c - T_{aw}}$

therefore: $e^*_c = \delta\,(T_c - T_{aw}) + e^*_{aw}$ (A3.22)

where δ = slope of the saturated vapour pressure curve at some temperature between T_c and T_{aw} in $Pa\,^{\circ}K^{-1}$

Substituting (A3.20) and (A3.22) into $(e_c^* - e_a)$ then:

$$\begin{aligned} e^*_c - e^*_a &= \delta\,(T_c - T_{aw}) + e^*_{aw} - [e_{aw} - \delta\,(T_a - T_{aw})] \\ &= \delta\,(T_c - T_{aw}) + \delta\,(T_a - T_{aw}) \end{aligned} \qquad \text{(A3.23)}$$

Combining (A3.18) and (A3.23) then:

$$\begin{aligned} L_{ca} &= \frac{\rho_{DA} Cp\,\delta\,[(T_c - T_{aw}) + \gamma\,(T_a - T_{aw})]}{r_c \gamma} \\ &= \frac{\rho_{DA} Cp\,[\delta\,(T_c - T_{aw})/\gamma + (T_a - T_{aw})]}{r_c} \\ &= E_{ce}\left[\frac{\delta\,(T_c - T_{aw})}{\gamma} + (T_a - T_{aw})\right] \end{aligned} \qquad \text{(A3.24)}$$

where

$E_{ce} = \dfrac{\rho_{DA} Cp}{r_c}$ = evaporative heat transfer coefficient ($Wm^{-2}\,^{\circ}C^{-1}$)

Since cover area is greater than floor area, LAI was introduced to convert L_{ca} into latent heat transfer per m^2 of floor. The final L_{ca} equation therefore stands as:

$$L_{ca} = CAI\,E_{ac}\left[\frac{\delta\,(T_c - T_{aw})}{\gamma} + (T_a - T_{aw})\right] \qquad (4.1g)$$

A3.2 THE PLANT ENERGY BALANCE

The energy balance for the standard greenhouse plant subsystem is given in Section 4.1.1.2 as:

$$P_p + N_p + R_p - H_{pa} - L_{pa} = 0 \qquad (4.2a)$$

A3.2.1 Deriving the P_p equation

The P_p equation:

$$P_p = S_P\tau_{cP}\alpha_{pP} + S_P\tau_{cP}\tau_{pP}\rho_{fP}\alpha_{pP} + S_P\tau_{cP}\rho_{pP}\rho_{cP}\alpha_{pP} \qquad (4.2b)$$

was derived in a manner similar to that of P_c in Appendix A3.1.

The first term is (4.2b) ($S_P\tau_{cP}\alpha_{pP}$) represents the S_P transmitted through the cover and then absorbed by the plant subsystem. It is therefore of 2nd order. The next term in (4.2b) ($S_P\tau_{cP}\tau_{pP}\rho_{fP}\alpha_{pP}$) represents the S_P transmitted through the cover, transmitted through the plants, reflected off the floor and absorbed by the underside of the plant canopy. It is therefore a 5th order term. The last term ($S_P\tau_{cP}\rho_{pP}\rho_{cP}\alpha_{pP}$) represents the S_P transmitted through the cover, reflected off the plants, reflected off the underside of the cover and absorbed by the plants. It is therefore a 4th order term.

A3.2.2 Deriving the N_p equation

The N_p equation:

$$N_p = S_N\tau_{cN}\alpha_{pN} + S_N\tau_{cN}\tau_{pN}\rho_{fN}\alpha_{pN} + S_N\tau_{cN}\rho_{pN}\rho_{cN}\alpha_{pN} \qquad (4.2c)$$

was derived in a manner similar to that used for deriving P_p with the exception that the NIR partitioning properties are used in conjunction with solar radiation in the NIR (S_N) waveband.

A3.2.3 Deriving the R_p equation

The R_p equation:

$$R_p = 4.6\alpha_{pF}(T_{sky} - T_c)[\tau_{cF}(1 + \rho_{pF}\rho_{cF} + \tau_{pF}\rho_{fF})] + 5.4\alpha_{pF}(T_c - T_p)[\rho_{cF}\rho_{pP}(1 - \rho_{cF}) + 1 - \rho_{cF} + \tau_{pF}\rho_{fF}] + 5.4_{pF}(T_f - T_p)[\tau_{pF}\rho_{cF}(1 + \rho_{cF}\rho_{pF} + \tau_{pF}\rho_{fF} - \rho_{fF}) + 1 - \rho_{fF}] \quad (4.2d)$$

was derived in a manner similar to that used for deriving R_c.

A3.2.4 Deriving the H_{pa} Equation

The H_{pa} equation:

$$H_{pa} = 2\,LAI\,h_{pa}(T_p - T_a) \quad (4.2e)$$

It was derived by applying Newton's cooling equation (Appendix 1) to the plant subsystem and the inside airspace.

LAI was introduced to convert the H_{pa} heat transfer from per m^2 of plant canopy into heat transfer per m^2 of floor. The factor '2' accounts for the fact that both upper and lower leaf surfaces exchange heat.

A3.2.5 Deriving the L_{pa} Equation

The L_{pa} equation:

$$L_{pa} = 2\,LAI\,E_{ap}\left[\frac{\delta\,(T_p - T_{aw})}{\gamma} + (T_a - T_{aw})\right] \quad (4.2f)$$

where E_{ap} = evaporative heat transfer coefficient ($Wm^{-2}{}^{\circ}C^{-1}$)

and where LAI and the factor '2' are introduced for the same reasons outlined in Section A3.2.4.

The L_{pa} equation was derived by following the methodology used for deriving L_{ca} in Section A3.1.5.

A3.3 THE FLOOR ENERGY BALANCE

The energy balance for the standard greenhouse floor subsystem is given in Section 4.1.1.3 as:

$$P_f + N_f + R_f - H_{fa} + C_{1f} - L_{fa} = 0 \qquad (4.3a)$$

P_f, N_f, R_f, H_{fa} and L_{fa} were derived using methodology similar to that outlined in Sections A3.1 and A3.2.

A3.3.1 Deriving the C_{1f} equation

The C_{1f} equation:

$$C_{1f} = K_1 (T_1 - T_f) \qquad (4.3f)$$

Beneath the model greenhouse were four 150mm soil layers (see Figures 4.1 and 4.2). If the floor is warmer than the deep soil layer, heat slowly moves towards the floor by conduction, via the four intervening layers.

The C_{1f} equation was derived by applying the Fourier heat equation (Appendix 1) to the floor subsystem and soil layer 1.

A3.4 SOIL LAYER 1 ENERGY BALANCE

The energy balance for soil layer 1 is given in Section 4.1.1.4 as:

$$C_{21} - C_{1f} = 0 \qquad (4.4a)$$

A3.4.1 Deriving the C_{21} equation

The C_{21} equation:

$$C_{21} = K_2 (T_2 - T_1) \qquad (4.4b)$$

was derived by applying the Fourier heat equation (Appendix 1) to soil layer 1 and soil layer 2.

A3.4.2 Deriving the C_{1f} equation

The procedure for deriving C_{1f} is given in Section A3.3.1.

A3.5 SOIL LAYER 2 ENERGY BALANCE

The energy balance for soil layer 2 is given in Section 4.1.1.5 as:

$$C_{32} - C_{21} = 0 \qquad (4.5a)$$

C_{32} and C_{21} were derived using the methodology outlined in Section A3.4.

A3.6 SOIL LAYER 3 ENERGY BALANCE

The energy balance for soil layer 3 is given in Section 4.1.1.6 as:

$$C_{42} - C_{32} = 0 \qquad (4.6a)$$

C_{42} and C_{32} were derived using the methodology outlined in Section A3.4.

A3.7 SOIL LAYER 4 ENERGY BALANCE

The energy balance for soil layer 4 is given in Section 4.1.1.7 as:

$$C_{d4} - C_{43} = 0 \qquad (4.7a)$$

C_{d4} and C_{43} were derived using the methodology outlined in Section A3.4.

A3.8 INSIDE AIRSPACE ENERGY BALANCE

The energy balance for the standard greenhouse inside airspace is given in Section 4.1.1.8 as:

$$H_{pa} - H_{ac} + H_{fa} - A_{ao} + AUX - D_{ao} + L_{pa} + L_{ca} + L_{fa} = 0 \qquad (4.8a)$$

The convective heat transfer terms H_{pa}, H_{ac} and H_{pa} were derived in Sections A3.2.4, A3.1.4 and A3.3 respectively. The latent heat transfer terms L_{pa}, L_{ca} and L_{fa} were derived in Sections A3.2.5, A3.1.6 and A3.3 respectively.

AUX is the auxiliary heat input to the greenhouse airspace in Wm^{-2} floor.

A3.1.8 Deriving the A_{ao} equation

Section 4.1.1.8 defines the A_{ao} equation as:

$$A_{ao} = \frac{\Phi_{ao}\,(\delta + \gamma)\,(T_{aw} - T_{ow})}{\gamma} \qquad (4.8b)$$

The advective heat transfer term A_{ao} represents the combined sensible and latent heat exchange associated with bulk moist air movement to and from the greenhouse. This movement occurs through openings in the cover such as vents, doorways extractor fans or loose construction and is driven by an enthalpy gradient either side of the cover.

The enthalpy of a moist air sample is a function of wet and dry bulb temperatures. Assuming air at 0°C has zero enthalpy and water in liquid state at 0°C has zero enthalpy then the enthalpy of moist air at barometric pressure of 101.3KPa is given by:

$$\mathcal{H} = \mathcal{H}_{DA} + \omega\mathcal{H}_{v} \qquad (A3.25)$$

where $\mathcal{H}$ = enthalpy of moist air (Jg_{DA}^{-1})

$\mathcal{H}_{DA}$ = specific enthalpy of dry air (Jg_{DA}^{-1})

ω = humidity ratio ($g_v g_{DA}^{-1}$)

$\mathcal{H}$ = specific enthalpy of water vapour (Jg_v^{-1})

The specific enthalpy of dry air between 0°C and 60°C is given by:

$$\mathcal{H}_{DA} = 1.01T \qquad \text{(A3.26)}$$

where 1.01 approximates the specific heat capacity of dry air at 0°C in $Jg_{DA}^{-1}\,°C^{-1}$ and T is temperature in °C.

The specific enthalpy of dry air at 20°C is therefore:

$$\mathcal{H}_{DA} = 1.01 \times 20$$
$$= 20.2\ Jg_{DA}^{-1}$$

and is entirely sensible heat.

The specific enthalpy of water vapour between 0°C and 60°C is given by:

$$\mathcal{H}_v = 2501 + 1.88T \qquad \text{(A3.27)}$$

where 2501 = latent heat of vaporization of water at 0°C in Jg_{DA}^{-1}

1.84 $\approx$ specific heat capacity of water vapour at 0°C in $Jg_v^{-1}\,°C^{-1}$ [2]

T = temperature (°C)

Assuming vaporization takes place at 0°C then the specific enthalpy of water vapour at 20°C is:

$$\mathcal{H}_v = 2501 + 1.88 \times 20$$
$$= 2501 + 37.6$$
$$= 2539\ Jg_v^{-1}$$

---

[2]According to monteith and Unsworth (1990) Cp_v can be treated as constant between -5 and 45°C.

where 2,501Jg_v^{-1} is latent enthalpy and 37.6Jg_v^{-1} is sensible enthalpy.

Figure A3.9 introduces a new property called equivalent temperature (Θ_a) which is defined as the temperature of a dry air sample having the same enthalpy as a moist air sample at T_a and T_{aw}. It is therefore possible to access the moist air enthalpy gradient either side of the greenhouse cover by working with dry bulb temperatures of equivalent enthalpy.

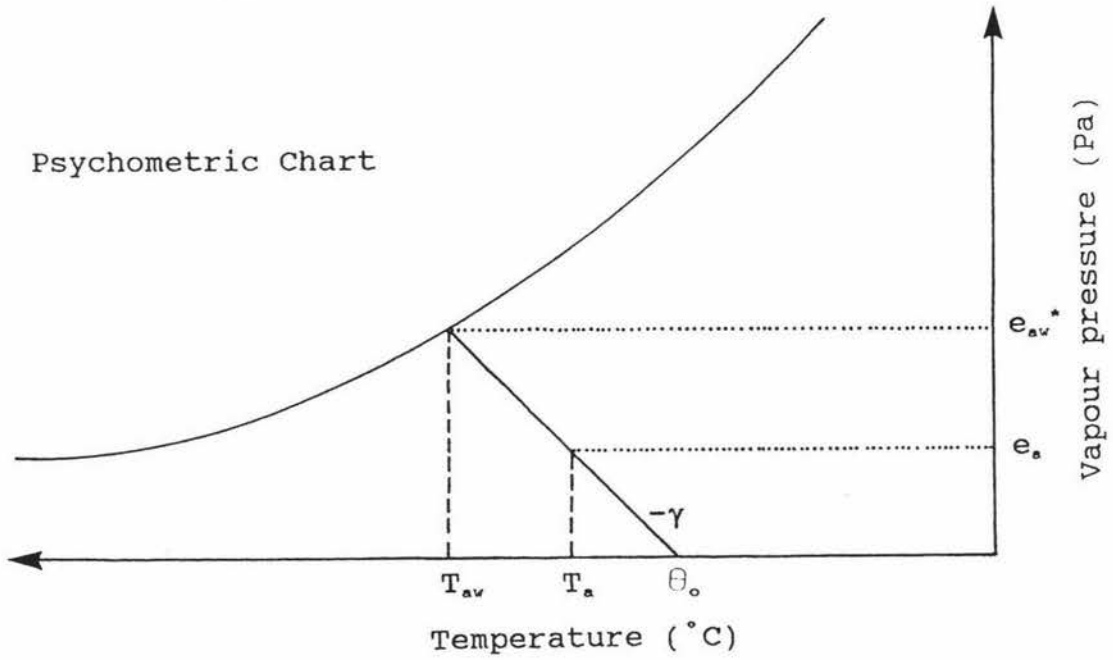

Figure A3.9 Equivalent temperature.

From Figure A3.9

$$-\gamma = \frac{e_a - 0}{T_a - \Theta_a} \quad \Rightarrow \Theta_a = T_a + \frac{e_a}{\gamma} \qquad \text{(A3.28)}$$

or $$-\gamma = \frac{e_{aw}^* - 0}{T_{aw} - \Theta_a} \quad \Rightarrow \Theta_a = T_{aw} + \frac{e_{aw}^*}{\gamma} \qquad \text{(A3.29)}$$

The enthalpy gradient is therefore:

$$\mathcal{H}_a - \mathcal{H}_o = Cp\,(\Theta_a - \Theta_o) \qquad \text{(A3.30)}$$

where $\mathcal{H}_a$ = specific enthalpy of inside dry air (Jg^{-1})

$\mathcal{H}_o$ = specific enthalpy of outside dry air (Jg^{-1})

Cp = specific heat capacity of dry air = $1.01 Jg_{DA}^{-1} {}^{\circ}C^{-1}$

Θ_a = equivalent temperature of inside air ($^{\circ}C$)

Θ_o = equivalent temperature of outside air ($^{\circ}C$)

Combining (A3.29) and (A3.30) then:

$$\begin{aligned} \mathcal{H}_a - \mathcal{H}_o &= Cp\left[\left(T_{aw} + \frac{e^*_{aw}}{\gamma}\right) - \left(T_{ow} + \frac{e^*_{ow}}{\gamma}\right)\right] \\ &= Cp\left(T_{aw} - T_{ow} + \frac{e^*_{aw}}{\gamma} - \frac{e^*_{ow}}{\gamma}\right) \\ &= Cp\,(T_{aw} - T_{ow}) + \frac{Cp}{\gamma}(e^*_{aw} - e^*_{ow}) \end{aligned} \qquad \text{(A3.31)}$$

Using the Penman-Monteith transformation (Figure A3.8) equation (A3.31) becomes:

$$\begin{aligned} \mathcal{H}_a - \mathcal{H}_o &= Cp\,(T_{aw} - T_{ow}) + \frac{Cp\,\delta}{\gamma}(T_{aw} - T_{ow}) \\ &= Cp\,\frac{(\delta + \gamma)}{\gamma}(T_{aw} - T_{ow}) \end{aligned} \qquad \text{(A3.32)}$$

As $\mathcal{H}_a$ and $\mathcal{H}_o$ are derived using equivalent temperatures, the dry air enthalpy gradient ($\mathcal{H}_a$ -$\mathcal{H}_o$) represents the actual moist air enthalpy gradient either side of the cover.

Advective heat transfer to and from the greenhouse is proportional to:

- moist air enthalpy gradient either side of the cover,
- the dry air density either side of the cover,
- the greenhouse volume,
- and the number of house air changes per unit time.

It can be shown that:

$$A = \rho_{DA} NV (\mathcal{H}_a - \mathcal{H}_o)$$
$$= \rho_{DA} NVCp \frac{(\gamma + \delta)}{\gamma} (T_{aw} - T_{ow}) \qquad \text{(A3.33)}$$

where A = advective heat transfer to and from the greenhouse (W)

ρ_{DA} = density of dry air = $1{,}200 g_{DA} m^{-3}$ [3]

N = number of air changes per second (s^{-1})

V = greenhouse volume (m^{-3})

The advective heat transfer per m^2 of floor area A_{ao}, is therefore:

$$A_{ao} = \frac{\rho_{DA} NVCp}{A_f} \frac{(\gamma + \delta)}{\gamma} (T_{aw} - T_{ow})$$
$$= \rho_{DA} NdCp \frac{(\gamma + \delta)}{\gamma} (T_{aw} - T_{ow}) \qquad \text{(A3.34)}$$
$$= \frac{\rho_{DA} Cp (\gamma + \delta)}{r_a \gamma} (T_{aw} - T_{ow})$$

where A_f = floor area (m^2)

r_a = advective resistance (sm^{-1}) = 1/Nd

d = average height of greenhouse (m) = V/A_f

Finally:

$$A_{ao} = \frac{\Phi_{ao} (\delta + \gamma) (T_{aw} - T_{ow})}{\gamma} \qquad \text{(4.8b)}$$

where Φ_{ao} = the advective heat transfer coefficient ($Wm^{-2} {}^{\circ}C^{-1}$)

$$= \frac{\rho_{DA} Cp}{r_a} - \frac{\rho_{DA} NVCp}{Af}$$

A3.8.2 Deriving the D_{ao} equation

The D_{ao} equation:

---

[3] $\rho_{DA} = 1{,}200 g_{DA} m^{-3}$ is assumed indicative of dry air density at typical inside and outside temperatures. In reality however, ρ_{DA} lies somewhere between $1{,}146 g_{DA} m^{-3}$ and $1{,}292 g_{DA} m^{-3}$; the 35°C and 0°C dry air densities respectively (Monteith and Unsworth, 1990).

$$D_{ao} = \mathcal{H}_v \Omega_{ao} CAI \left[\frac{(\delta + \gamma)(T_{aw} - T_{ow})}{\gamma} - (T_a - T_o) \right] \qquad (4.8c)$$

Water vapour may move advectively within bulk air currents, or diffusively in response to water vapour molecule gradients. When water vapour diffuses from one region to another it carries both sensible and latent energy. The overall energy (sensible + latent) associated with water vapour per unit mass is called the enthalpy of water vapour. In Section A3.81 a term known as the specific enthalpy of water vapour $\mathcal{H}_v$ was defined under the assumption water vapour at 0°C has $0Jg_v^{-1}$ sensible enthalpy and $2{,}501Jg_v^{-1}$ latent enthalpy.

In Section A3.81 the $\mathcal{H}_v$ equation is given as:

$$\mathcal{H}_v = 2501 + 1.88T \qquad (A3.27)$$

In Section A3.16 water vapour density is derived as:

$$\chi = \frac{e \epsilon \rho_{DA}}{p} \qquad (A3.13)$$

The water vapour density gradient in $g_v m^{-3}$ either side of the greenhouse cover is given by:

$$\begin{aligned} \chi_a - \chi_o &= \frac{e_a \epsilon \rho_{DA}}{p} - \frac{e_o \epsilon \rho_{DA}}{p} \\ &= \frac{\epsilon \rho_{DA}}{p} (e_a - e_o) \end{aligned} \qquad (A3.35)$$

Using the approach of Penman-Monteith again (Figure A3.10) it can be shown that:

$$e_o = e^*_{ow} - \gamma (T_o - T_{ow}) \qquad (A3.36)$$

Substituting (A3.20) and (A3.36) into (A3.35) then:

$$\begin{aligned} \chi_a - \chi_o &= \frac{\epsilon \rho_{DA}}{p} \{ [e^*_{aw} - \gamma (T_a - T_{aw})] - [e^*_{ow} - \gamma (T_o - T_{ow})] \} \\ &= \frac{\epsilon \rho_{DA}}{p} [(e^*_{aw} - e^*_{ow}) - \gamma (T_a - T_{aw}) + \gamma (T_o - T_{ow})] \end{aligned} \qquad (A3.37)$$

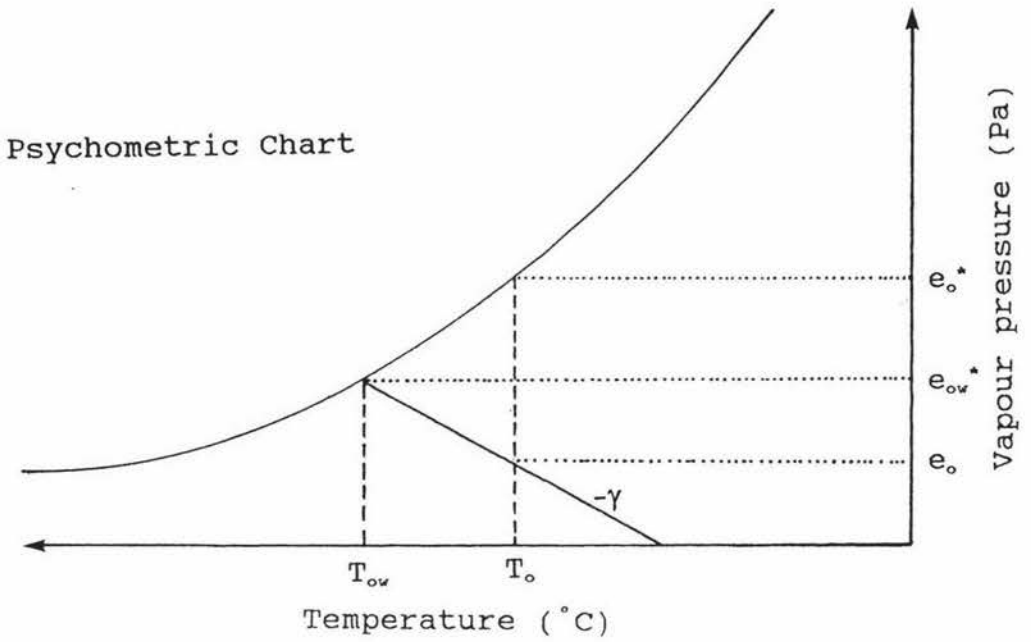

Figure A3.10 Penman-Monteith transformation II.

From Figure A3.10:

$$\delta = \frac{e^*_{aw} - e^*_{ow}}{T_{aw} - T_{ow}} \qquad \text{(A3.38)}$$

$$\Rightarrow \quad e^*_{aw} - e^*_{ow} = \delta\,(T_{aw} - T_{ow})$$

Substituting (A3.38) into (A3.37) then:

$$\begin{aligned}\chi_a - \chi_o &= \frac{\epsilon \rho_{DA}}{p}\left[\delta\,(T_{aw} - T_{ow}) - \gamma\,(T_a - T_{aw}) + \gamma\,(T_o - T_{ow})\right] \\ &= \frac{\epsilon \rho_{DA}}{p}\left[\delta\,(T_{aw} - T_{ow}) + \gamma\,(T_{aw} - T_{ow}) - \gamma\,(T_a - T_o)\right] \\ &= \frac{\epsilon \rho_{DA}}{p}\left[(\delta + \gamma)\,(T_{aw} - T_{ow}) - \gamma\,(T_a - T_o)\right]\end{aligned} \qquad \text{(A3.39)}$$

Multiplying through by γ/γ then:

$$\begin{aligned}\chi_a - \chi_o &= \frac{\epsilon \rho_{DA}}{p}\frac{\gamma}{\gamma}\left[(\delta + \gamma)\,(T_{aw} - T_{ow}) - \gamma\,(T_a - T_o)\right] \\ &= \frac{\rho_{DA} Cp}{\mathcal{L}}\left[\frac{(\delta + \gamma)}{\gamma}\,(T_{aw} - T_{ow}) - (T_a - T_o)\right]\end{aligned} \qquad \text{(A3.40)}$$

where $\gamma = \frac{Cp\,p}{\lambda\,\epsilon}$

According to Fick's Law of Diffusion the rate of mass transfer per unit area (the mass flux density) may be derived by dividing the mass gradient by the diffusion resistance.

Hence $$Zc_{ao} = \frac{(\chi_a - \chi_o)}{r} \qquad \text{(A3.40)}$$

where Zc_{ao} = water vapour flux density ($g_v s^{-1} m^{-2}$cover) ie. rate of water vapour diffusion through the greenhouse cover

r = resistance to water vapour diffusion (sm^{-1})

Zc_{ao} can also be given in terms of water vapour pressure and permeance.

$$Zc_{ao} = \phi(e_a - e_o) \qquad \text{(A3.42)}$$

where ϕ = permeance ($g_v s^{-1} m^{-2}$coverPa^{-1})

$(e_a - e_o)$ = water vapour pressure gradient either side of the cover (Pa)

Combining (A3.41) and (A3.42) then:

$$r = \frac{(\chi_a - \chi_o)}{\phi(e_a - e_o)} \qquad \text{(A3.43)}$$

Now $$\chi = \frac{eM_v}{RT} \qquad \text{(A3.9)}$$

Combining (A3.43) and (A3.41) then:

$$r = \frac{\frac{e_a M_v}{RT} - \frac{e_o M_v}{RT}}{\phi(e_a - e_o)} \qquad \text{(A3.44)}$$

$$= \frac{M_v}{\phi RT}$$

Combining (A3.44) and (A3.41)then:

$$Zc_{ao} = \frac{\varnothing RT(\chi_a - \chi_o)}{M_v} \qquad (A3.45)$$

where $\frac{\varnothing RT}{M_v}$ = diffusion resistance term based on permeance (sm^{-1})

Now $$Z_{ao} = \frac{\varnothing RTCAI(\chi_a - \chi_o)}{M_v} \qquad (A3.46)$$

where Z_{ao} = rate of water vapour diffusion through the cover per m^2 of floor ($g_v s^{-1} m^{-2}$floor)

Combining (A3.40) and (A3.46) then:

$$Z_{ao} = \frac{\varnothing RTCAI\rho_{DA}Cp}{M_v \mathcal{L}}\left[\frac{(\gamma + \delta)}{\gamma}(T_{aw} - T_{ow}) - (T_a - T_o)\right] - \Omega_{ao}CAI\left[\frac{(\gamma + \delta)}{\gamma}(T_{aw} - T_{ow}) - (T_a - T_o)\right] \qquad (4.9f)$$

where Ω_{ao} = mass transfer coefficient ($g_v s^{-1} m^{-2}$cover$^\circ K^{-1}$)

$$= \frac{\varnothing RT\rho_{DA}Cp}{M_v \mathcal{L}}$$

The heat associated with the diffusing water vapour is therefore derived by combining (5.9f) and (A3.27). Hence:

$$D_{ao} = \mathcal{H}_v Z_{ao} - \mathcal{H}_v \Omega_{ao} CAI\left[\frac{(\delta + \gamma)(T_{aw} - T_{ow})}{\gamma} - (T_a - T_o)\right] \qquad (4.8c)$$

where D_{ao} = diffusion heat transfer (Wm^{-2}floor)

(As water vapour density inside a greenhouse is almost always greater than that outside the T used in Equation (A3.27) to find $\mathcal{H}_v$ is assumed to be the inside temperature T_a).

A3.9 INSIDE AIRSPACE MASS BALANCE

The mass balance for the standard greenhouse inside airspace is given in Section 4.1.1.9 as:

$$M_{pa} + M_{ca} + M_{fa} - M_{ao} - Z_{ao} + EMF = 0 \qquad (4.9a)$$

M_{pa}, M_{ca}, M_{fa}, M_{ao}, Z_{ao} and EMF all have units of $g_v s^{-1} m^{-2}$floor.

EMF symbolises the water vapour input by evaporative cooling, misting or fogging.

A3.9.1 Deriving the M_{pa} equation

M_{pa} quantifies the advective exchange of water vapour between the plants and the inside airspace.

A negative M_{pa} indicates transpiration by giving the mass of water vapour emigrating the leaf stand above $1m^2$ of floor every second. A positive M_{pa} indicates water vapour condensing on leaves above $1m^2$ of floor every second.

M_{pa} is derived by dividing the latent heat exchange L_{pa} (derived in Section A3.2.5) by the latent heat of vaporization, L. Therefore:

$$M_{pa} = \frac{L_{pa}}{\lambda} = \frac{2 LAI E_{ap}}{\lambda} \left\{ \left[\frac{\delta (T_p - T_{aw})}{\gamma} \right] + (T_a - T_{aw}) \right\} \qquad (4.9b)$$

A3.9.2 Deriving the M_{ca} equation

M_{ca} quantifies the advective exchange of water vapour between the cover and the inside airspace.

A negative M_{ca} indicates the mass of water vapour evaporating from liquid water on the underside of the cover above $1m^2$ of floor every second. A positive M_{ca} indicates the mass water vapour condensing on the underside of the cover above $1m^2$ of floor every second.

M_{ca} is derived by dividing the latent heat exchange L_{ca} (derived in Section A3.1.6) by the latent heat of vaporization, L. Therefore:

$$M_{ca} = \frac{L_{ca}}{\mathcal{L}} = \frac{CAIE_{ac}}{\mathcal{L}} \left\{ \left[\frac{\delta (T_c - T_{aw})}{\gamma} \right] + (T_a - T_{aw}) \right\} \qquad (4.9c)$$

A3.9.3 Deriving the M_{fa} equation

M_{fa} quantifies the advective exchange of water vapour between the floor and inside airspace.

A negative M_{fa} indicates the mass of water vapour evaporating from $1m^2$ of floor every second. A positive M_{fa} indicates water vapour condensing on $1m^2$ of floor every second.

M_{fa} is derived by dividing the latent heat exchange L_{fa} (derived in Section A3.3) by the latent heat of vaporization, L. Therefore:

$$M_{fa} = \frac{L_{fa}}{\mathcal{L}} = \frac{E_{af}}{\mathcal{L}} \left\{ \left[\frac{\delta (T_f - T_{aw})}{\gamma} \right] + (T_a - T_{aw}) \right\} \qquad (4.9d)$$

A3.9.4 Deriving the M_{ao} Equation

Section 4.1.1.9 defines the M_{ao} equation as:

$$M_{ao} = \frac{\Phi_{ao} \left\{ \left[\frac{(\delta + \gamma)(T_{aw} - T_{ow})}{\gamma} \right] - (T_a - T_o) \right\}}{\mathcal{L}} \qquad (4.9e)$$

M_{ao} quantifies the advective exchange of water vapour between the inside air space and outside air.

A negative M_{ao} indicates water vapour leaving the greenhouse airspace by advection and a positive M_{ao} indicates water vapour entering the greenhouse airspace by advection.

In Section A3.8.1 the total advective heat exchange (sensible + latent) A_{ao}, was derived as:

$$A_{ao} = \frac{\Phi_{ao}(\delta + \gamma)(T_{aw} - T_{ow})}{\gamma} \qquad (4.8b)$$

The sensible heat exchange by advection is given by:

$$A_{ao}(sen.) = \Phi_{ao}(T_a - T_o) \qquad (A3.47)$$

where $A_{ao}(sen.)$ = sensible advective heat exchange (Wm^{-2})

Now: *Total advective heat exchange* = *Sensible advective heat exchange* + *Latent advective heat exchange*

$$\Rightarrow \quad A_{ao} = A_{ao}(sens.) + A_{ao}(lat.)$$

therefore

$$A_{ao}(lat.) = A_{ao} - A_{ao}(sens.)$$

$$= \frac{\Phi_{ao}(\delta + \gamma)(T_{aw} - T_{ow})}{\mathcal{L}} - \Phi_{ao}(T_a - T_o)$$

$$= \Phi_{ao}\left[\frac{(\delta + \gamma)(T_{aw} - T_{ow})}{\gamma} - (T_a - T_o)\right]$$

and knowing $M_{ao} = \frac{A_{ao}(lat.)}{\mathcal{L}}$

then:

$$M_{ao} = \frac{\Phi_{ao}\left\{\left[\frac{(\delta + \gamma)(T_{aw} - T_{ow})}{\gamma}\right] - (T_a - T_o)\right\}}{\mathcal{L}} \qquad (4.9e)$$

A3.9.5 Deriving the Z_{ao} equation

Section 4.1.1.9 defines the Z_{ao} equation as:

$$Z_{ao} = \Omega_{ao} CAI \left\{ \left[\frac{(\delta + \gamma)(T_{aw} - T_{ow})}{\gamma} \right] - (T_a - T_o) \right\} \qquad (4.9f)$$

Z_{ao} quantifies the diffusive exchange of water vapour between the inside airspace and outside air.

A negative Z_{ao} indicates water vapour diffusing from the greenhouse airspace to the outside airspace and a positive Z_{ao} indicates water vapour diffusing from the outside airspace to the greenhouse airspace.

The derivation of Z_{ao} is given in Section A3.8.2.

APPENDIX 4: PHASE 1 INPUTS

A4.1 PARAMETERS

In this section Phase 1 parameters are tabulated according to type. For materials that are non-transparent, the symbols (u) and (l) were used to differentiate the upper surface from the lower.

The bracketed characters in the right hand column of the following tables indicate the information source. A key is given below.

Information source

(1) Wells, (1990a).

(2) Threlkeld, (1962).

(3) Wells, (1989a).

(4) Goudriaan, (1977).

(5) Monteith and Unsworth, (1990).

(6) Bailey, (1978c).

(A) Assumed values.

(C) Calculated values (see Appendix 5).

(E) Experimental values (see Appendix 6).

(I) Based on manufacturer or distributor brochures.

(O) Based on other tabulated figures.

(S) Values set by author.

A4.1.1 PAR parameters

Table A4.1a PAR Absorptivity.

Subsystem	Symbol	Material	Absorptivity
Cover	α_{cP}	Glass	0.25 (1)
		Agphane	0.25 (1)
		Double *Agphane*	0.44 (O)
Screen	α_{uP} or α_{lP}	*Marix*	0.25 (O)
		LS 13 (u)	0.10 (O)
		LS 13 (l)	0.13 (O)
		LS 15 (u)	0.05 (O)
		LS 15 (l)	0.15 (O)
		LS 18 (u)	0.00 (O)
		LS 18 (l)	0.20 (O)
		LS 18F (u)	0.00 (O)
		LS 18F (l)	0.20 (O)
		Clear PE	0.25 (O)
		Black PE	0.80 (O)
		Infrane X30	0.25 (O)
		Infansol	0.25 (O)
		Durafilm	0.25 (O)
		Duratherm	0.25 (O)
		Hyperlyte	0.25 (O)
		Agphane	0.25 (O)
Plant	α_{pP}		$1-\tau_{pP}-\rho_{pP}$ (A)
Floor	α_{fP}		0.15 (2)

Table A4.1b PAR Transmissivity.

Subsystem	Symbol	Material	Transmissivity
Cover	τ_{cP}	Glass	0.70 (3)
		Agphane	0.70 (3)
		Double *Agphane*	0.49 (O)
Screen	τ_{sP}	*Marix*	0.50 (I)
		LS 13	0.60 (I)
		LS 15	0.45 (I)
		LS 18	0.15 (I)
		LS 18F	0.15 (I)
		Clear PE	0.70 (3)
		Black PE	0.00 (A)
		Infrane X30	0.70 (3)
		Infansol	0.70 (3)
		Durafilm	0.70 (3)
		Duratherm	0.70 (3)
		Hyperlyte	0.70 (3)
		Agphane	0.70 (3)
Plant	τ_{pP}		e^{-KL} † (4)
Floor	τ_{fP}		0.00 (2)

† where K is the extension coefficient and is given by:

$$K = K_b \sqrt{(1 - (\tau_L + \rho_L))}$$

where K_b = 0.8

τ_L = leaf transmissivity to PAR = 0.1

ρ_L = leaf reflectivity to PAR = 0.1

$(\tau_L + \rho_L)$ = the Scattering Coefficient

L = LAI

(Goudriaan, 1977)

Table A4.1c PAR Reflectivity.

Subsystem	Symbol	Material	Reflectivity
Cover	ρ_{cP}	Glass	0.05 (1)
		Agphane	0.05 (1)
		Double *Agphane*	0.07 (O)
Screen	ρ_{uP} or ρ_{lP}	*Marix*	0.25 (I)
		LS 13 (u)	0.30 (I)
		LS 13 (l)	0.27 (I)
		LS 15 (u)	0.50 (I)
		LS 15 (l)	0.40 (I)
		LS 18 (u)	0.85 (I)
		LS 18 (l)	0.65 (I)
		LS 18F (u)	0.85 (I)
		LS 18F (l)	0.65 (I)
		Clear PE	0.05 (I)
		Black PE	0.20 (2)
		Infrane X30	0.05 (I)
		Infansol	0.05 (I)
		Durafilm	0.05 (I)
		Duratherm	0.05 (I)
		Hyperlyte	0.05 (I)
		Agphane	0.05 (I)
Plant	ρ_{pP}		† (4)
Floor	ρ_{fP}		0.15 (5)

† The reflectivity of a dense stand of horizontal leaves (ie. a closed canopy) ρ_∞, is given by:

$$\rho_\infty = 0.9 \times \left(\frac{1 - \sqrt{(1 - (\tau_L + \rho_L))}}{1 + \sqrt{(1 - (\tau_L + \rho_L))}} \right)$$

where τ_L = leaf transmissivity to PAR = 0.1

ρ_L = leaf reflectivity to PAR = 0.1

$(\tau_L + \rho_L)$ = the Scattering Coefficient)

and where:

$$\rho_{pP} = \rho_{\infty} (1 - e^{LK_b})$$

where L = LAI

and $K_b = 0.8$

(Goudriaan, 1977)

A4.1.2 NIR parameters

Table A4.2a NIR Absorptivity.

Subsystem	Symbol	Material	Absorptivity
Cover	α_{cN}	Glass	0.25 (1)
		Agphane	0.25 (1)
		Double *Agphane*	0.44 (O)
Screen	α_{uN} or α_{lN}	*Marix*	0.25 (O)
		LS 13 (u)	0.10 (O)
		LS 13 (l)	0.13 (O)
		LS 15 (u)	0.05 (O)
		LS 15 (l)	0.15 (O)
		LS 18 (u)	0.00 (O)
		LS 18 (l)	0.20 (O)
		LS 18F (u)	0.00 (O)
		LS 18F (l)	0.20 (O)
		Clear PE	0.25 (O)
		Black PE	0.80 (O)
		Infrane X30	0.25 (O)
		Infansol	0.25 (O)
		Durafilm	0.25 (O)
		Duratherm	0.25 (O)
		Hyperlyte	0.25 (O)
		Agphane	0.25 (O)
Plant	α_{pN}		$1-\tau_{pN}-\rho_{pN}$ (A)
Floor	α_{fN}		0.15 (2)

Table A4.2b NIR Transmissivity.

Subsystem	Symbol	Material	Transmissivity
Cover	τ_{cN}	Glass	0.70 (3)
		Agphane	0.70 (3)
		Double *Agphane*	0.49 (O)
Screen	τ_{sN}	*Marix*	0.50 (I)
		LS 13	0.60 (I)
		LS 15	0.45 (I)
		LS 18	0.15 (I)
		LS 18F	0.15 (I)
		Clear PE	0.70 (3)
		Black PE	0.00 (A)
		Infrane X30	0.70 (3)
		Infansol	0.70 (3)
		Durafilm	0.70 (3)
		Duratherm	0.70 (3)
		Hyperlyte	0.70 (3)
		Agphane	0.70 (3)
Plant	τ_{pN}		e^{-KL} † (4)
Floor	τ_{fN}		0.00 (2)

† where K is the extension coefficient and is given by:

$$K = K_b \sqrt{(1 - (\tau_L + \rho_L))}$$

where K_b = 0.8

τ_L = leaf transmissivity to NIR = 0.4

ρ_L = leaf reflectivity to NIR = 0.4

$(\tau_L + \rho_L)$ = the Scattering Coefficient

L = LAI

(Goudriaan, 1977)

Table A4.2c NIR Reflectivity.

Subsystem	Symbol	Material	Reflectivity
Cover	ρ_{cN}	Glass	0.05 (1)
		Agphane	0.05 (1)
		Double *Agphane*	0.07 (O)
Screen	ρ_{uN} or ρ_{lN}	*Marix*	0.25 (I)
		LS 13 (u)	0.30 (I)
		LS 13 (l)	0.27 (I)
		LS 15 (u)	0.50 (I)
		LS 15 (l)	0.40 (I)
		LS 18 (u)	0.85 (I)
		LS 18 (l)	0.65 (I)
		LS 18F (u)	0.85 (I)
		LS 18F (l)	0.65 (I)
		Clear PE	0.05 (I)
		Black PE	0.20 (2)
		Infrane X30	0.05 (I)
		Infansol	0.05 (I)
		Durafilm	0.05 (I)
		Duratherm	0.05 (I)
		Hyperlyte	0.05 (I)
		Agphane	0.05 (I)
Plant	ρ_{pN}		† (4)
Floor	ρ_{fN}		0.15 (5)

† The reflectivity of a dense stand of horizontal leaves (ie. a closed canopy) ρ_∞, is given by:

$$\rho_\infty = 0.9 \times \left(\frac{1 - \sqrt{(1 - (\tau_L + \rho_L))}}{1 + \sqrt{(1 - (\tau_L + \rho_L))}} \right)$$

where τ_L = leaf transmissivity to NIR = 0.4

ρ_L = leaf reflectivity to NIR = 0.4

$(\tau_L + \rho_L)$ = the Scattering Coefficient

and where:

$$\rho_{pP} - \rho_{\infty} (1 - e^{LK_b})$$

where L = LAI

K_b = 0.8

(Goudriaan, 1977)

A4.1.3 FIR parameters

Table A4.3a FIR Absorptivity.

Subsystem	Symbol	Material	Absorptivity
Cover	α_{cF}	Glass	0.95 (2)
		Agphane	0.48 (E)
		Double *Agphane*	0.69 (O)
Screen	α_{uF} or α_{lF}	*Marix*	0.59 (E)
		LS 13 (u)	0.45 (E)
		LS 13 (l)	0.61 (E)
		LS 15 (u)	0.45 (E)
		LS 15 (l)	0.48 (E)
		LS 18 (u)	0.47 (E)
		LS 18 (l)	0.61 (E)
		LS 18F (u)	0.42 (E)
		LS 18F (l)	0.56 (E)
		Clear PE	0.20 (E)
		Black PE	0.67 (E)
		Infrane X30	0.49 (E)
		Infansol	0.39 (E)
		Durafilm	0.15 (E)
		Duratherm	0.72 (E)
		Hyperlyte	0.76 (E)
		Agphane	0.48 (E)
Plant	α_{pF}		$0.95(1-\tau_{pF})$ (5)
Floor	α_{fF}		0.90 (5)

Table A4.3b FIR Transmissivity.

Subsystem	Symbol	Material	Transmissivity
Cover	τ_{cF}	Glass	0.00 (A)
		Agphane	0.37 (E)
		Double *Agphane*	0.14 (E)
Screen	τ_{sF}	*Marix*	*0.20 (E)*
		LS 13	0.26 (E)
		LS 15	0.18 (E)
		LS 18	*0.04* (E)
		LS 18F	0.09 (E)
		Clear PE	0.66 (E)
		Black PE	0.09 (E)
		Infrane X30	*0.32 (E)*
		Infansol	*0.44 (E)*
		Durafilm	*0.57 (E)*
		Duratherm	*0.10 (E)*
		Hyperlyte	*0.00 (E)*
		Agphane	*0.37* (E)
Plant	τ_{pF}		e^{-KL} † (5)
Floor	τ_{fF}		*0.00 (A)*

† $K = K_b\sqrt{((1-\tau_L)^2 - \rho_L^2)}$

where: $K_b = 0.8$

$\tau_L = 0$

$\rho_L = 0.05$

Table A4.3c FIR Reflectivity.

Subsystem	Symbol	Material	Reflectivity
Cover	ρ_{cF}	Glass	0.05 (O)
		Agphane	0.15 (O)
		Double *Agphane*	0.17 (O)
Screen	ρ_{uF} or ρ_{lF}	*Marix*	0.21 (E)
		LS 13 (u)	0.27 (E)
		LS 13 (l)	0.13 (E)
		LS 15 (u)	0.37 (E)
		LS 15 (l)	0.34 (E)
		LS 18 (u)	0.49 (E)
		LS 18 (l)	0.35 (E)
		LS 18F (u)	0.49 (E)
		LS 18F (l)	0.35 (E)
		Clear PE	0.14 (E)
		Black PE	0.24 (E)
		Infrane X30	0.19 (E)
		Infansol	0.17 (E)
		Durafilm	0.28 (E)
		Duratherm	0.18 (E)
		Hyperlyte	0.24 (E)
		Agphane	0.15 (E)
Plant	ρ_{pF}		$0.05(1-\tau_{pF})$ (5)
Floor	ρ_{fF}		0.10 (O)

A4.1.3 Transfer coefficients

Table A4.4 Convective heat transfer coefficients in $Wm^{-2}{}^{\circ}K^{-1}$.

Name	Value
h_{co}	10 (C)
h_{cg}	2 (C)
h_{ca}	2 (C)
h_{sg}	1 (C)
h_{sa}	1 (C)
h_{pa}	5 (C)
h_{fa}	1.5 (C)

Table A4.5 Advective heat transfer coefficients in $Wm^{-2}{}^{\circ}K^{-1}$ and symbolised Φ_{ao}, for advective heat transfer through standard greenhouse covers.

Cover	Fans	Value
Glass	On	60 (C)
	Off	1.5 (C)
Agphane	On	60 (C)
	Off	1.0 (C)
Double *Agphane*	On	60 (C)
	Off	0.5 (C)

Table A4.6a Advective heat transfer coefficients in $Wm^{-2}{}^{\circ}K^{-1}$ and symbolised Φ_{qo}, for advective heat transfer through screened greenhouse covers (with the screen in its drawn position).

Cover	Fans	Value
Glass	On	60 (C)
	Off	1.5 (C)
Agphane	On	60 (C)
	Off	1.0 (C)
Double *Agphane*	On	60 (C)
	Off	0.5 (C)

Table A4.6b **Advective heat transfer coefficients in $Wm^{-2}{}^{\circ}K^{-1}$ and symbolised Φ_{sq}, for advective heat transfer through thermal screens.**

Screen	Value
LS 13	3 (C)
LS 15	3 (C)
LS 18	3 (C)
LS 18F	3 (C)
Marix	3 (C)
Clear PE	0.5 (C)
Black PE	0.5 (C)
Infrane X30	0.5 (C)
Infrasol	0.5 (C)
Durafilm	0.5 (C)
Duratherm	0.5 (C)
Hyperlyte	0.5 (C)
Agphane	0.5 (C)

Table A4.7 Evaporative heat transfer coefficients in $Wm^{-2}{}^{\circ}K^{-1}$.

Name	Value
E_{cq}	2.2 (C)
E_{ca}	2.2 (C)
E_{sq}	1.0 (C)
E_{sa}	1.0 (C)
E_{fa}	1.5 (C)
E_{pa} (daytime)	6.0 (C)
E_{pa} (night-time)	1.0 (C)

Table A4.8 Conductive heat transfer coefficients in $Wm^{-2}{}^{\circ}K^{-1}$.

Name	Value
K_1	5 (1)
K_2	5 (1)
K_3	5 (1)
K_4	5 (1)

Table A4.9 Permeance figures for cover and screen materials in $g_{vap}\,s^{-1}\,m^{-2}\,Pa^{-1}$ (symbolised ø).

Material	Permeance ø
Glass Cover	5×10^{-7} (6&C)
Double *Agphane* Cover	5×10^{-9} (6&C)
Marix	5×10^{-6} (6&C)
LS 13	5×10^{-6} (6&C)
LS 15	5×10^{-6} (6&C)
LS 18	5×10^{-6} (6&C)
LS 18F	5×10^{-6} (6&C)
Clear PE	5×10^{-8} (6&C)
Black PE	5×10^{-8} (6&C)
Infrane X30	5×10^{-9} (6&C)
Infrasol	5×10^{-9} (6&C)
Durafilm	5×10^{-9} (6&C)
Duratherm	5×10^{-9} (6&C)
Hyperlyte	5×10^{-8} (6&C)
Agphane	5×10^{-8} (6&C)

The mass transfer coefficient Ω, units of $gs^{-1}m^{-2}{}^{\circ}K^{-1}$, was calculated using the following equation:

$$\Omega = \frac{\varnothing . R . T . \rho_{DA} . Cp}{M_{vap.}\, \mathcal{L}}$$

where R = Universal Gas Constant = $8.314 Jmol^{-1}{}^{\circ}K^{-1}$

T = temperature ($^{\circ}K$)

ρ_{DA} = density of dry air = $1200 g_{DA}\, m^{-3}$

Cp = specific heat capacity of dry air = $1.01 Jg_{DA}{}^{-1}{}^{\circ}K^{-1}$

$M_{vap.}$ = molecular weight of water = $18 gmol^{-1}$

$\mathcal{L}$ = latent heat of vaporisation of water at $0^{\circ}C$ = $2{,}501 Jg_{DA}{}^{-1}$

A4.1.4 Constants

Table A4.10 Phase 1 constants.

Name	Symbol	Value
Cover area index	CAI	1.2 or 1.6 (S)
Leaf area index	LAI	1 or 5 (S)
Cloud factor	C	0 or 1 (S)
Leaf absorptivity to FIR	$\alpha_{leaf.F}$	0.95 (5)
Leaf transmissivity to FIR	$\tau_{leaf.F}$	0 (5)
Leaf reflectivity to FIR	$\rho_{leaf.F}$	0.05 (5)
Stefan-Boltzmann Constant	σ	$5.67\times10^{-8}Wm^{-2}{}^{\circ}K^{-4}$ (5)
Slope of the Saturated Vapour Pressure Curve	δ	* (C)
Psychometric Constant	γ	66 $Pa\,^{\circ}K^{-1}$ (3)
Latent Heat of Vaporisation at 20°C	$\mathcal{L}$	2454 Jg^{-1} (3)
Radiation Potential 1.	$R_{potl}1$	4.1 (App. A3.1.3)
Radiation Potential 2.	$R_{potl}2$	5.4 (App. A3.1.3)

* $$\delta = \frac{e^{*}_{dry} \times 18}{8.31 \times T_o^2}$$

where e^{*}_{dry} = saturated water vapour pressure of dry air (Pa)

T_o = outside air temperature (°K)

A4.2 INDEPENDENT VARIABLES

Table A4.11 Known variables of Phase 1.

Name	Symbol	Value
Incoming PAR radiation	S_P	0 Wm^{-2}
Incoming NIR Radiation	S_N	0 Wm^{-2}
Outside temperature	T_o	5°C or 10°C
Outside wetbulb temperature	T_{ow}	2.2°C or 4.5°C when T_o=5°C
		6.5°C or 9.0°C when T_o=10°C
Inside temperature	T_a	15°C or 20°C
Deep ground temperature	T_d	15°C
Evaporative cooling, Misting, and Fogging	EMF	0 $gs^{-1}m^{-2}_{floor}$

APPENDIX 5: CALCULATED VALUES

A5.1 CONVECTIVE HEAT TRANSFER COEFFICIENTS

h_{co}, h_{cq}, h_{ca}, h_{sq}, h_{sa}, h_{pa}, and h_{fa} were estimated using the forced and free convection formulae given in Appendix A1.2.

A5.2 ADVECTIVE HEAT TRANSFER COEFFICIENTS

Assuming 0.5, 1, and 1.5 air changes/hour when the fans are off inside twin skin *Agphane*, single skin *Agphane*, and glass greenhouses respectively and 60 air changes/hour when the fans are on; the advective heat transfer coefficients were calculated using:

$$\frac{A_f}{NV} = r_a$$

$$\frac{V}{A_f} = d$$

and

$$\Phi_{ao},\ \Phi_{qo}\ , and\ \Phi_{aq} = \frac{\rho_{DA} Cp}{r_a}$$

where A_f = floor area (m^2)

N = number of air changes/second (s^{-1})

V = greenhouse volume (m^{-3})

r_a = advective resistance (sm^{-1})

Φ_{ao} = advective heat transfer coefficient ($Wm^{-2}\,^{\circ}K^{-1}$)

A5.3 EVAPORATIVE HEAT TRANSFER COEFFICIENTS

From Monteith and Unsworth (1990) and Wells (1989a):

$$r_v = 0.93 r_H$$

where r_v = resistance offered by the boundary layer for water vapour transfer (sm^{-1})

r_H = resistance offered by the boundary layer for heat transfer (sm^{-1})

also $$r_H = \frac{\rho_{DA} Cp}{h_c}$$

and $$r_v = \frac{\rho_{DA} Cp}{E_v}$$

therefore $$E_v = \frac{h_c}{0.93}$$

where h_c = convective heat transfer coefficient ($Wm^{-2}{}^{\circ}K^{-1}$)

E_v = evaporative heat transfer coefficient ($Wm^{-2}{}^{\circ}K^{-1}$)

A5.3.1 E_{cq} and E_{ca}

Since h_{cq} and h_{ca} = 2.0 $Wm^{-2}{}^{\circ}K^{-1}$ (from Table A4.4) then:

$$E_{cq} \text{ and } E_{ca} = \frac{2.0}{0.93} \approx 2.2\ Wm^{-2\circ}K^{-1}$$

A5.3.2 E_{sq} and E_{sa}

Since h_{sq} and h_{sa} = 1.0 $Wm^{-2}{}^{\circ}K^{-1}$ (from Table A4.4) then:

$$E_{sq} \text{ and } E_{sa} = \frac{1.0}{0.93} \approx 1.0\ Wm^{-2\circ}K^{-1}$$

A5.3.3 E_{fa}

Since h_{fa} = 1.5 $Wm^{-2}{}^{\circ}K^{-1}$ (from Table A4.4) then:

$$E_{fa} = \frac{1.5}{0.93} \approx 1.5\ Wm^{-2\circ}K^{-1}$$

A5.3.4 E_{pa}

Now $$r_b = \frac{\rho_{DA} Cp}{E_v}$$

where r_v = boundary resistance of the leaf (sm^{-1})

$$E_v = \frac{h_{pa}}{0.93}$$

and

$$= \frac{5}{0.93}$$

$$= 5.4\ Wm^{-2\circ}K^{-1}$$

therefore $$r_b = \frac{1200}{5.4}$$

$$= 222\ sm^{-1}$$

Now $$r_i = \frac{r_e(r_s + r_a)}{r_s + r_a + r_e}$$

$$= \frac{5000\,(150 + 20)}{150 + 20 + 5000} = \frac{850000}{5170} = 165\ sm^{-1}$$

where r_i = combined internal resistance (sm^{-1})

r_e = epidermal resistance (typically 2000-10000sm^{-1} for mesophytes)

r_s = stomatal resistance (typically 100-200sm^{-1} for mesophytes)

r_a = intercellular airspace resistance ($\approx$20sm^{-1})

Assuming leaves are amphistomatal then the total resistance (r_{vT}) is:

$$r_{vT} = \frac{r_b + r_i}{2} = \frac{222 + 165}{2} = 200 sm^{-1}$$

Therefore during the day:

$$E_{pa} = \frac{\rho_{DA} Cp}{r_{vT}} = \frac{1200}{200} = 6\ Wm^{-2\circ}K^{-1}$$

Assume E_{pa} = 1$Wm^{-2}{}^{\circ}K^{-1}$ during the night.

A5.4 PERMEANCE

The permeance figures in Table A4.9 were obtained from water vapour transmission tests. These tests are described in Heatley (1990).

APPENDIX 6: LONG WAVE TEST

Transmissivity, reflectivity and emissivity tests were conducted on each of the thirteen screen materials. The experiment was based on that of Horiguchi et al (1982).

METHOD AND MEASUREMENTS

(1) Reflectivity and Transmissivity

Diagrams showing the radiative heat exchange (radiation flux) for the measuring of reflectivity and transmissivity are shown in Figure A6.1. The radiation flux emitted by the two radiative cabinets, A and B, are dependent on their absolute temperatures, T_A and T_B, respectively. The radiative exchange of the ambient field between A and B may be written as:

$$R_o = R_A - R_B \qquad \text{(A6.1)}$$

under the assumption that the reflectivity of A and B are equal to zero (see Figure A6.1a) where:

R_o = net radiation between A and B,
R_A = radiation flux from A, and
R_B = radiation flux from B.

When a material such as a thermal screening material is placed between cabinet A and a net radiometer as shown in Figure A6.1b, the radiation exchange of the field is expressed as:

$$R_{NA} = (\tau R_A + R_{AM} + \rho R_B) - R_B \qquad \text{(A6.2)}$$

where R_{NA} = net radiation between AM and B,
R_{AM} = radiation flux of material AM,
τ = transmissivity of material AM or BM, and
ρ = reflectivity of material AM or BM.

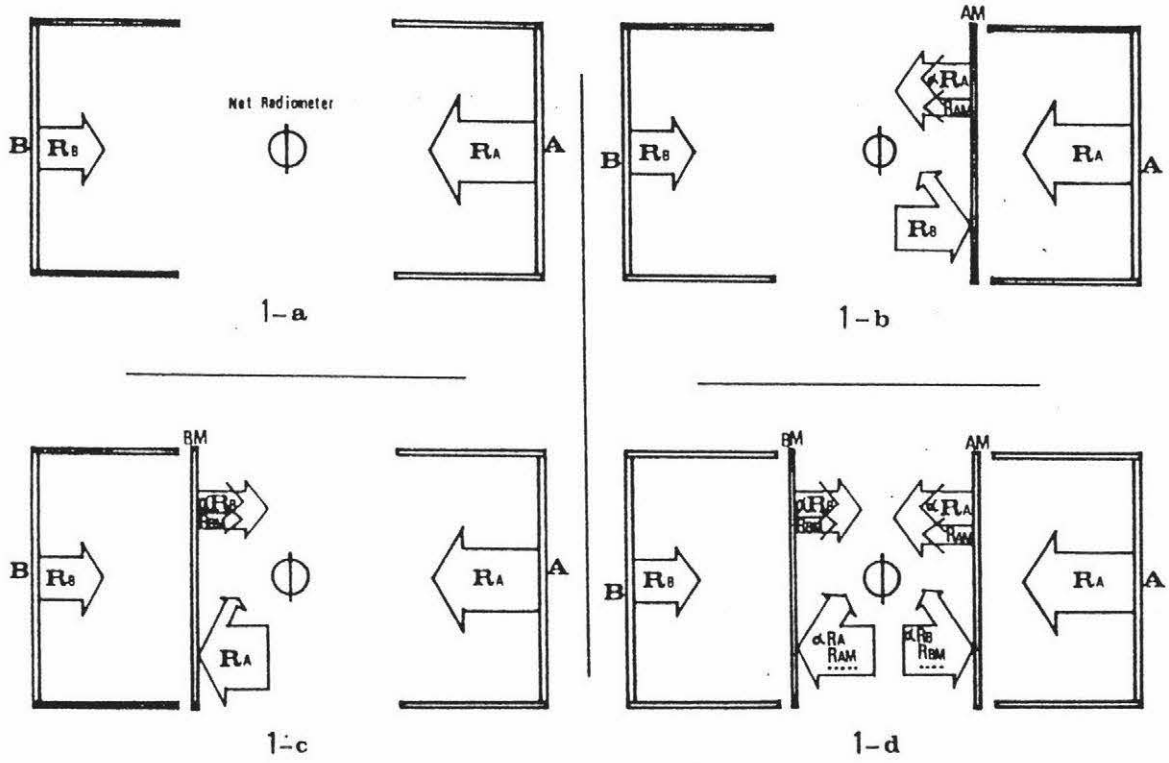

Figure A6.1 Radiative heat exchanges for the measurements of reflectivity and transmissivity.

On the other hand, if the screen material is placed between cabinet B and a net radiometer as shown in Figure A6.1c, the equation becomes as follows:

$$R_{NB} = R_A - (\tau R_B + R_{BM} + \rho R_A) \qquad \text{(A6.3)}$$

where R_{NB} = net radiation between BM and A, and

R_{BM} = radiation flux of material BM,

If the screen materials are placed on both sides of the net radiometer as shown in Figure A6.1d, the radiative exchange of the field is written as:

$$\begin{aligned} R_{NAB} &= \tau R_A - \tau R_B + R_{AM} - R_{BM} + \tau\rho R_B - \tau\rho R_A + \ldots.) \\ &= \tau (R_A - R_B)\ (1 - \rho + \rho^2 - \rho^3 + \ldots.) \\ &\quad + (R_{AM} - R_{BM})\ (1 - \rho + \rho^2 - \rho^3 + \ldots.) \\ &= [\tau (R_A - R_B) + (R_{AM} - R_{BM})]\frac{1}{1 + \rho} \end{aligned} \qquad \text{(A6.4)}$$

where R_{NAB} = net radiation between AM and BM.

From equations (A6.1) and (A6.2), (R_{AM} - R_{BM}) can be expressed as:

$$R_{AM} - R_{BM} = R_{NA} + R_{NB} - (\tau + 1 - \rho) R_o \qquad \text{(A6.5)}$$

Furthermore, substituting equations (A6.2) and (A6.5) into equation (A6.4), we get:

$$R_{NAB} = [R_{NA} + R_{NB} - R_o (1 - \rho)] \frac{1}{1 + \rho}$$

Therefore,

$$\rho = \frac{2R_o - (R_{NA} + R_{NB})}{R_o - R_{NAB}} - 1 \qquad \text{(A6.6)}$$

To obtain ρ values in the four cases shown in Figures A6.1a-A6.1d, the following net radiometer readings were taken:

1. R_o net radiation with no screening material in place
2. R_{NA} net radiation with a screen material across cabinet A
3. R_{NB} net radiation with a screen material across cabinet B
4. R_{NAB} net radiation with screen materials across both cabinets

In equation (A6.4), if the radiation flux, R_{AM}, is equal to that of R_{BM}, the equation can be simplified to:

$$R_n = \frac{\tau (R_A - R_B)}{1 + \rho} \qquad \text{(A6.7)}$$

Thus,

$$\tau = \frac{R_n (1 + \rho)}{R_o} \qquad \text{(A6.8)}$$

where R_n = net radiation in the case of $R_{AM} = R_{BM}$

To maintain the radiation flux from AM equal to that from BM, the test material was rotated continuously around the fixed net radiometer.

(2) Emissivity

The procedure for the measurement of emissivity is shown in Figure A6.2. In Figure A6.2a, the exchange of radiation between the water and the ceiling is expressed as:

$$R_w = \epsilon_w \sigma T^4 + \rho_w R_c \qquad (A6.9)$$

where R_w = radiation flux from the water surface
ϵ_w = water emissivity (0.95) at 20°C
ρ_w = water reflectance (0.05)
R_c = radiation flux from the ceiling
σ = Stefan-Boltzmann constant

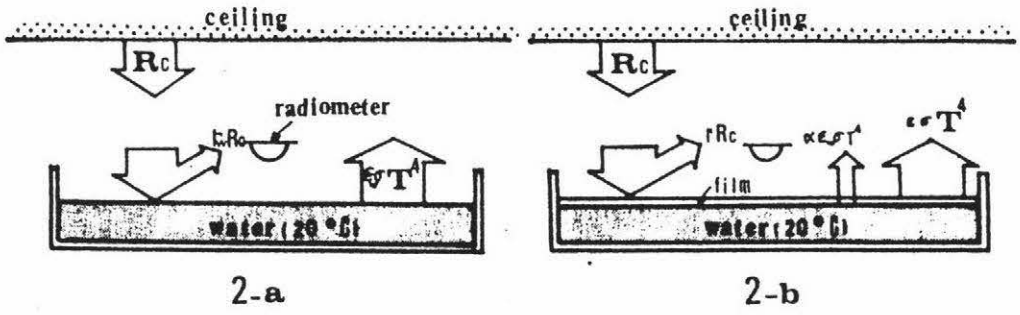

Figure A6.2 Radiative heat exchange for measurement of emissivity.

The reflectivity of the ceiling was assumed to be zero as it was painted ultra matt black.

The radiometer was placed above the water surface, and the surface water

temperature was controlled at 20°C ∓0.5°C, during the measurement of R_w. After the measurement of R_w, a screen material was stretched across the water surface as shown in Figure A6.2b. The exchange of radiation fluxes shown in Figure A6.2b can be expressed as:

$$R_p = \epsilon\sigma T^4 + \tau\epsilon_w\sigma T^4 + \rho R_c \qquad \text{(A6.10)}$$

where R_p = radiation flux from the screen surface
ϵ = emissivity of the screen
ρ = reflectivity of the screen
τ = transmissivity of the screen

In equation (A6.10), it is assumed that the surface water temperature is equal to that of the surface temperature of the screen. Thus, ϵ is expressed from equations (A6.9) and (A6.10) as:

$$\epsilon = \left[\frac{R_p - \rho R_c}{R_w - \rho_w R_c} - \tau\right]\epsilon_w \qquad \text{(A6.11)}$$

where ϵ_w and ρ are constants and are assumed to be 0.95 and 0.05, respectively. Thus,

$$\epsilon = \left[\frac{R_p - \rho R_c}{R_w - 0.05R_c} - \tau\right] \times 0.95 \qquad \text{(A6.12)}$$

To calculate emissivity, radiations from the plastic film, water surface, and ceiling must be measured.

MEASURING EQUIPMENT

The equipment used for the measurements of reflectivity and transmissivity is shown in Figure A6.3. The radiative heating cabinets were made of an insulating material called rock wood. A sheet metal lining, wrapped with a heating cable, sat within cabinet B. The surface temperature of the lining was continuously monitored with copper-constantan thermocouples and a 'Campbell' data logger. Cabinet A stayed at ambient temperature. The inward facing surfaces of both cabinets were painted ultra matt black so as to be emitters of completely diffuse

radiation. Since the surface temperature of the cabinets are affected by the surrounding temperature, the temperature difference between A and B was carefully controlled at 8°C ∓0.3°C using an output signal from the 'Campbell' to activate a simple on/off relay box.

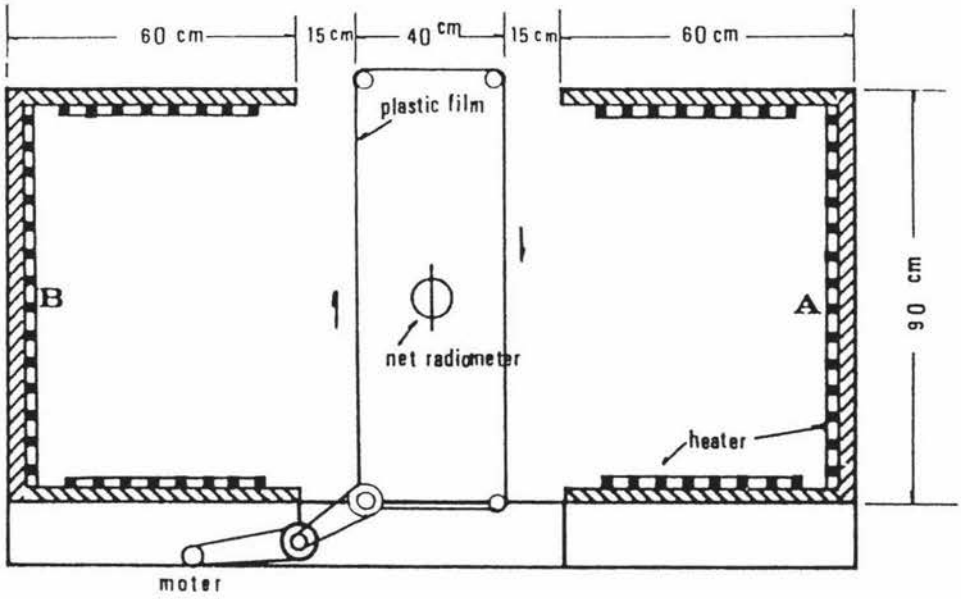

Figure A6.3 Equipment for measuring transmissivity and reflectivity of screen materials.

For the reflectivity test the screen materials were taped to the cabinets. In the transmissivity test the screens were fastened around dual rollers, located between the cabinets, and rotated at 20 rpm around the net radiometer.

The measuring equipment for emissivity is shown in Figure A6.4. The near surface temperature of the water was maintained at 20°C ∓0.5°C with an 'Omron' temperature controller, receiving signals from a copper-constantan thermocouple just below the water surface. The radiometer was set at 30mm above the water surface. The test material was floated on the water surface and taped to the tank at its periphery.

The results are given in Tables A4.3a-A4.3c.

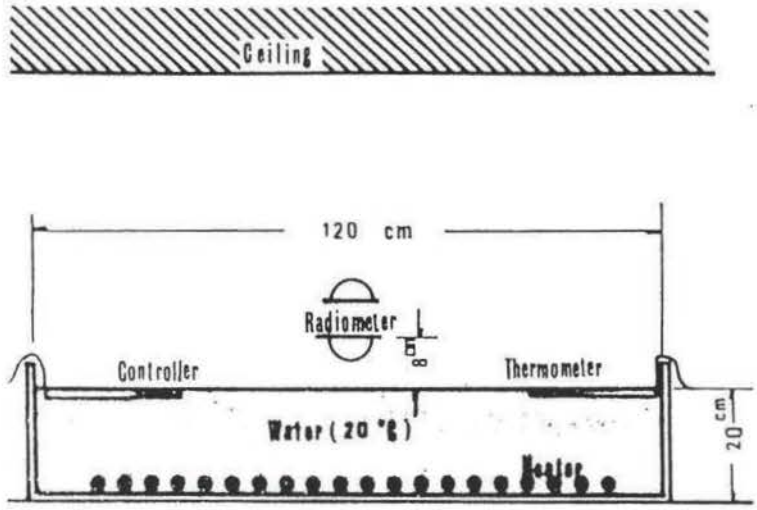

Figure A6.4 Equipment for emissivity measurement.